2022

Geological Survey Paper 8:

Structural Geology of the Arthur Range, Southern Tyennan Domain, Tasmania

Authors: D. R. Gray
M. J. Vicary
Date: 28/01/2022
Email: info@mrt.tas.gov.au
Website: www.mrt.tas.gov.au

REPORT No: GSP8

Panoranic view down the Western Arthur Range looking to the southeast from Mt Sirius (1151m). The foreground shows Lake Oberon with the glaciated and serrated quartzite ridgeline including Mt Pegasus (1063m) above the lake left side, and Mt Capricorn (1037m) in centre middle-ground beyond, extending through to the Crags of Andromeda with West Portal (1160m) the high peak visible in the distance (centre-right). The Eastern Arthur Range is the distant range (background right) with Federation Peak (1225m) and Geeves Bluff (1165m) defining the high ridgeline in the far-right background. The spine of the Range is occupied by the Devonian Western Arthur Anticline with the anticline limbs approximating the range flanks. The hinge of a northeast-closing, recumbent, isoclinal macro-fold hinge is visible in the right-hand peak above Lake Oberon and in Mt Capricorn behind. (Photo credit: David Noble)

Tasmanian Government
Mineral Resources Tasmania
mrt

CONTENTS

Abstract

The Arthur Ranges lie in the northeast corner of the Southern Tyennan domain. They consist of a Proterozoic low-grade quartzite-pelite sequence dominated by a series of Cambrian regional-scale, recumbent-isoclinal folds. The northeast flank of the Arthur Ranges is defined by a Devonian reverse fault system that truncates and offsets these Cambrian recumbent folds. The faults are associated with a sub-parallel series of open, upright northwest-trending Devonian folds that swing to a more east-west trend towards the eastern end of the Western Arthur Range. Spacing of the Devonian axial surface traces is on the order of ~1.5 km. This younger folding refolds the older Cambrian large-scale recumbent folds that are also northwest-trending.

The spine of the Western Arthur Range consists of a major northeast-closing recumbent macro-fold that extends the length of the range (~21 km) and is folded by the younger open Western Arthur Anticline. An oppositely, southwest-closing recumbent fold sits in the footwall to the Devonian reverse fault system, but to current knowledge this is only preserved at Mt Hayes, Dorado Peak and Mt Scorpio along the north flank of the range.

The Eastern Arthur Range consists of a fold-pair of regional-scale, Cambrian recumbent-isoclinal macro-folds, with a structurally higher southwest-closing closure overlying a structurally lower northeast-closing closure. Hinge zones of these folds can be seen at "The Needles" and Devils Thumb (southwest-closing hinge zones) and at Geeves Bluff and Federation Peak (northeast-closing hinge zones).

Lithofacies of the Arthur Ranges include quartzite (both thick and thin bedded), banded quartzite-pelite (interlayered quartzite, quartz schist and schist) and pelite (carbonaceous schist/phyllite). These lithologies dictate the geometry and character of the early recumbent isoclinal folding. Most of the structural profiles show 1) a thin-bedded, chevron folded quartzite in the macro-fold core (exposed on the eastern flanks of the range), and 2) more thick-bedded quartzites within the north-closing macro-fold hinge (exposed in the central to northern part of the range). Chevron folding is dominant in thinner-bedded quartzites whereas the transposition layering is more associated with the intercalated black carbonaceous siliceous pelite/phyllite.

In the Western Arthur Range cross-bedding was observed in quartzites above Alpha Moraine and on ridgeline south of Lake Cygnus. Both indicate right-way-up, bedding-parallel foliation (So/Sm) on the upper limb of the northeast-closing recumbent fold.

Shear sense indicators in the low-grade metamorphic sheet indicate recumbent macro-fold evolution and internal sheet deformation involves south-southwest-over- north-northeast transport, with shear displacement to the north (003° to 013°) in the Western Arthur Range and to the north-northeast (022° to 026°) in the Eastern Arthur Range. The Devonian fold and thrusting is also south-southwest-over-north-northeast, with transport towards ~025° in the Western Arthurs and towards ~035° in the Eastern Arthurs (assuming transport is approximately orthogonal to fault strike-traces).

Tasmanian Government

Mineral Resources Tasmania

Department of State Growth
www.mrt.tas.gov.au

Structural Geology of the Arthur Range, Southern Tyennan Domain, Tasmania

David R. Gray[1] and Michael J. Vicary[2]
[1] *Consultant Structural Geologist to Mineral Resources Tasmania*
[2] *Geological Survey Branch - Mineral Resources Tasmania*

ARTICLE INFO

Published: 28 January 2022
Publisher: Mineral Resources Tasmania
Report No.: GSP8

KEYWORDS

Structural Geology
Western Arthur Range
Southern Tyennan Region

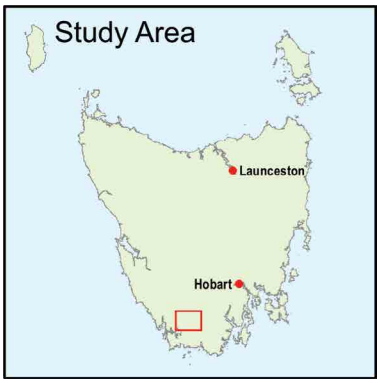

1.0 INTRODUCTION

The Arthur Range lies in the north-easternmost part in the south of the Southern Tyennan region. It includes the Western and Eastern Arthur Ranges (Figure 1) that represent the topographic interface between the Eastern and Southern Tyennan domains in the south.

The Western Arthur Range is an elongated northwest-southeast trending mountain range in folded Proterozoic quartzite (Figures 2 and 3). One of the most dramatic landforms in the southwest it is a range of jagged peaks and sharp ridges at an average elevation of 1000m (Collins, 1990, p.94). Some 21 km in length and 4 km in width the range is a "glacial legacy of 30 lakes, ridges and deep cirques" (Collins, 1990, p.244). The structure of the Western Arthur Range is defined by two major, Cambrian recumbent macro-folds that extend the length of the range from Mt Hesperus to the Crags of Andromeda. These macro-folds are truncated and offset by a Devonian reverse fault-thrust system as well as folded by an open Devonian anticline in the thrust-system hanging wall (Figures 3 and 4).

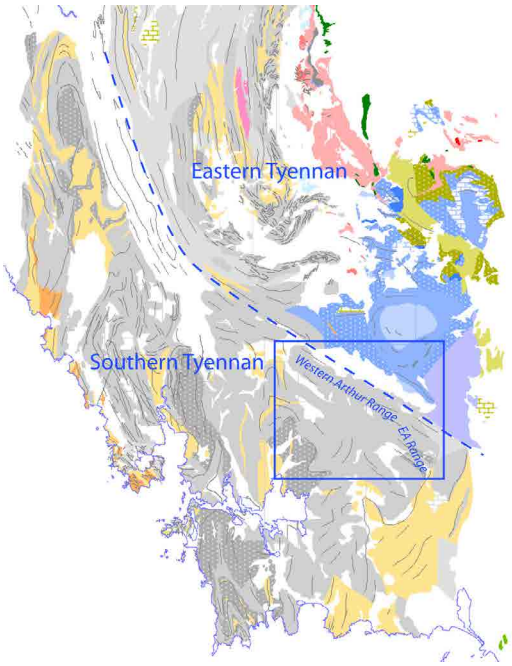

Figure 1. Litho-tectonic map of southwest Tasmania based on the Mineral Resources Tasmania 1:250000 digital atlas. The map shows the positions of the Arthur Ranges with respect to the Southern and Eastern Tyennan domains. The highlighted box shows the region covered by Figures 3 and 4 with the Western and Eastern Arthur Ranges. The Southern Tyennan Proterozoic litho-tectonic stratigraphy is as follows: *dark orange: HG metamorphic rocks; light orange: LG dominant pelitic sequence; light grey: LG quartzite dominant sequence; white stipple-darker grey: platy schistose quartzite]*

The Eastern Arthur Range has a more north-south trend where the spine of the range is at a high angle to both the Cambrian recumbent macro-folds and the open, upright Devonian folds. This is distinct from the northwest-trending Western Arthur Range where the Cambrian and Devonian structural trends are sub-parallel (Figures 1, 3 and 4). The Eastern Arthur Range is transected by three Devonian folds that also re-fold a series of older Cambrian recumbent folds (Figure 4).

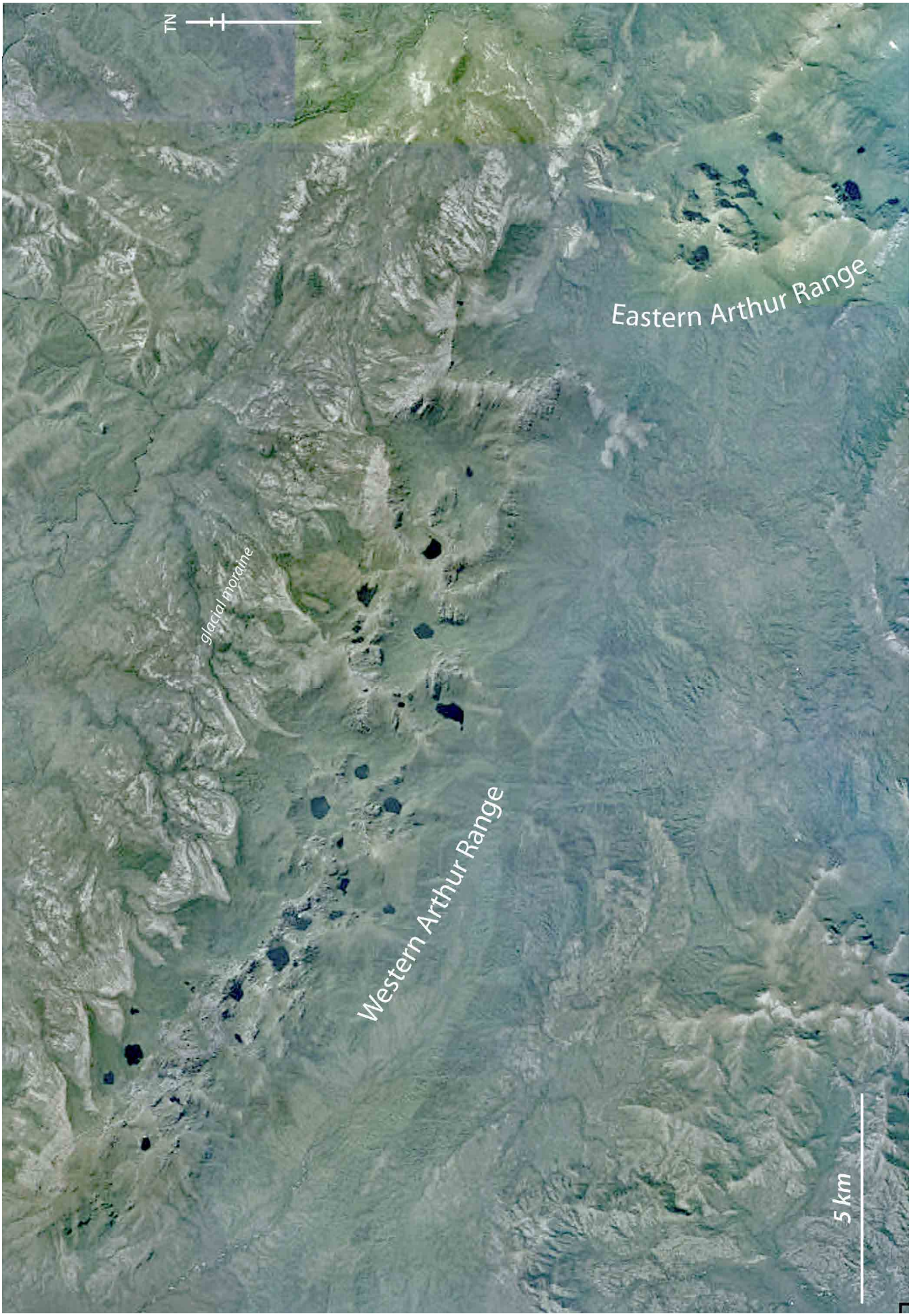

Figure 2a. Satellite image of the Western and Eastern Arthur Ranges showing the numerous glacial cirque lakes and the extensive moraine developed along the northern face of the Western Arthur Range.

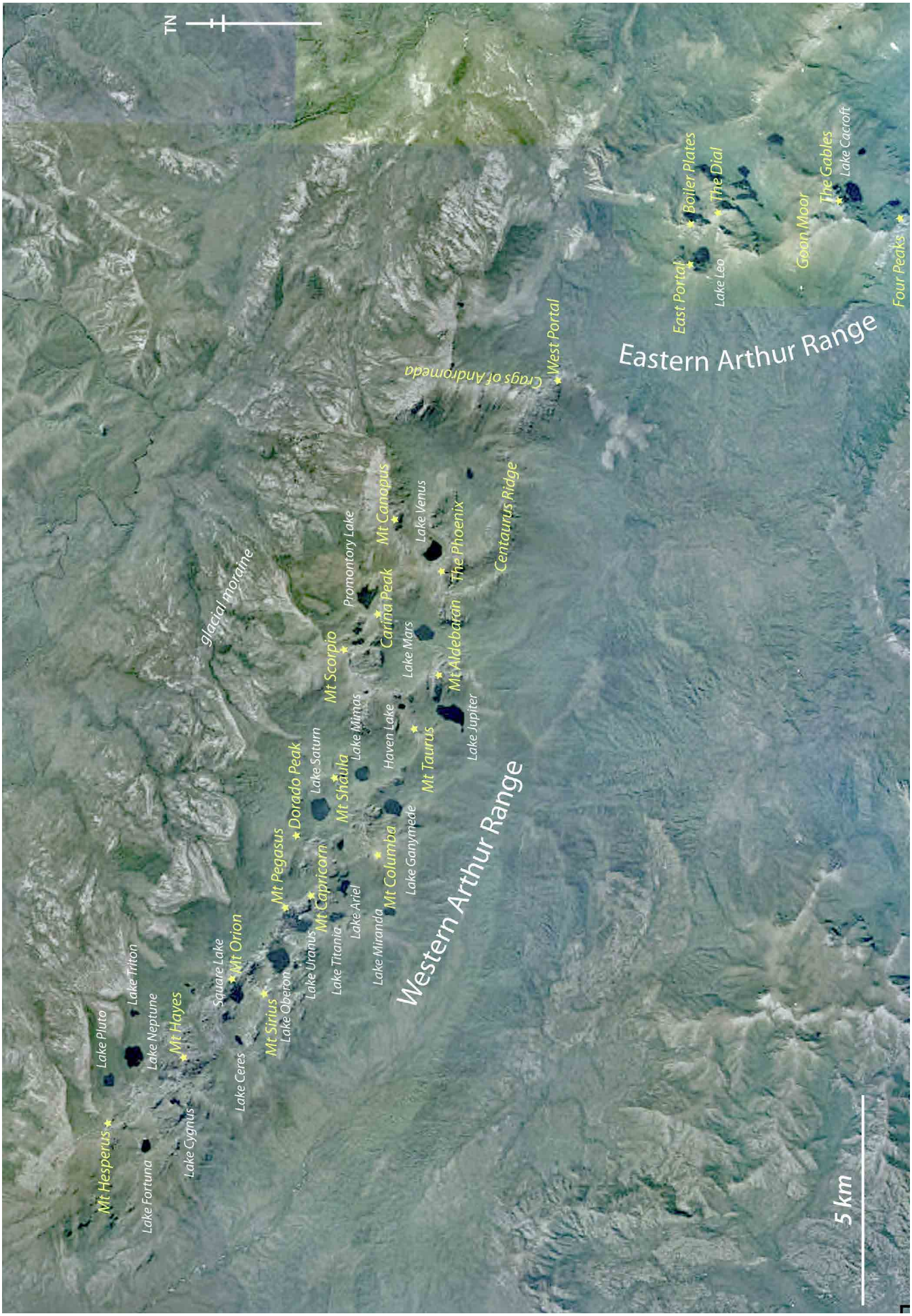

Figure 2b. Satellite image of the Western and Eastern Arthur Ranges naming the numerous glacial cirque lakes, peaks and ridges.

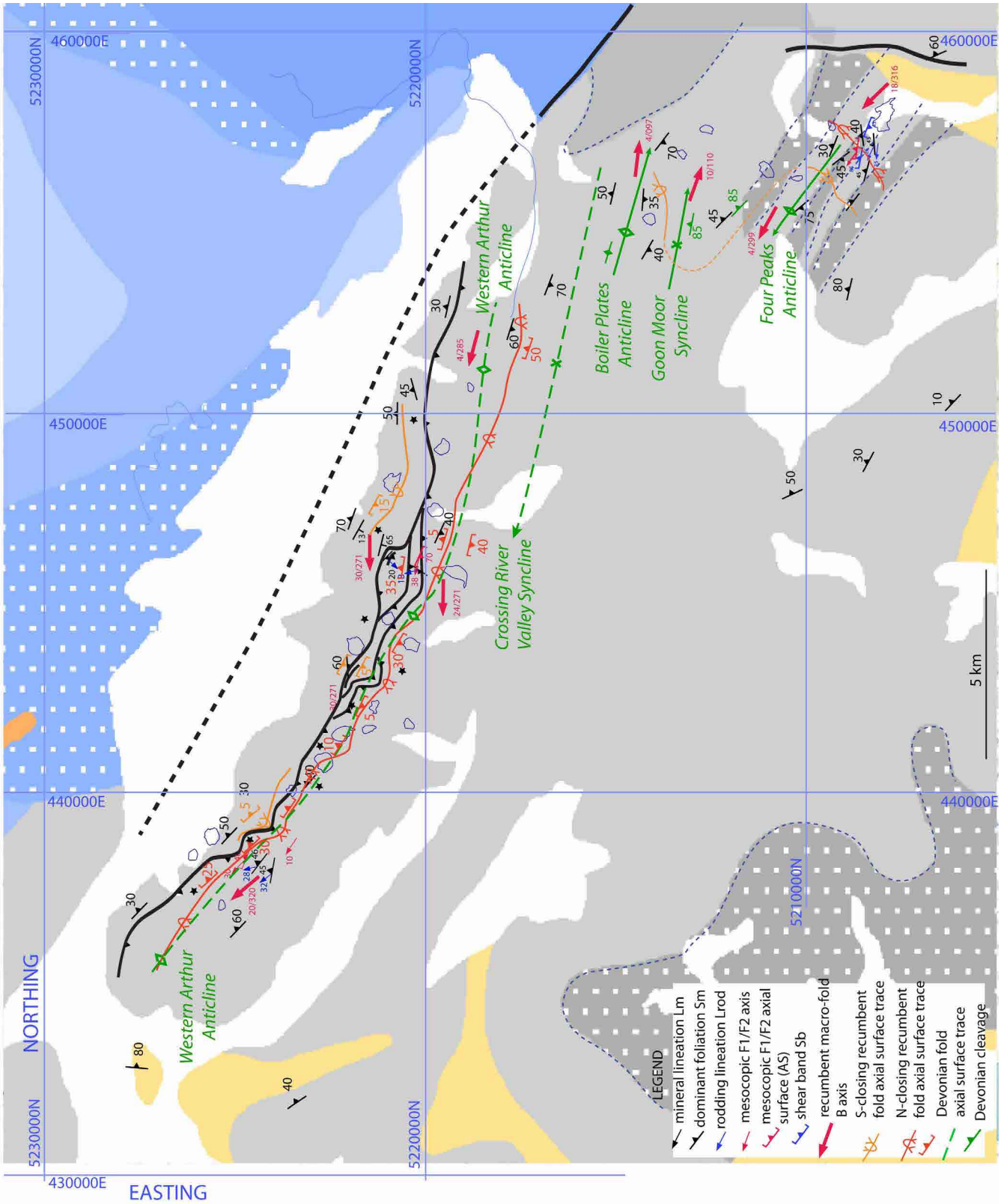

Figure 3. Structural map of the Arthur Ranges area. Map base is from the Mineral Resources Tasmania 1:250000 Digital Geological Atlas. The map shows reverse fault traces (heavy black lines), the recumbent isoclinal macro-fold axial surface traces (red trace: northeast-closing recumbent fold; orange trace: the southwest-closing recumbent fold), and the Western Arthur anticline axial surface trace (green dashed line). Attitudes of the axial surfaces of the recumbent folds are shown by the red and orange barbed dip symbols. The younger Devonian Western Arthur Anticline is shown by the dashed green trace. Darker green axial surface traces are shown for the Eastern Arthur Range including the Boiler Plates and Four Peaks Anticlines and the Goon Moor Syncline.

light grey: un-differentiated low-grade Proterozoic quartzite sequence
dark grey: undifferentiated Proterozoic sequence
dark grey with white stipple: platy or schistose quartzite
orange: low-grade Proterozoic pelite dominant sequence
blue with white stipple: Unmetamorphosed Proterozoic pelite dominant sequence
light blue: Unmetamorphosed Proterozoic quartzite sequence
dark blue: Unmetamorphosed Proterozoic quartz-rich lithicwacke conglomerate and black slate

2.0 BACKGOUND

The only geological mapping undertaken in the Arthur Range has been by Taylor (1959) in the Lake Cracroft-Federation Peak area, as part of mapping the region from Bathurst Harbour-Old River mouth to Norold Mountains to Lake Cracroft-Federation Peak. Taylor (1959) established a litho-stratigraphy of sericite-quartz schist (Old River Schist) in-folded with and overlying quartzite (Solly River Quartzite) with the quartzites cropping out in antiformal fold cores (see Taylor, 1959, fig.9). He identified 130° trending "tight overfolds", mapped as south-closing recumbent folds folded by an upright anticline through Four Peaks (see Taylor, 1959, fig.9). Taylor (1959, p.42 and p.44) also describes a semi-imbricate reverse fault system in the Federation Peak area.

With limited or no mapping done in the Western Arthur Range and the north end of the Eastern Arthur Range the following structural interpretation (Figures 3 and 4) is based on 1) a profile traverse by the authors on the ridgeline above and south of Lake Cygnus in the Western Arthur Range (Section 3.2.3 and profile 3, Figure 5), 2) profile traverse from Haven Lake-Mt Scorpio-K Moraine by the authors (Section 3.2.4 and profile 10, Figure 5), 3) a profile traverse by the authors along the Federation Peak ridgeline to Geeves Bluff in the Eastern Arthur Range (Section 4.2.4 and profile 15, Figure 5), 4) examination of published and un-published bushwalker photographs, and photos taken from "Wandering Foxbat" videos, and 5) photos by the authors on a March 26, 2020 helicopter flight along the Western Arthur Range into the Eastern Arthur Range to Federation Peak.

The overall lack of mapping and field-measured structural data, apart from the data collected by the authors, means that this is a preliminary structural interpretation. Form-line mapping has been undertaken on field outcrop photographs and onto Lands Department aerial photographs, BUT depending on clarity and distance from subject this can lead to erroneous interpretations without field checking. Multiple checks from different sources have been undertaken where possible.

Structural data is tabulated in Appendix 1.

The following **structural terminology** is used:

So/Sm	metamorphic foliation parallel to bedding (commonly a transposition layering)
So/Sm env	enveloping surface to folded So/Sm
Sm	dominant or main metamorphic foliation
Sb	shear band (S-C' structure)
AS	fold axial surface
AS/Sm	dominant foliation sub-parallel to fold axial surfaces
Sm/Sb	dominant foliation developing from Sb, shear band foliation
Scc	crenulation cleavage
Scl	Devonian overprinting low-grade cleavage
S_1	early slaty cleavage
Lm	mineral lineation
Lstretch	stretching lineation
TD	transport direction
Lint	intersection lineation
Lrod	rodding lineation developed from deforming Lint
FA	fold axis
F1, F2, F3	local age of fold axes (oldest to youngest)

The Arthur Range structural geology is largely the result of Cambrian and Middle Devonian tectonics with the main deformation and metamorphism of the Proterozoic rocks occurring during a Cambrian collision and obduction event at ~510 Ma (Berry, 2014).

The older structures referred to in this paper are considered to have formed during this Cambrian event. These include the regional scale, recumbent isoclinal macro-folds including all of the above structural elements

The younger Devonian structures include the regional scale open folds and the thrust-reverse faults that refold, truncate and offset the older structures.

2.1 Lithology

Quartzites dominate the Arthur Range Ranges (Figures 6 and 7) but are generally thinly bedded with bed thicknesses ~10-15cm (Figure 8). Some thicker bedded quartzite (~30-40 cm) has occasional cross-bedding (Figure 8). Quartzite in places is intercalated with dark, quartz-rich pelitic phyllite (Figure 9). Thicker bands of black carbonaceous mica-quartz phyllite occur at Federation Peak (cf. Taylor, 1959, fig.9).

2.2 Structural Elements

Small-scale, mesoscopic structural elements in the Arthur Range are dominated by chevron folds in the bedding foliation So/Sm (Figures 8, 10 and 11), transposition foliation Sm (Figure 12) and shear bands (Figure 13).

2.2.1 Chevron Folding

Chevron folding at all scales dominates the structure of the Western Arthur Range, (Figures 8, 10 and 11). Folds typically have long straight limbs and narrow hinge zones, either with rounded, sub-rounded to angular hinge form.

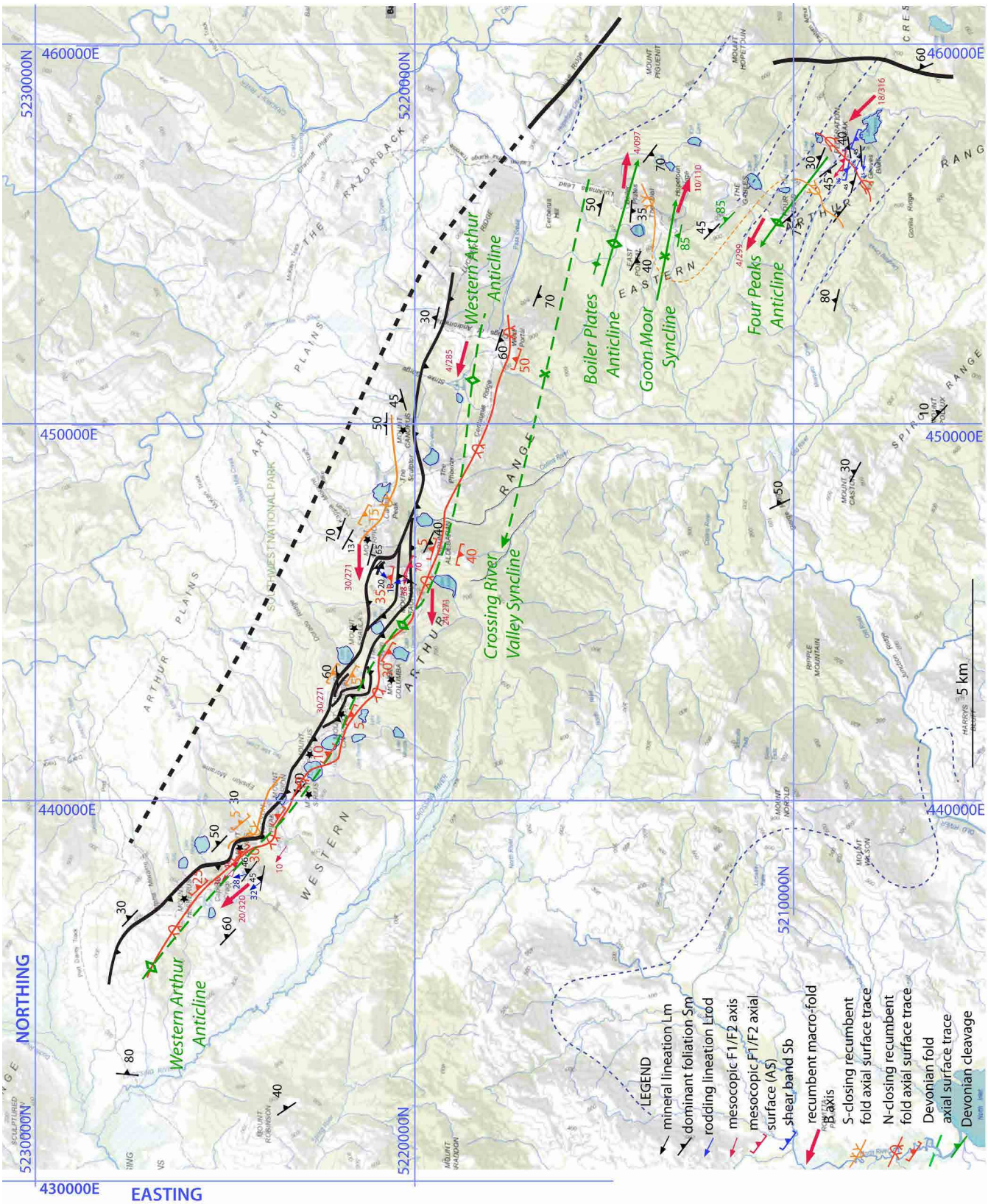

Figure 4. Structural map of the Arthur Range area on a ListMap topographic base. The map shows reverse fault traces (heavy black lines), the recumbent isoclinal macro-fold axial surface traces (red trace: northeast-closing recumbent fold; orange trace: the southwest-closing recumbent fold), and the Western Arthur Anticline axial surface trace (green dashed line). Attitudes of the axial surfaces of the recumbent folds are shown by the red and orange barbed dip symbols. The younger Devonian Western Arthur Anticline is shown by the dashed green trace. Darker green axial surface traces are shown for the Eastern Arthur Range including the Boiler Plates and Four Peaks Anticlines and the Goon Moor Syncline.

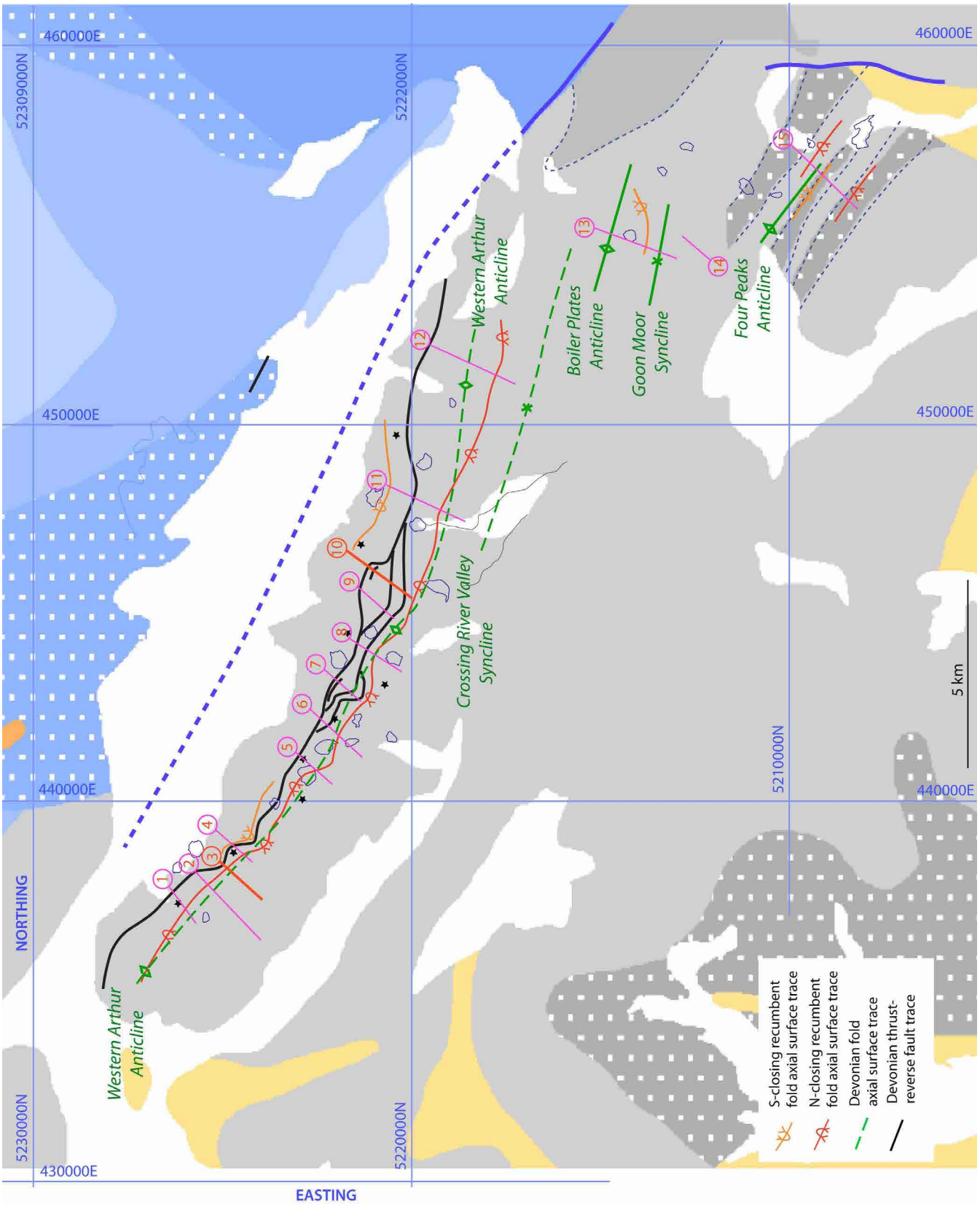

Figure 5. Section line location map used to construct the structural architecture of the Arthur Range. Map base is from the Mineral Resources Tasmania 1:250000 Digital Geological Atlas. Pink section lines are Photo profiles, that is photos with structural form-line interpretation. Thick red are constructed traverse topographic profiles. These are linked to specific figures throughout the text. See Figure 4 for map lithological lines.

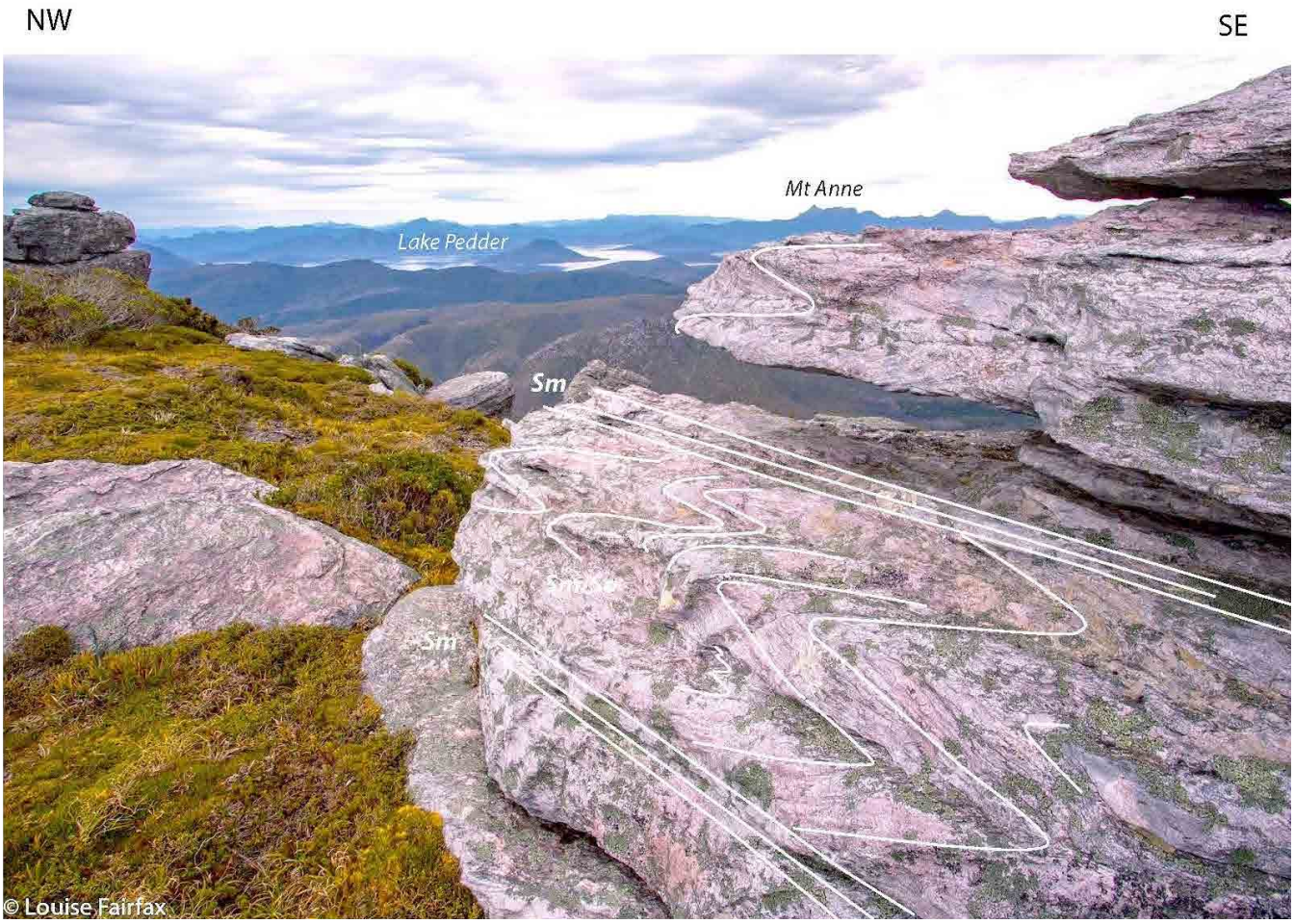

Figure 6. Pink quartzite on ridgeline at the head of Alpha moraine showing bands of transposition Sm bounding chevron-folded zones in Sm/So. Initial inspection showed alternating zones of "cross-bedding-like" features but closer inspection shows the hinge zones that can be traced along the inferred axial surface traces. Fold axial surfaces are at low angles to the transposition Sm. (photo credit: Louise Fairfax)

Figure 7. Thicker bedded quartzite with cross-bedding. Truncated top sets indicate right way up. Outcrop on ridge east of Lake Cygnus (see outcrop photo 3, Figure 44a).

Figure 8. Typical chevron folded thin-bedded quartzite of the Western Arthur range at Mt Hesperus (photo credit David Noble). View is to the southeast.

Figure 9. More pelitic sequence at Federation Peak ridgeline showing thin banding of intercalated black carbonaceous, mica-quartz phyllite and rare thin quartzite bands.

Figure 10. Recumbent tight to isoclinal chevron folds in thin-bedded quartzite north of Lake Ceres. Hinge parallel view to the northwest with helicopter for scale (photo credit: Jason Bradbury). So/Sm (white lines) define the chevron folds with steeply northeast-dipping So/Sm enveloping surfaces (So/Sm env) essentially subparallel to the edge of the cliff-face (dip photo right). Fold axial surfaces (AS) are gently southwest-dipping (to photo left).

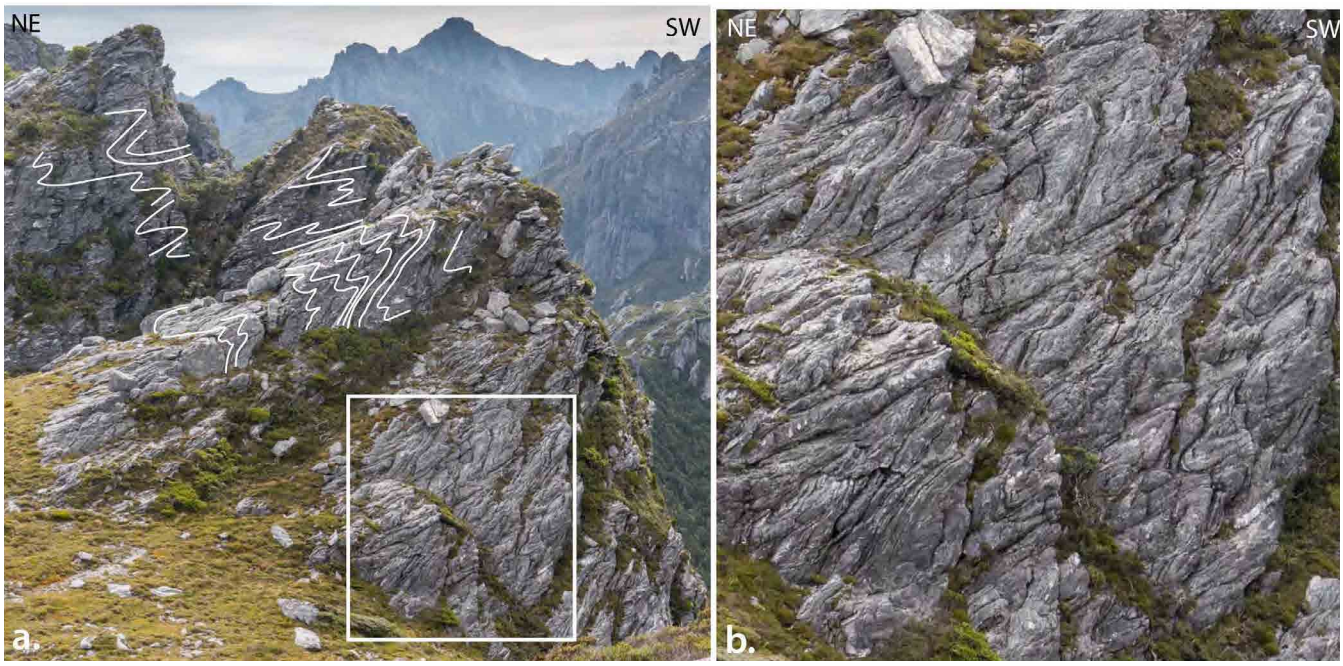

Figure 11. Chevron-folded thin-bedded quartzite in cliff, High Moor (photo credit: David Noble).

2.2.2 Transposition Layering

In the eastern flank of the Western Arthur range zones of transposition layering (Figure 12) separate or bound the chevron-folded zones made up of asymmetric folds with an axial surface cleavage. This is observed at all scales. The transposition layering commonly has centimetre-spacing and is an intense foliation where the earlier So/Sm foliation is folded and acutely intersected by the younger transposition foliation.

2.2.3 Shear Bands

Shear bands (or S-C' structures) occur within the dominant foliation (Sm) in more pelitic sequences intercalated with the the quartzites (Figure 13). Two sets of shear bands can occur as synthetic or antithetic sets. These have been used to determine transport directions for the Arthur Range and this part of the Southern Tyennan domain (see Section 6).

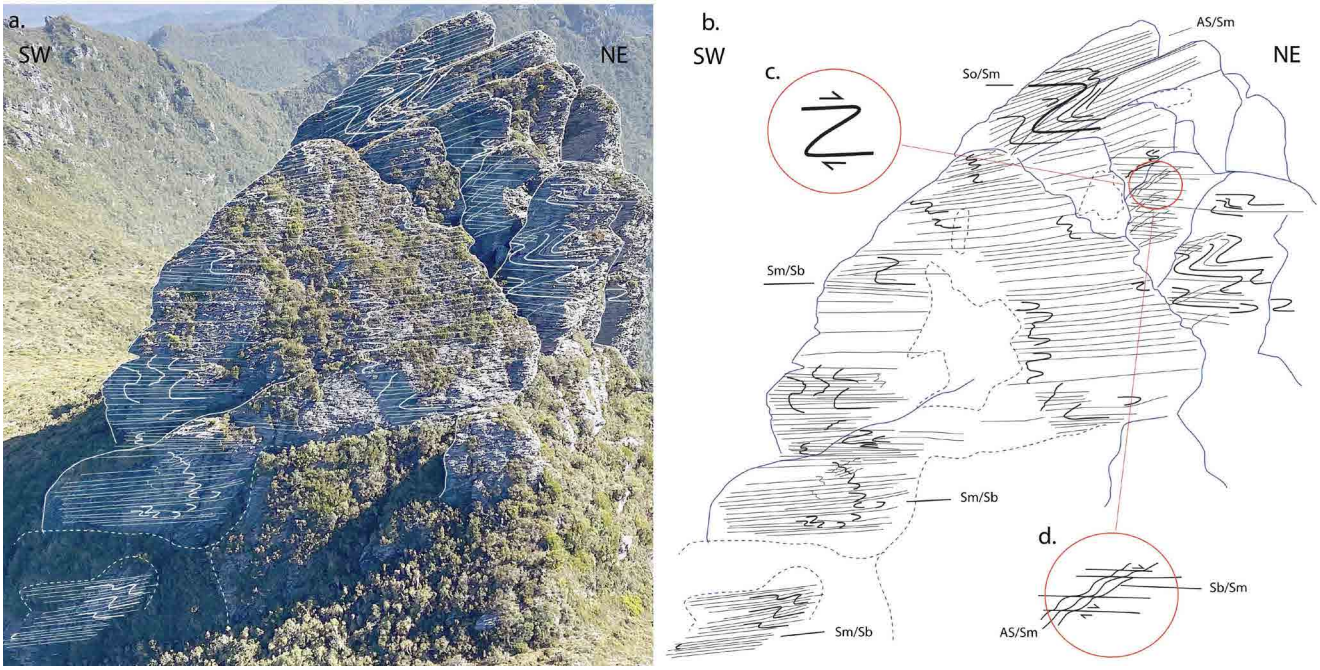

Figure 12. The ridge north of Haven Lake (a and b) showing asymmetric chevron folds in foliation So/Sm, an axial surface foliation to the chevron folds (AS/Sm) both folded by an intense subhorizontal transposition foliation Sm/Sb. Inset c) shows the general asymmetry of the meso-folds and inset d) the nature and sense of the transposition layering (Sm/Sb). Sb: shear band

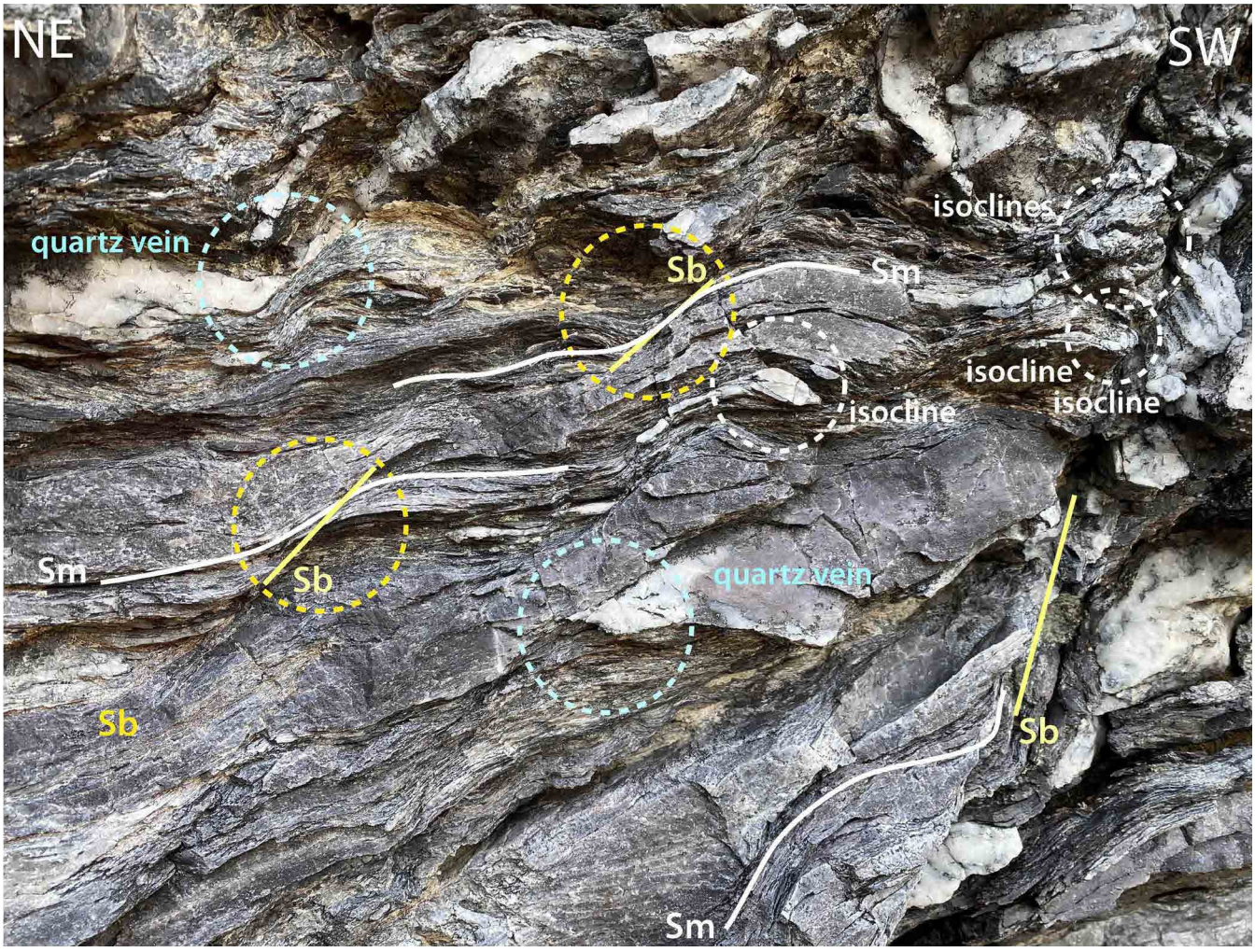

Figure 13. Shear bands (Sb) in the dominant foliation Sm in more pelitic sequence along the Federation Peak ridgeline. Relict isoclines (highlighted by white dashed circles) occur within this foliation, along with Sm-parallel boudinaged quartz veins (highlighted by light blue dashed circles), and shear bands Sb (highlighted by the yellow dashed circles). Shear bands show northeast-over-southwest (northeast down) shear sense.

3.0 WESTERN ARTHUR RANGE

The major structural elements shown in Figure 14 are:

1. A major Devonian thrust-reverse fault system along the north flank of the range.
2. A northwest-trending, open, upright Devonian anticline that extends the length of the range and sits in the reverse fault-system hanging wall.
3. A northeast-closing recumbent, isoclinal macro-fold that extends the length of the range and also sits in the reverse fault-system hanging wall.
4. A southwest-closing recumbent, isoclinal fold that sits in the reverse fault-system footwall.
5. The Devonian and Cambrian hinge zones show slight obliquity.
6. Both the Cambrian and Devonian folds have a northwest plunge.
7. Cross faults, commonly north-south trending, offset the major Devonian anticlinal hinge and the major northeast-closing recumbent macro-fold hinge.
8. A sub-vertical, northwest-trending Devonian cleavage. This has an orientation consistent with the axial surface attitude of the anticline and overprints the early-formed So/Sm, Sm and Sb fabrics.

3.1 Structure of the Western Arthur Range

The regional scale structure of the Western Arthur Range (Figure 14) is based on structural relationships from the section and profile lines shown in Figure 15. These include Mt Hesperus (profile1), the Capella Crags and ridgelines bounding Lake Cygnus (profile 2 and Section 3), Haven Lake-Mt Scorpio (Section 10) as well as a number of photo profiles including Mt Hayes (profile 4), Lake Oberon (profile 5), Mt Capricorn (profile 6), Dorado Peak (profile 7), Mt Columba-The Dragon-Dorado Peak (profile 8), Mt Taurus (profile 9), The Phoenix (profile 11) and Crags of Andromeda (profile 12).

3.1.1 Macro-Scale Recumbent Folds

Oppositely closing and facing recumbent isoclinal macro-folds are truncated and offset by a Devonian, southwest-dipping thrust-reverse fault system (Figures 14 and 16). These relationships can be observed at two places along the northeast slopes of the Western Arthur Range, at Mt Hayes (Figures 17) and Dorado Peak (Figure 18). The same relationships (Figure 16c) can also be inferred from structural data collected along the Haven Lake - Mt Scorpio traverse (see Section 3.2.4).

The northeast-closing recumbent macro-fold along with the younger Devonian Western Arthur Anticline can be variably seen in almost all the hillside-mountain-peak profiles shown in Figures 19, 20, 21 22, and 23. Both folds occupy the spine of the Western Arthur Range (see Figure 19) and extend the length of the range (Figure 14). The form and geometry of the northeast-closing fold can also be seen in the photo profiles shown in Figures 19, 20, 21 22, and 23. The serial profiles in Figures 21 and 23 show changes in the recumbent fold axial surface dip and dip-direction due to refolding by the Western Arthur Anticline. The recumbent fold axial surface on the northeast limb of the Anticline dip to the northeast, whereas in the Anticline hinge it is sub-horizontal and on the southwest limb dips to the southwest (see Figures 23, 24 and 25).

The southwest-closing recumbent fold hinge is preserved in erosional remnants along the northeast flank of the Western Arthur Range. The geometry and form of this fold can be seen in Figures 17 and 18.

Refolded recumbent isoclinal folds are also visible at Mt Pegasus (Figure 24) and Mt Capricorn (Figure 25). At Mt Capricorn, the orthogonal relationship between the axial surfaces and the So/Sm enveloping surfaces (Figure 24b and 24c) indicates this outcrop is in a hinge zone position of the recumbent macro-fold.

3.1.2 The Western Arthur Anticline

Photographs of the Western Arthur Range topography highlight the broad scale Devonian Western Arthurs Anticline depicted by broad arching of the generalised Sm foliation (see Figures 26, 27 and 28).

Throughout parts of the range the hingeline of the Anticline is difficult to locate (see dashed axial surface trace in Figure 14) due to the refolding of the older recumbent macro-folds (Figures 27 and 28), as well as the truncation and offset by both the reverse fault system and the north-trending oblique slip faults (see Section 3.2). The hingeline was determined in several instances by utilising the dip direction of the northeast-closing recumbent fold axial surface (equivalent to the foliation Sm attitude); for example see orange dashed traces in profiles shown in Figure 23.

At the eastern end of the range, the Crags of Andromeda ridgeline (Figure 29a) shows a broadened hinge zone for the Western Arthurs Anticline with gentle undulating folds in So/Sm defining most of the ridge crest from West Portal (Figure 29b) to the central part of the ridge (Figure 29c). The approximately upright nature of the folding (Figures 29c and 30), the flat enveloping surface to the broadly warped layering and the pronounced lack of cleavage (Figure 30) all suggest continuation of the Western Arthur Anticline through the Crags of Andromeda. The broad hinge form, the open nature of the folding in the hinge and the lack of cleavage suggest lower strain/shortening at shallow crustal levels and potential die-out of the anticline into the Pass Creek-Hopetoun Creek watershed area (i.e. fold amplitude is decreasing to zero to the east of the Crags of Andromeda).

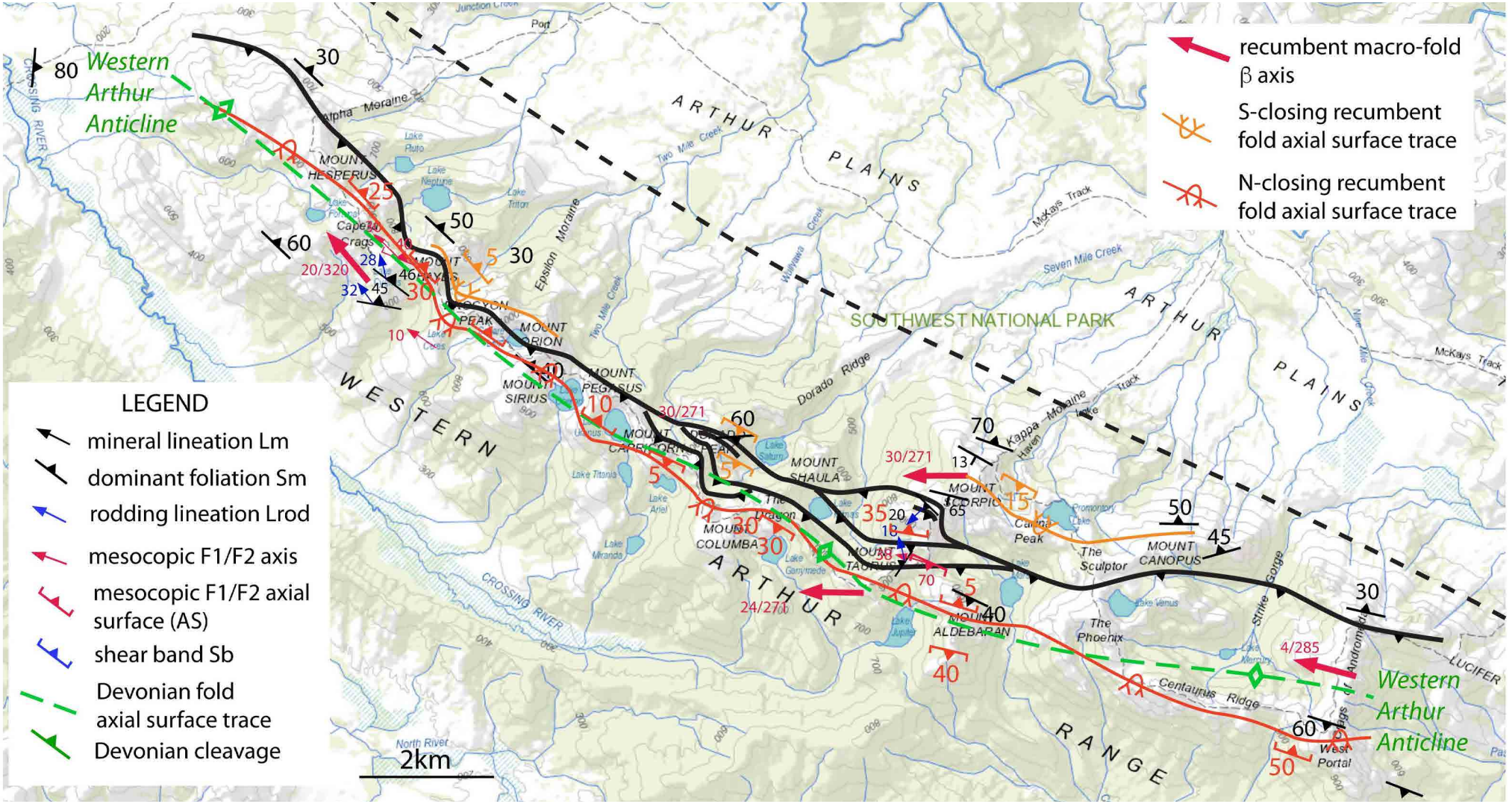

Figure 14. Structure map of the Western Arthur Range with topographic LISTmap base. The map shows reverse fault traces (heavy black lines), the recumbent isoclinal macro-fold axial surface traces (red trace: northeast-closing recumbent fold; orange trace: the southwest-closing recumbent fold), and the Western Arthur Anticline axial surface trace (green dashed line). Attitudes of the axial surfaces of the recumbent folds are shown by the red and orange barbed dip symbols.

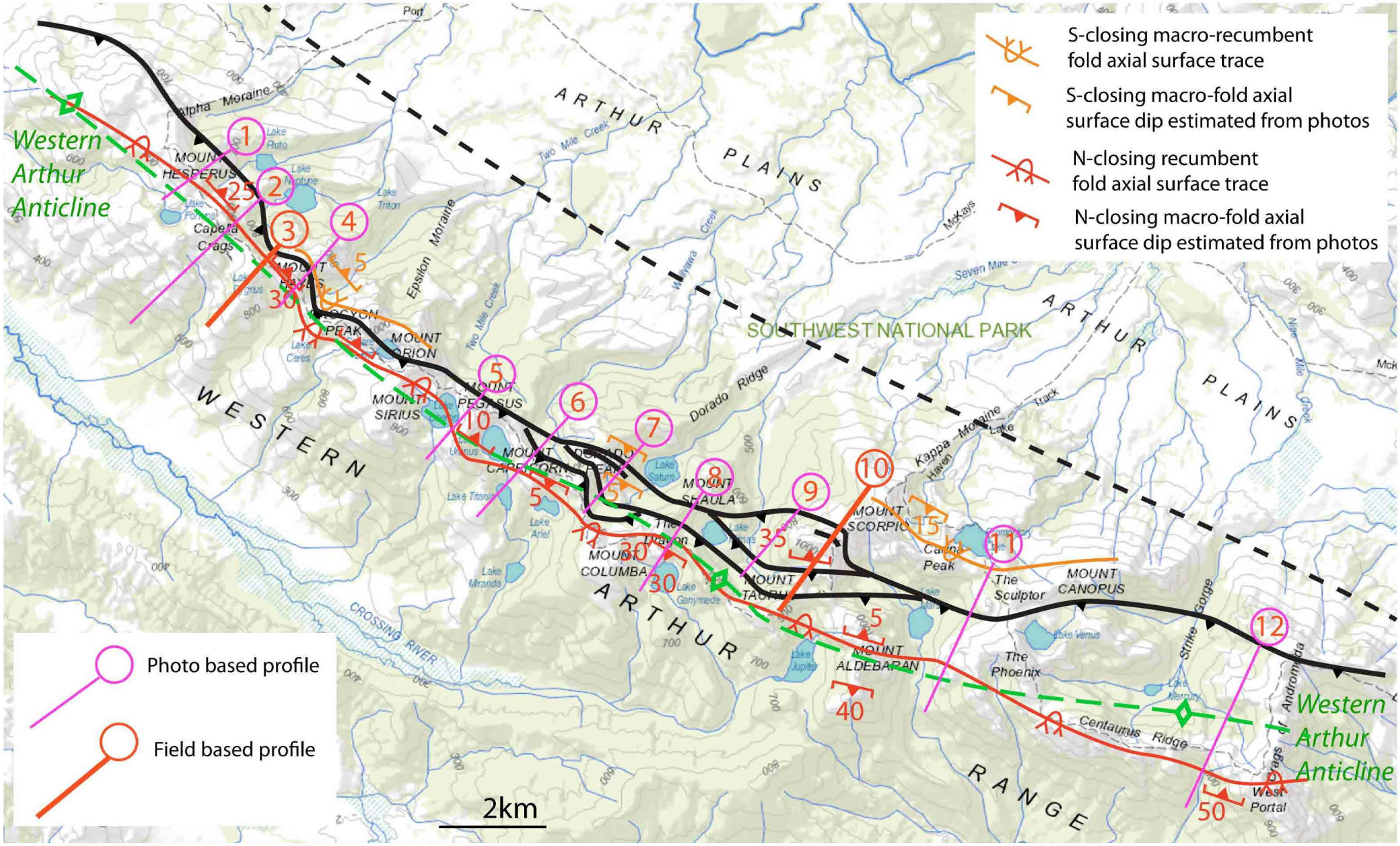

Figure 15. Simplified structural map of the Western Arthur Range with ListMap topographic map base. The map shows the positions of the field based section lines (thick red section lines) and photo profiles (pink section lines) used to establish the Western Arthur Range large-scale structure and structural geometry.

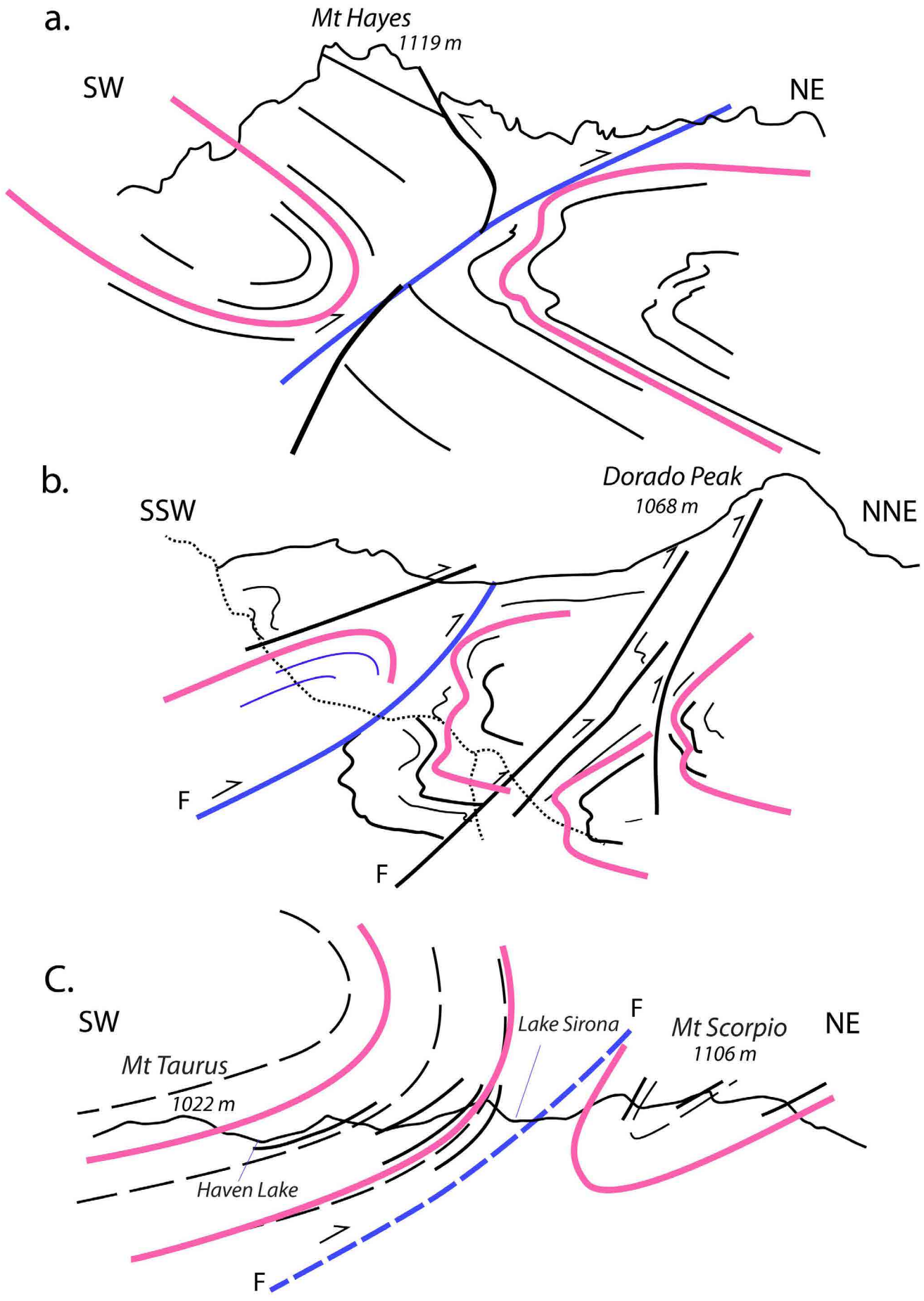

Figure 16. Structural profiles along the northeast margin of the Western Arthur Range showing the northeast-closing recumbent isoclinal fold in fault-juxtaposition with a major southwest-closing recumbent isoclinal fold in the footwall. Heavy pink lines highlight recumbent fold closures in bedding foliation So/Sm. Heavy blue lines highlight the major thrust fault that separates the northeast- and southwest closing recumbent fold hinges. Thin black lines are bedding foliation (So/Sm) traces and heavy black lines are faults (F).

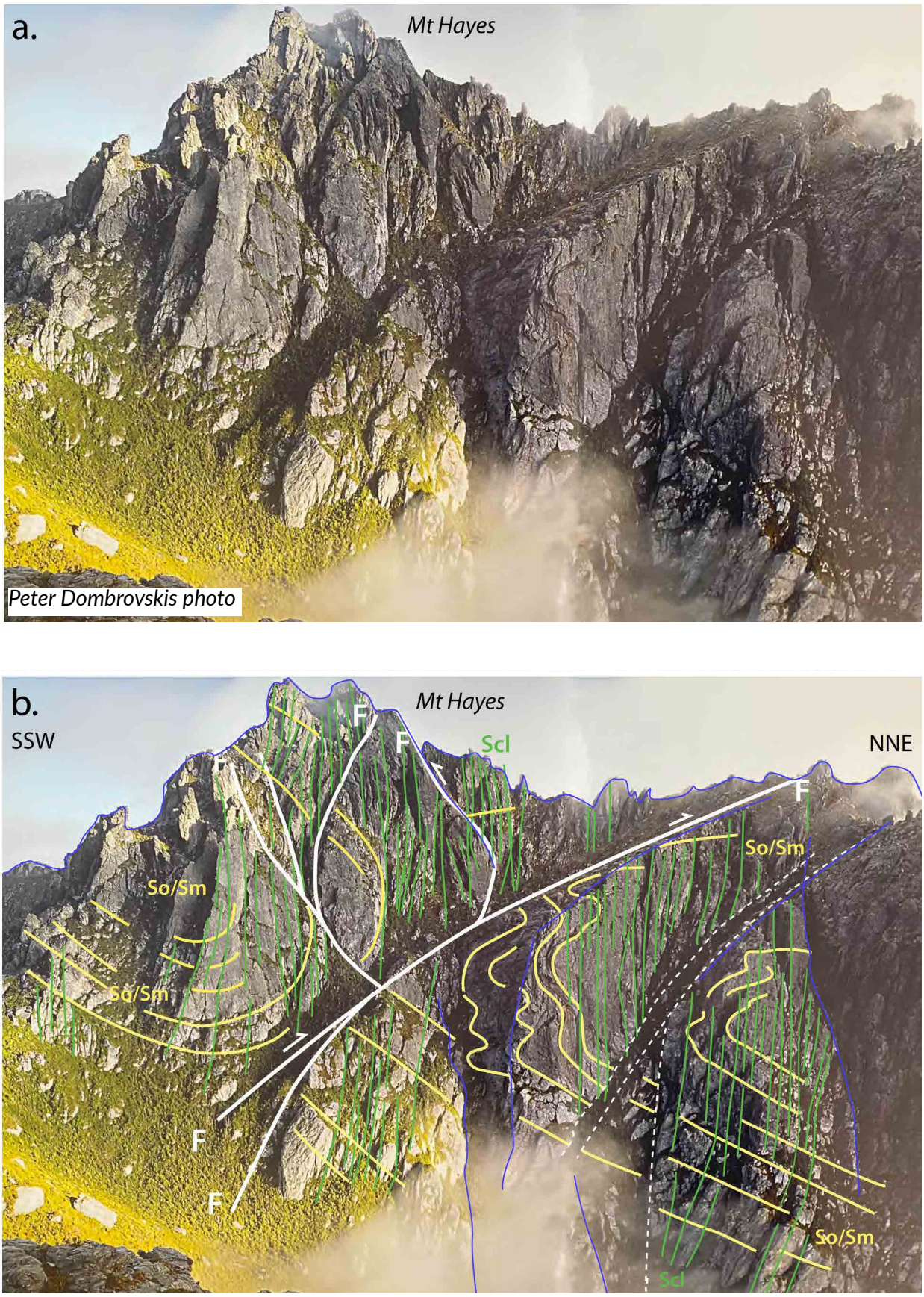

Figure 17. Structural profile across Mt Hayes (1119m). View is to the west. a) Peter Dombrovskis photo in Brown (2017, p.13) [Peter Dombrovskis, National Library of Australia, nla.cat-vn4937364]. b) Annotated photo with formline interpretation showing the oppositely facing and closing macro-fold hinges cut by a major thrust fault. The position of the photo profile in (b) corresponds to Profile 4 in Figure 15. Note the Devonian cleavage (Scl) is enhanced in the more pelitic layers and can be used to define the layering and the So/Sm foliation formlines.

Yellow lines: bedding -parallel foliation So/Sm traces. White lines: major fault traces. Thin green lines: sub-vertical Devonian cleavage traces (Scl) that are axial surface cleavage to Western Arthur Anticline). Blue lines are the topographic surface.

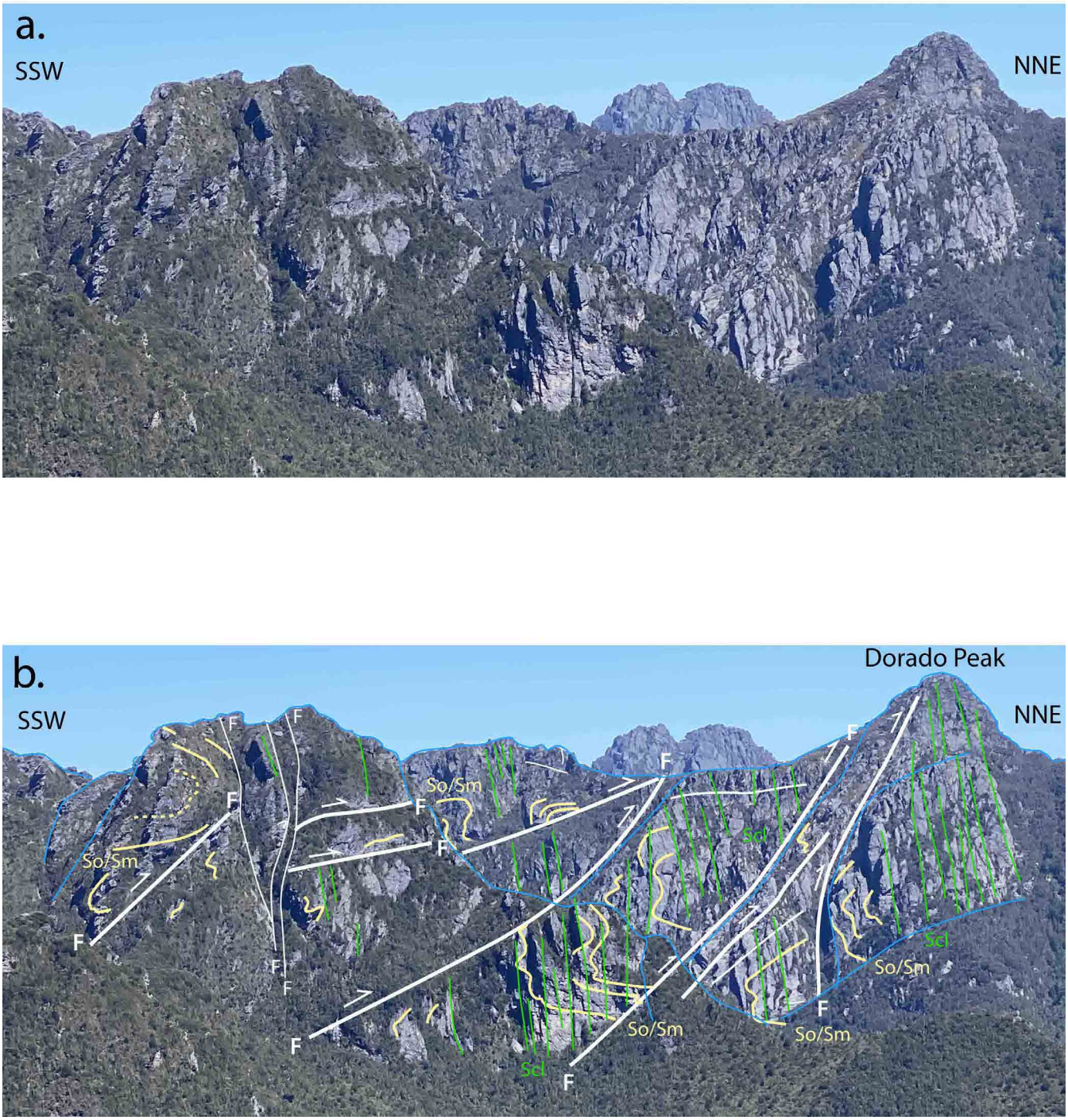

Figure 18. Dorado Peak (1068m) ridgeline profile with part of Beggary Bump in left foreground (ridgeline highlighted by the blue line trace). A series of flat thrusts and steeper reverse faults truncate and offset a major southwest-closing recumbent fold (right side of photo). The northeast-closing recumbent fold is faulted within the Beggary Bump ridgeline and is truncated by both flat thrust-faults and a steep fault set. View is to the northwest from the ridgeline above Haven Lake, looking towards Dorado Peak. The position of the photo profile in (b) corresponds to Profile 7 in Figure 15.

Yellow lines: bedding -parallel foliation So/Sm traces. White lines: major fault traces. Thin green lines: sub-vertical Devonian cleavage traces (Scl) that are axial surface cleavage to Western Arthur Anticline). Blue lines are the topographic surface.

a.

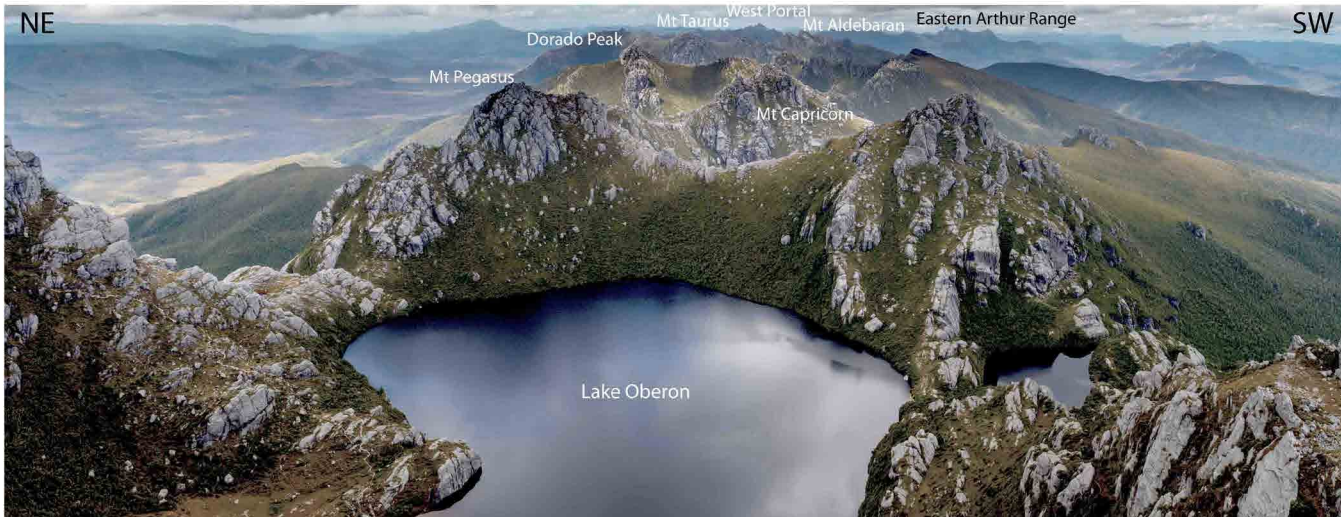

b.

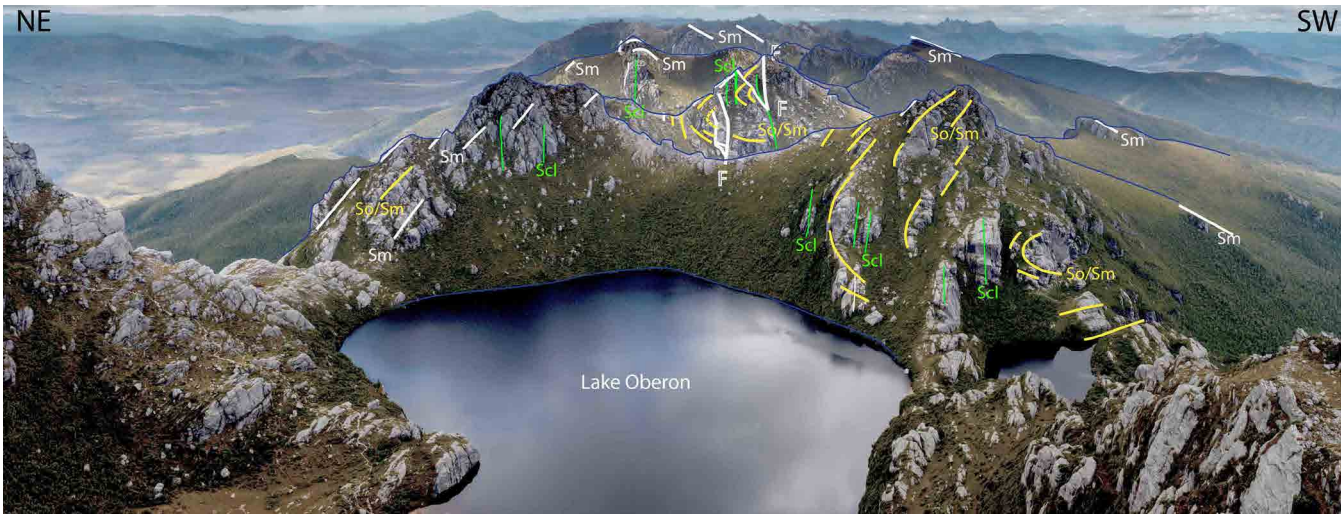

Figure 19. a) View from Mt Sirius at 1151m of the ragged and jagged peaks of the Western Arthur Range sculptured by glacial action with numerous glacial cirque lakes (photo credit: David Noble). b) Form-line interpretion of the image showing a northeast-closing recumbent macro-fold hinge in So/Sm (yellow lines) exposed in the southeast corner of Lake Oberon. This recumbent macro-fold is re-folded by the broad arch of the Western Arthurs Anticline along the spine of the Range. Dip slopes in the Sm foliation (white lines) dip away from the ridge crest along both flanks of the range. This younger Devonian anticline has a strong to intense sub-vertical, axial surface cleavage Scl (fine green lines). The recumbent fold hinge continues to Mt Capricorn (next ridgeline) and beyond. The position of the photo profile in (b) corresponds to Profile 5 in Figure 15.

Yellow lines: bedding -parallel foliation So/Sm traces. heavy white lines: foliation Sm. Fine white lines: major fault traces. Thin green lines: sub-vertical Devonian cleavage traces (Scl) that are axial surface cleavage to Western Arthur Anticline). Blue lines are the topographic surface.

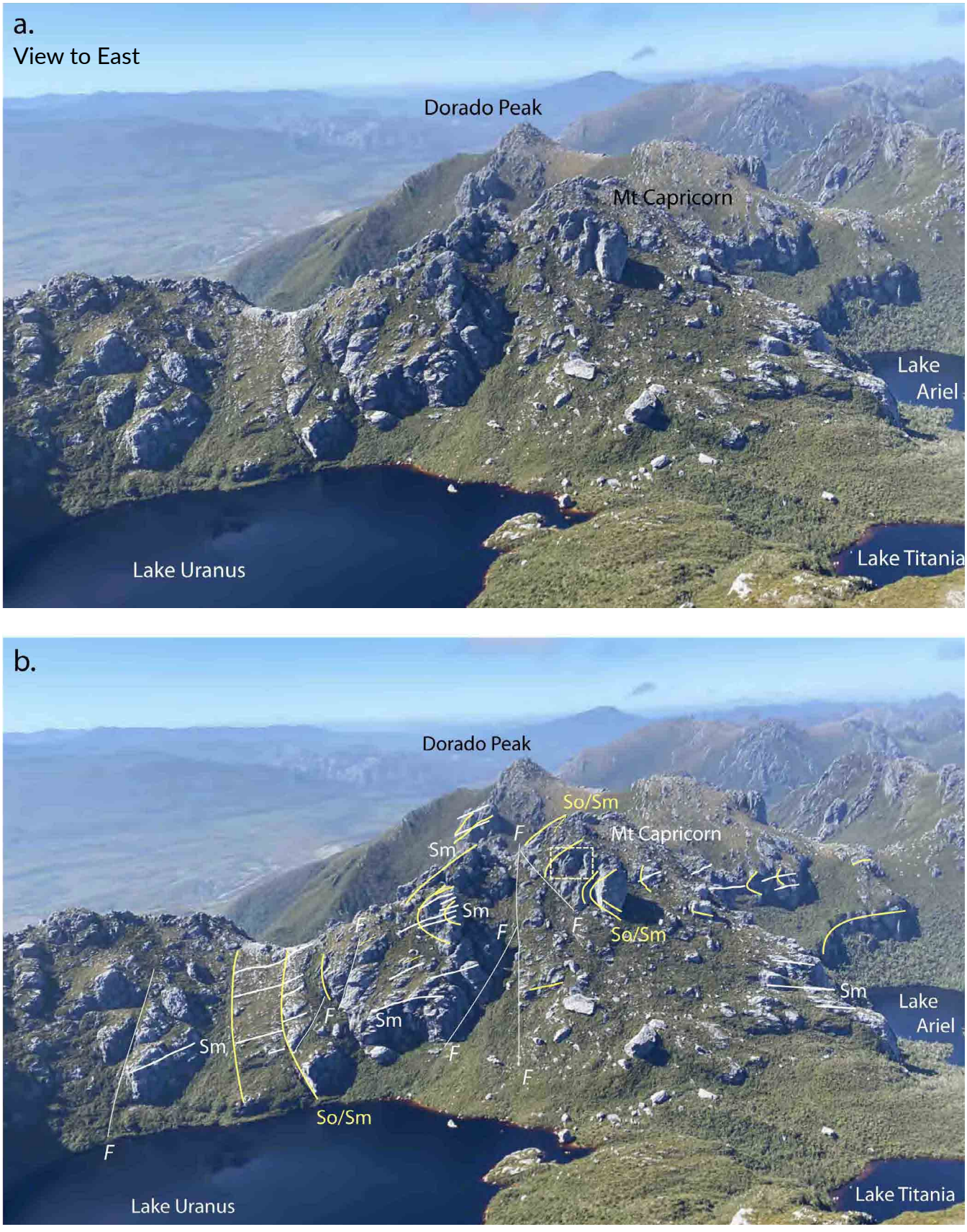

Figure 20. View, from near Mt. Pegasus, of Lake Uranus cirque wall and Mt Capricorn showing northeast-closing recumbent hinge below Mt Capricorn (1037m). Steep faults offset the hinge. Dorado Peak (1068m) ridgeline is in the middle ground. The position of the photo profile in b) corresponds to Profile 6 in Figure 15. The box outlined below Mt Capricorn is the photo in Figure 25 below.

Yellow lines: bedding -parallel foliation So/Sm traces. Heavy white lines: foliation Sm. Fine white lines: major fault traces. Thin green lines: sub-vertical Devonian cleavage traces (Scl) that are axial surface cleavage to Western Arthur Anticline).

Note the change in axial surface dip, towards the northeast (left side of photo) and sub-horizontal (right side of photo). The hinge of the Western Arthur Anticline passes between Mt Capricorn and Lake Ariel (i.e. where the recumbent macro-fold axial surface and the associated foliation Sm is sub-horizontal).

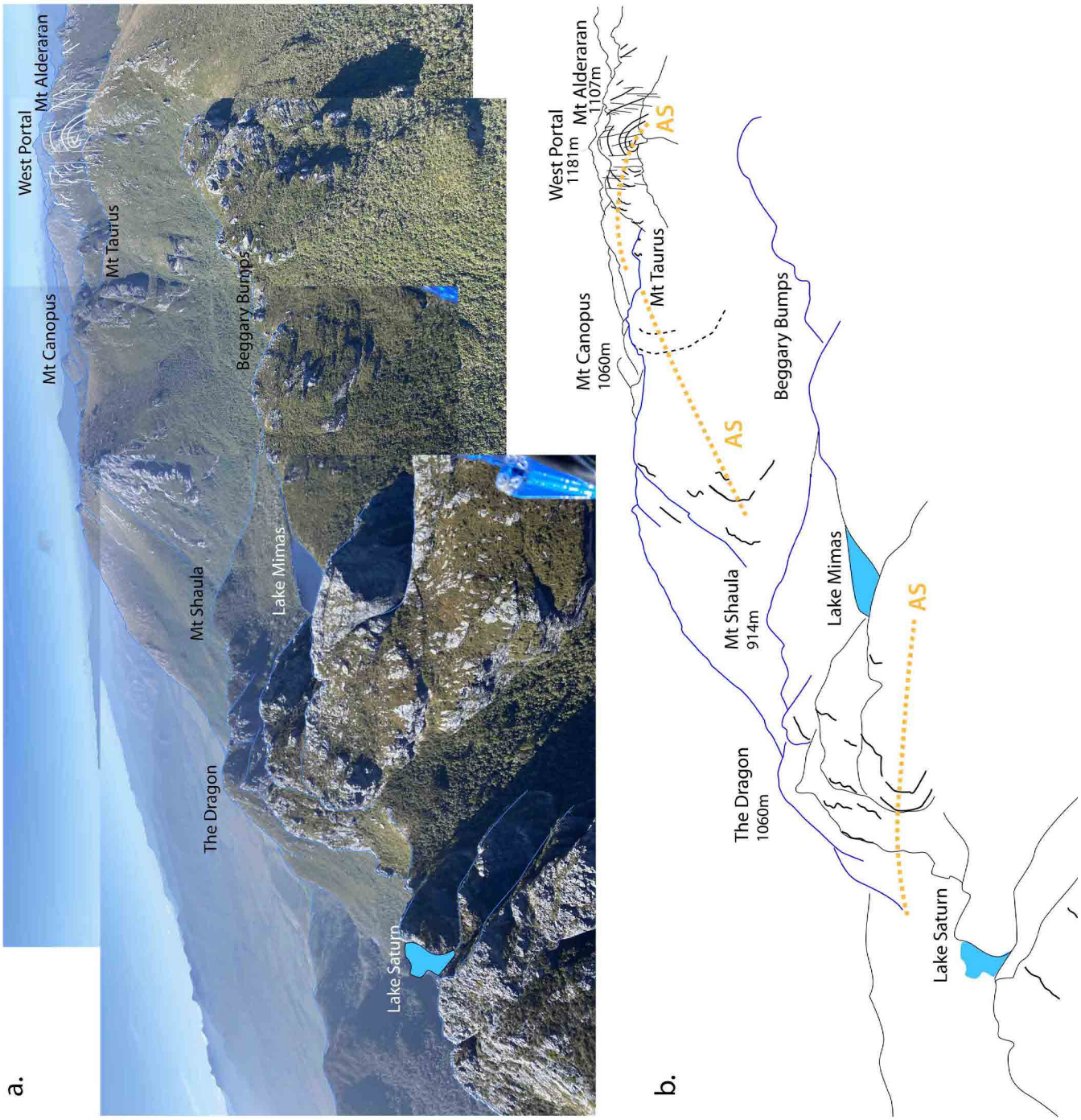

Figure 21. Composite photo-profile in a) with form-line interpretation in b). The composite profile encompasses serial ridgelines from Lake Saturn and the Beggary Bumps, Dorado Peak and Mt. Shaula, and Mt. Taurus and Mt. Aldebaran (see Figure 23d). It essentially consists of stacked profiles 7 through 10 in Figure 15. The composite profile in (b) shows a projection of the northeast-closing recumbent macro-fold hinge through these ridgelines with the axial surface (AS: shown by the orange dashed lines) generally northeast-dipping on the northeast limb of the Western Arthur Anticline.

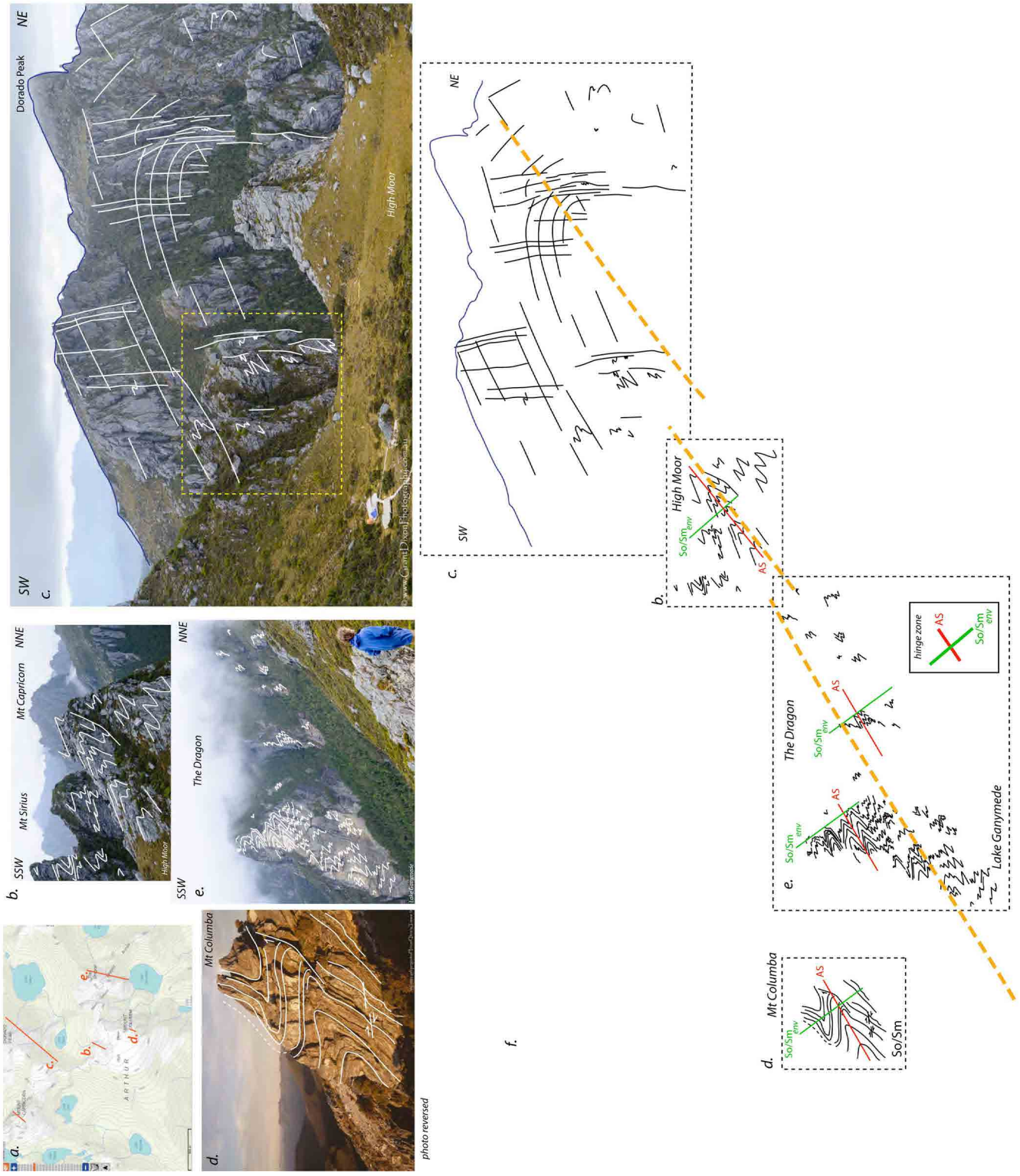

Figure 22. Composite fold-nappe profile through Mt Columba (1042m)-The Dragon (1006m)-Dorado Peak (1068m). This is profile 8 in Figure 15. The profile view is to the NW. (All photos by Grant Dixon). The axial surface (AS) of the northeast-closing recumbent macro-fold is shown by the orange dashed line. This aligns with points in the closures exposed in the hillsides where the AS (red line segment) is at high angles to the So/Sm enveloping surface (green line segment). The position of the photo profile in a) corresponds to Profile 8 in Figure 15. The view from High Moor towards Dorado Peak (c) gives an oblique view of the Dorado Peak structure. Compare with Dorado Peak ridgeline view in Figure 18.

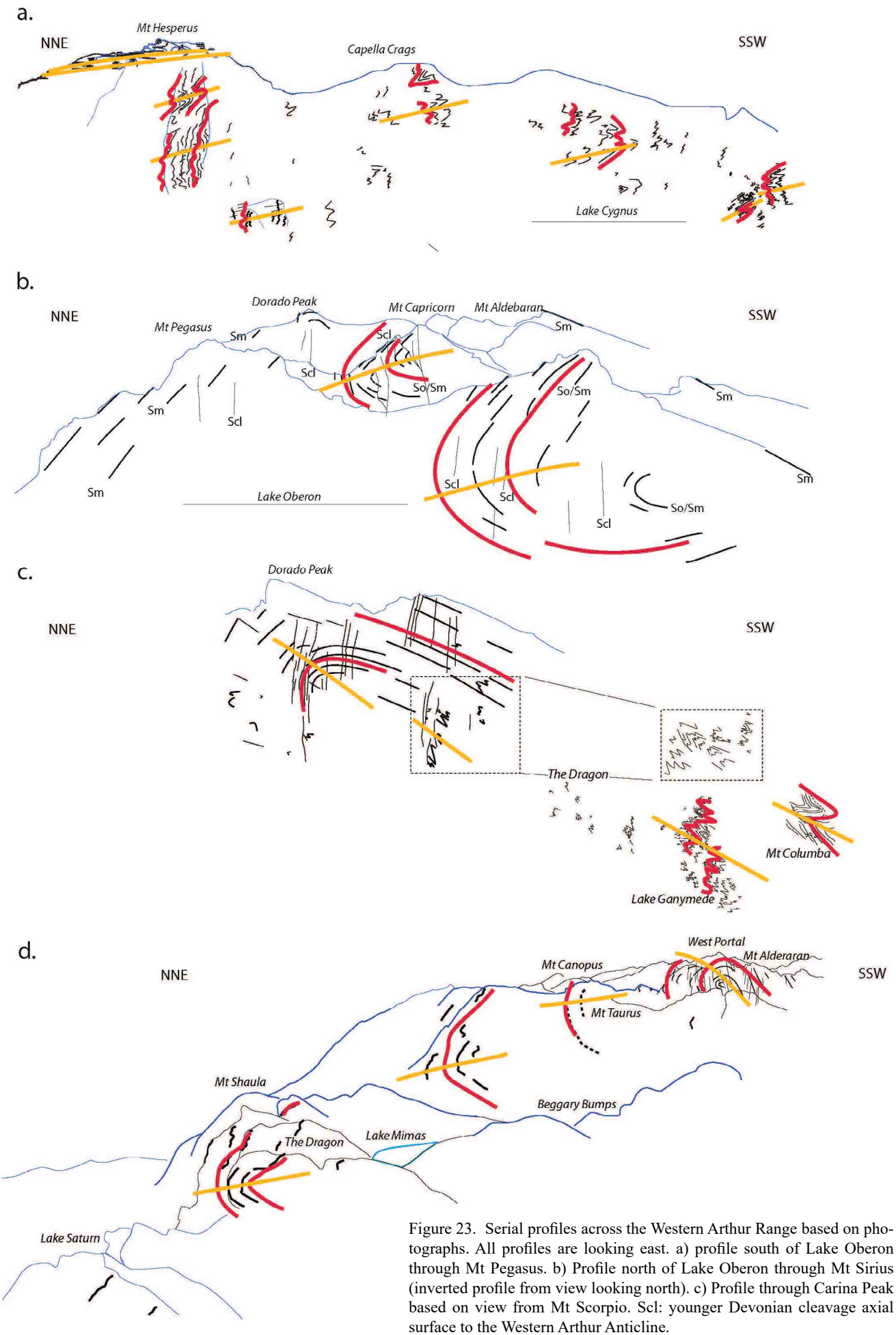

Figure 23. Serial profiles across the Western Arthur Range based on photographs. All profiles are looking east. a) profile south of Lake Oberon through Mt Pegasus. b) Profile north of Lake Oberon through Mt Sirius (inverted profile from view looking north). c) Profile through Carina Peak based on view from Mt Scorpio. Scl: younger Devonian cleavage axial surface to the Western Arthur Anticline.

Pink traces: So/Sm. Orange lines: axial surface traces (Sm foliation).

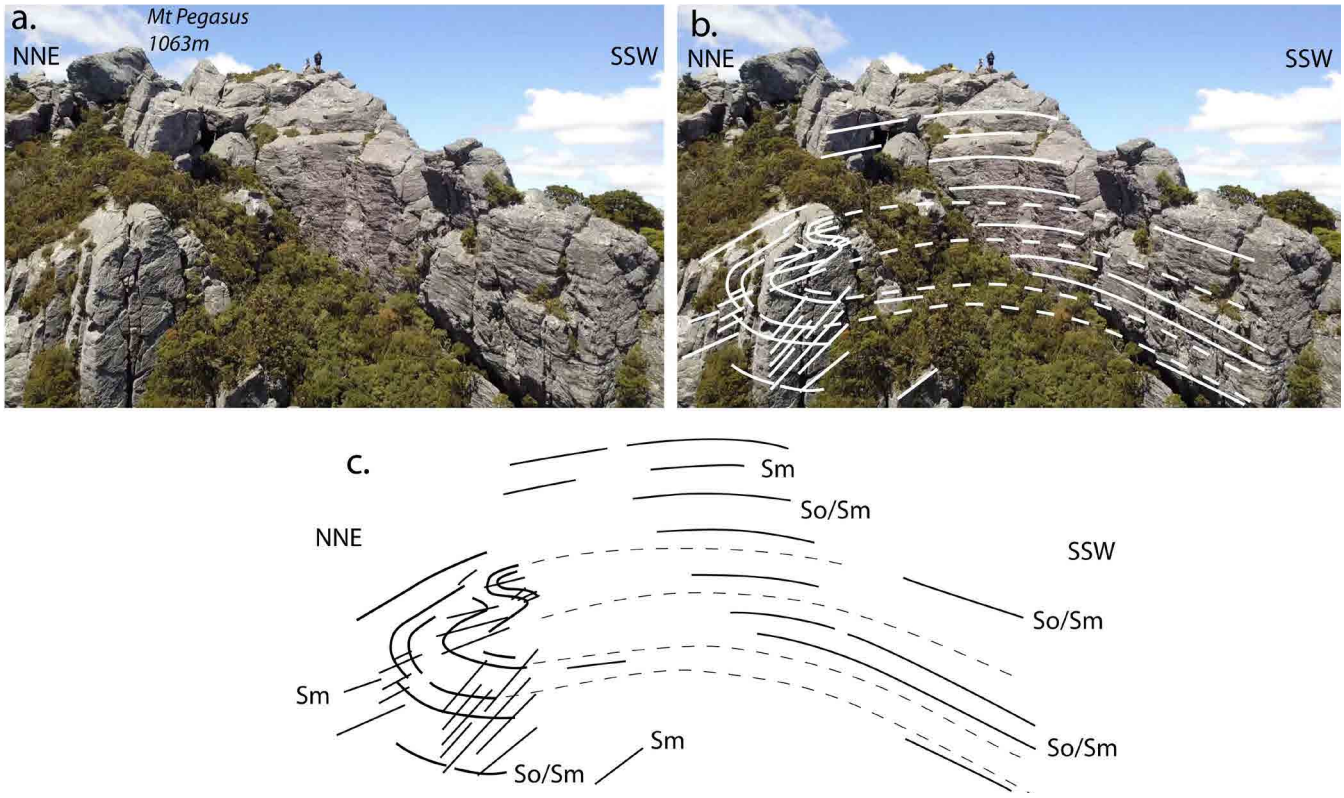

Figure 24. Upright refolding of a small, northeast-closing recumbent isocline on Mt Pegasus (1063m). (unpublished bushwalker drone photo: source unknown). Main anticlinal hinge of Western Arthur Anticline occurs in centre of photo.

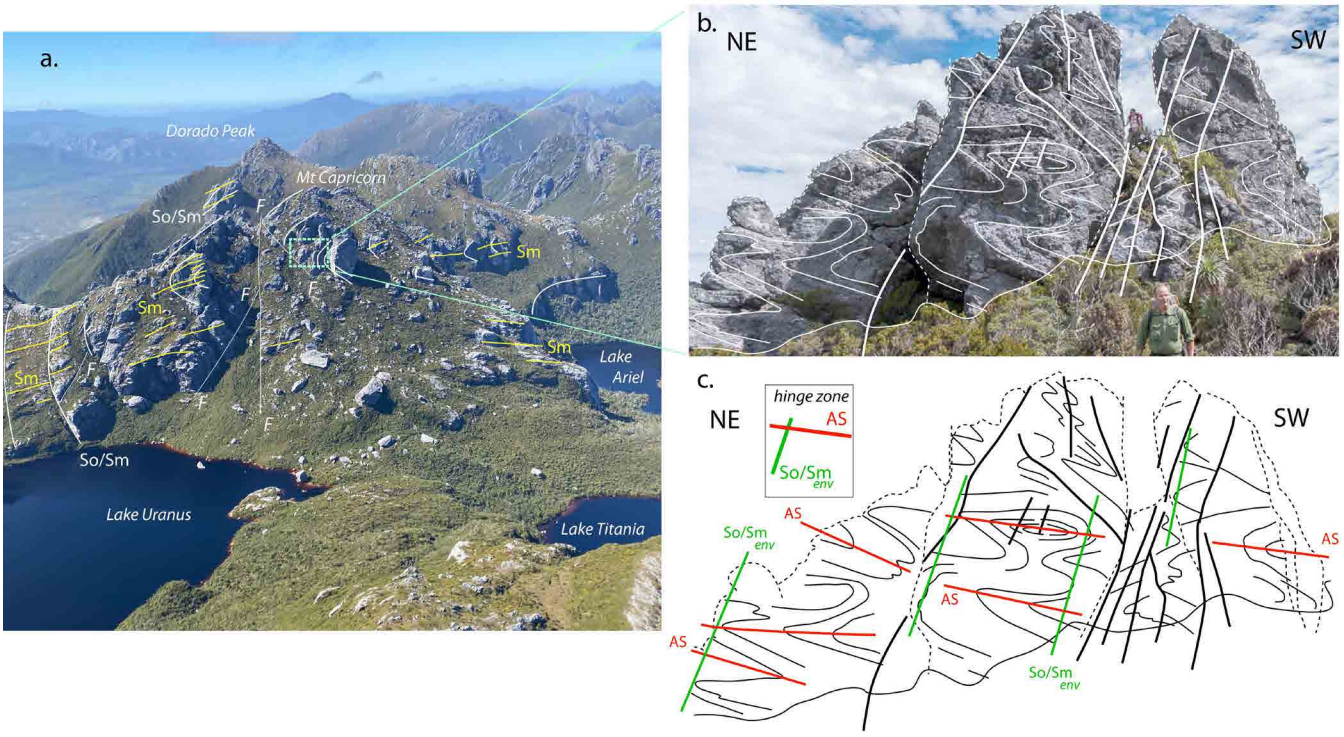

Figure 25. Structure of Mt Capricorn (1037m). a) The northeast-closing recumbent isoclinal macro-fold at Mt Capricorn with rectangle showing position of photo in (b). b) Summit structural relationships at Mt Capricorn (photo credit: David Noble). c) Formline interpretation of (b) showing foliation So/Sm traces (thin black lines), axial surface traces of small-scale recumbent folds (red line traces), enveloping surface of the So/Sm foliation (green line traces). Heavy black lines are fault traces.

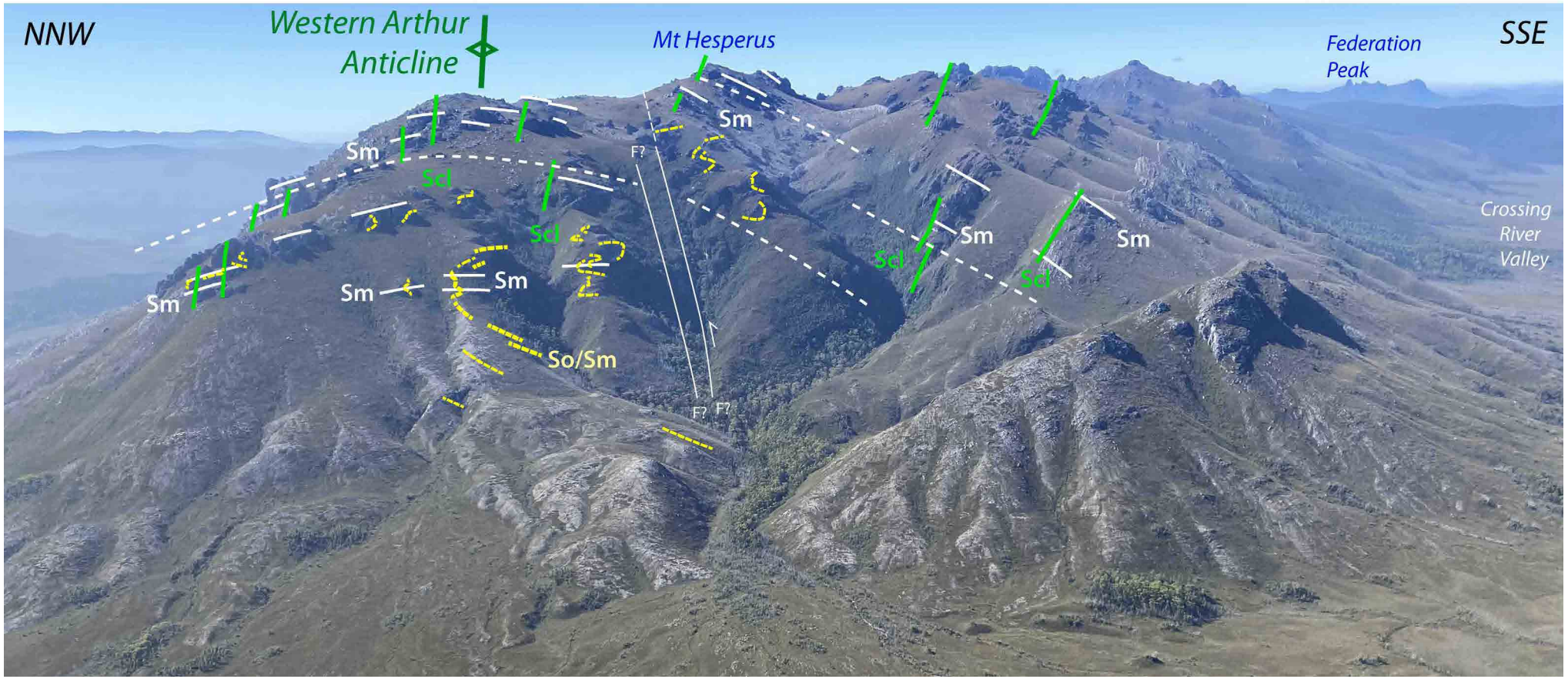

Figure 26. Oblique aerial helicopter view of the north end of the Western Arthur Range with Mt Hesperus (1098m) in photo-centre and Federation Peak (1225m) visible in the background ridgeline (far right). The Crossing River valley floor on photo-right is at ~200m elevation. The photo shows a broad arching within the dominant foliation Sm (white traces) to define the younger Devonian Western Arthur Anticline that occupies the spine of the range. A slightly fanning to the steeply dipping axial surface cleavage (Scl: green traces) can be seen overprinting the early-formed, northeast-closing, recumbent macro-fold (photo middle left). The recumbent macro-fold closure is suggested by interpreted form-lines in the dominant layering So/Sm (yellow dashed lines). Note this is based on digital photo interpretation and needs field checking.

Figure 27. Refolded northeast-closing recumbent fold exposed in the Mt Aldebaran (1107m) ridgeline (background) with Mt Taurus (1020m) ridgeline in foreground. The position of the photo profile in (b) corresponds to Profile 9 in Figure 15.

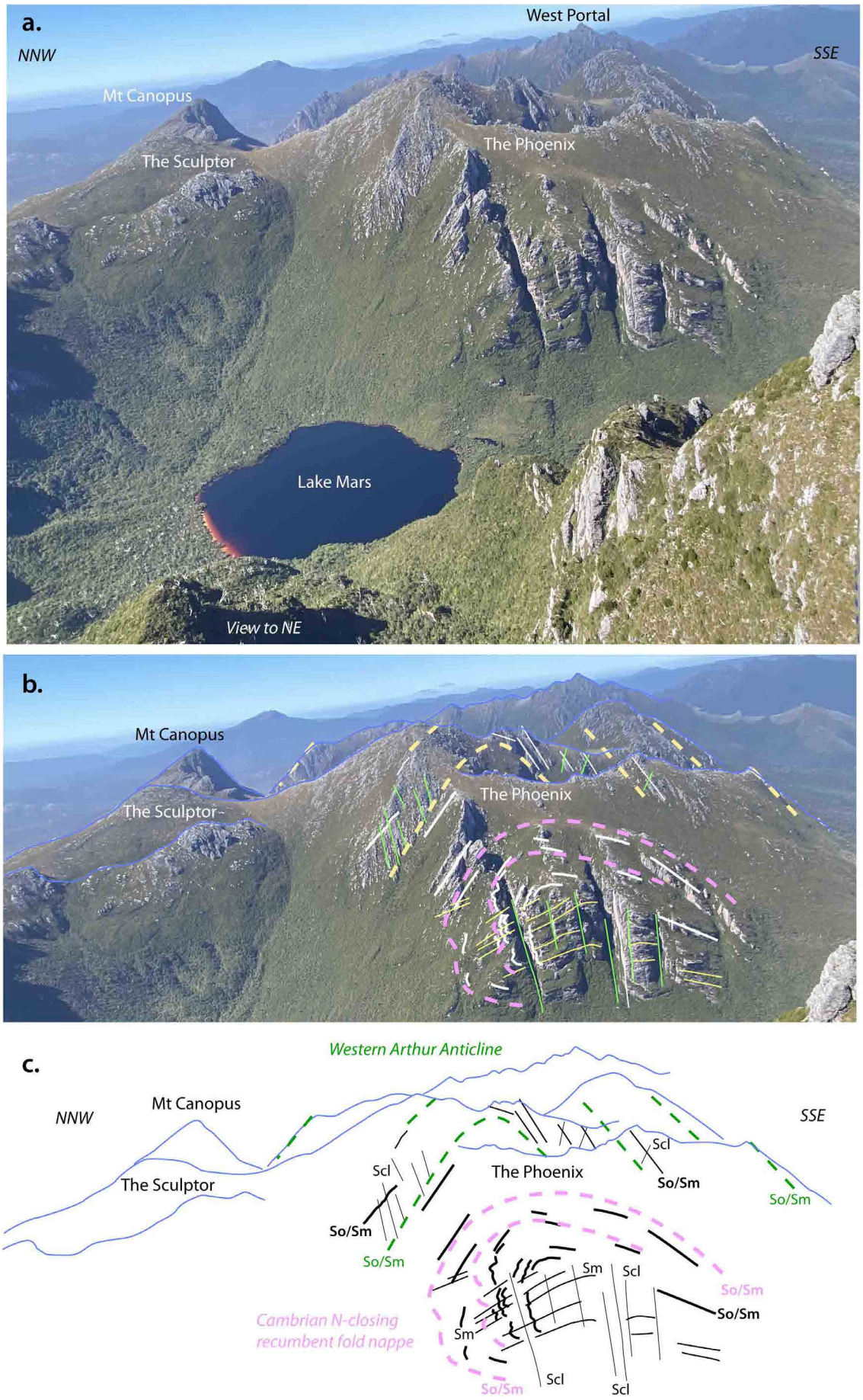

Figure 28. a) and b) Photos of The Sculptor-Mt Phoenix ridgeline with Lake Mars in the foreground. This corresponds to Profile 11 in Figure 15. b) and c) show the structural profile with formline interpretation traces in the Phoenix (1091m) ridgeline. The lower part of the ridge shows the northeast-closing recumbent macro-fold. This is arched by the Western Arthur Anticline seen in the upper part of the ridge and ridges in the middle ground. So/Sm: bedding parallel foliation (pink and green dashed line traces). Sm: foliation axial surface to the recumbent fold (heavy black lines). Scl: Devonian cleavage axial surface to the Western Arthur Anticline (thin black lines).

Throughout parts of the range the hingeline of the Anticline is difficult to locate (see dashed axial surface trace in Figure 14) due to the refolding of the older recumbent macro-folds (Figures 27 and 28), as well as the truncation and offset by both the reverse fault system and the north-trending oblique slip faults (see Section 3.2, Figure 31). The hingeline was determined in several instances by utilising the dip direction of the north-east-closing recumbent fold axial surface (equivalent to the foliation Sm attitude); for example see orange dashed traces in profiles shown in Figure 23.

At the eastern end of the range, the Crags of Andromeda ridgeline (Figure 29a) shows a broadened hinge zone for the Western Arthurs Anticline with gentle undulating folds in So/Sm defining most of the ridge crest from West Portal (Figure 29b) to the central part of the ridge (Figure 29c). The approximately upright nature of the folding (Figures 29c and 30), the flat enveloping surface to the broadly warped layering and the pronounced lack of cleavage (Figure 30) all suggest continuation of the Western Arthur Anticline through the Crags of Andromeda. The broad hinge form, the open nature of the folding in the hinge and the lack of cleavage suggest lower strain/shortening at shallow crustal levels and potential die-out of the anticline into the Pass Creek-Hopetoun Creek watershed area (i.e. fold amplitude is decreasing to zero to the east of the Crags of Andromeda).

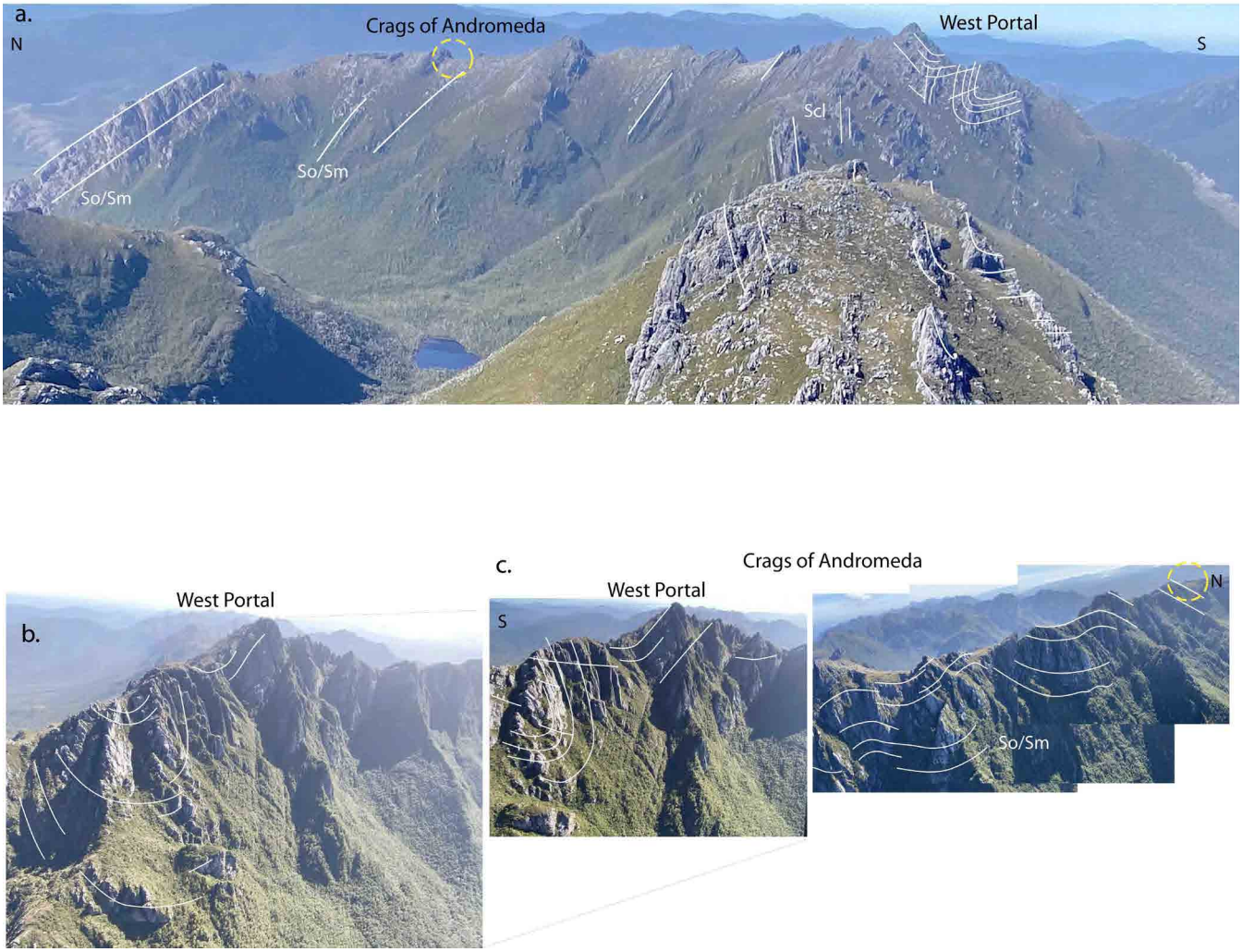

Figure 29. Crags of Andromeda photo profile. This corresponds to Profile 12 in Figure 15. a) View of ridgeline looking to the east showing part of the northeast-closing recumbent macro-fold at West Portal (1160m) and northeast-dipping foliation Sm defining the northeast flank of the range (photo left side). b) View of West Portal with plunging, northeast-closing recumbent macro-fold hinge (view looking west). c) Composite photo-collage of eastern side of the Crags of Andromeda ridge showing the gently undulating open folds in the bedding foliation So/Sm. The upright folds in Figure 30 are from the ridgeline position shown by the circle in a) and c).

Figure 30. Upright to steeply inclined chevron folds in thin-bedded, poorly cleaved quartzite-pelite sequence in the central part of the Crags of Andromeda ridgeline (all photos by Grant Dixon). The thin quartzite layers are heavily veined with all layers showing a noticeable lack of cleavage.

3.2. Western Arthur Structural Profiles

3.2.1 Mt Hesperus and the north end of the Western Arthur Range (Section 1, Figure 15)

There is an apparent double closure in formlines in the northwestern part of the range (white traces in Figure 31). The first closure is where bedding-foliation formlines appear to wrap around or close at the northwest end of the range. This relates to intersection of the gently, northwest-plunging Western Arthur Anticline with the topography at range termination (Figure 26). The northeast- facing and closing recumbent macro-fold (red line trace in Figure 31) also shows apparent termination within this broader closure (see Figures 26 and 31).

The second closure shows as a convergence in the bedding foliation formlines in the southwest flank of the range between Lake Cygnus and Mt Hayes (see white traces in Figure 31). This either relates 1) to the intersection of the northeast-closing recumbent macro-fold through Mt Hayes and the ridgeline south of Lake Cygnus, and/or 2) a gentle synformal warping in the bedding foliation observed through the ridgeline south of Lake Cygnus (see Figure 43c).

The northeast range flank is both defined and cut by a southwest-dipping reverse fault network. This in turn is offset by a series of north-trending dextral-normal oblique-slip faults particularly across the Capella Crags.

A series of photographs at the north end of the Western Arthur range provide a composite structural profile (Figure 32; see yellow profile lines f, g and e-h in Figure 31 for locations). A flat-lying transposition layering (Sm) caps the north end of the range at the head of Alpha moraine (Figures 32f, 32g, 33 and 34). Occasional metre-scale recumbent, isoclinal fold hinges lie within the Sm/So (Figures 33a). Less deformed Sm/So is sub-parallel to this Sm with apparent cross bedding (Figure 34).

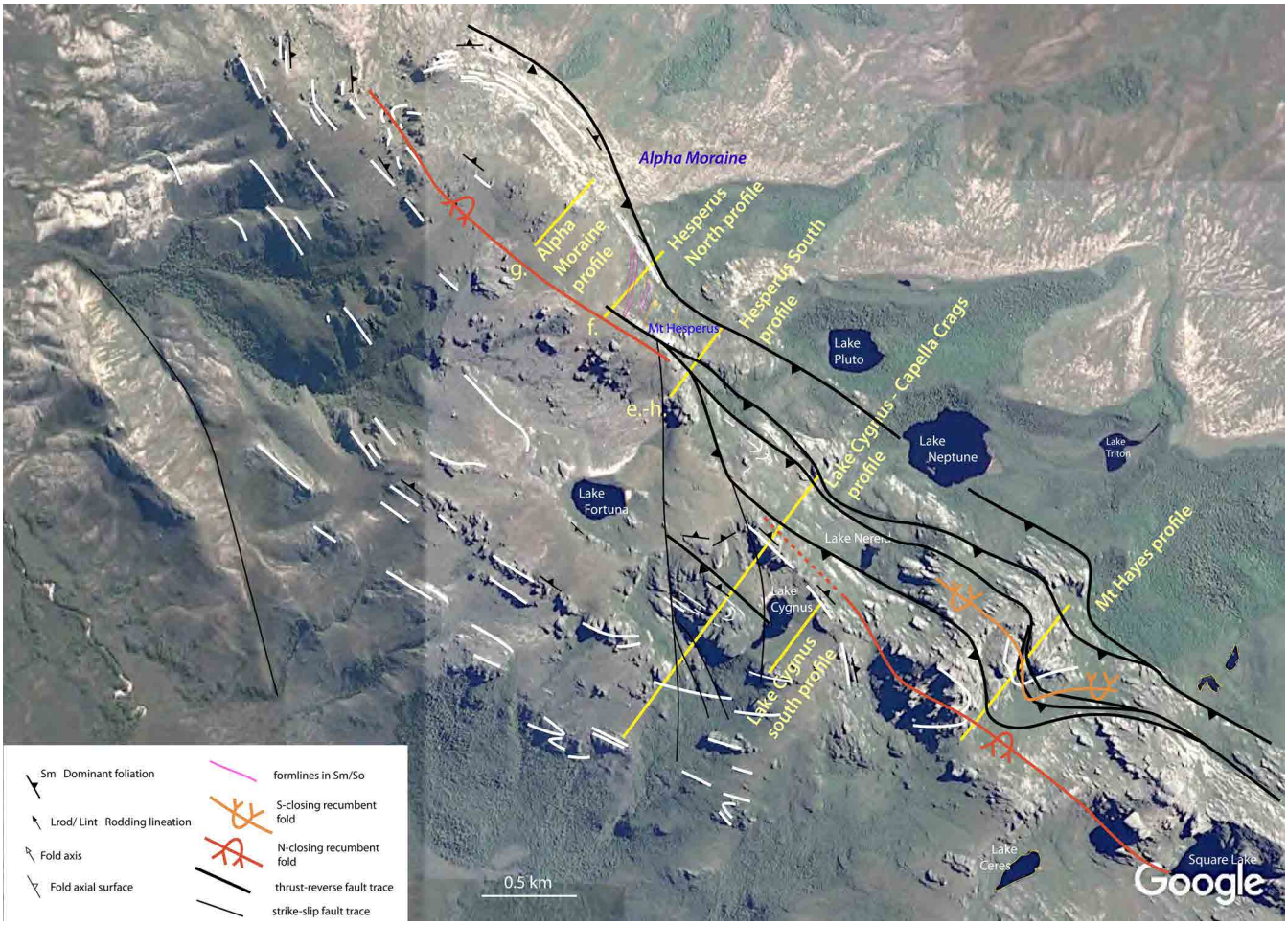

Figure 31. Structure map of the northern end of the Western Arthur Range from Square Lake through Mt Hesperus. Heavy black lines with barbs highlight a southwest-dipping reverse fault system.

Red trace is the axial surface trace of the northeast-closing recumbent macro-fold.
Orange trace is the axial surface trace of the southwest-closing recumbent fold.
Thin black lines are the dextral-normal oblique slip faults that offset the folds and the reverse faults.
Yellow lines are the Section lines referred to in the text. White line traces are the formlines in So/Sm (pink in Legend).

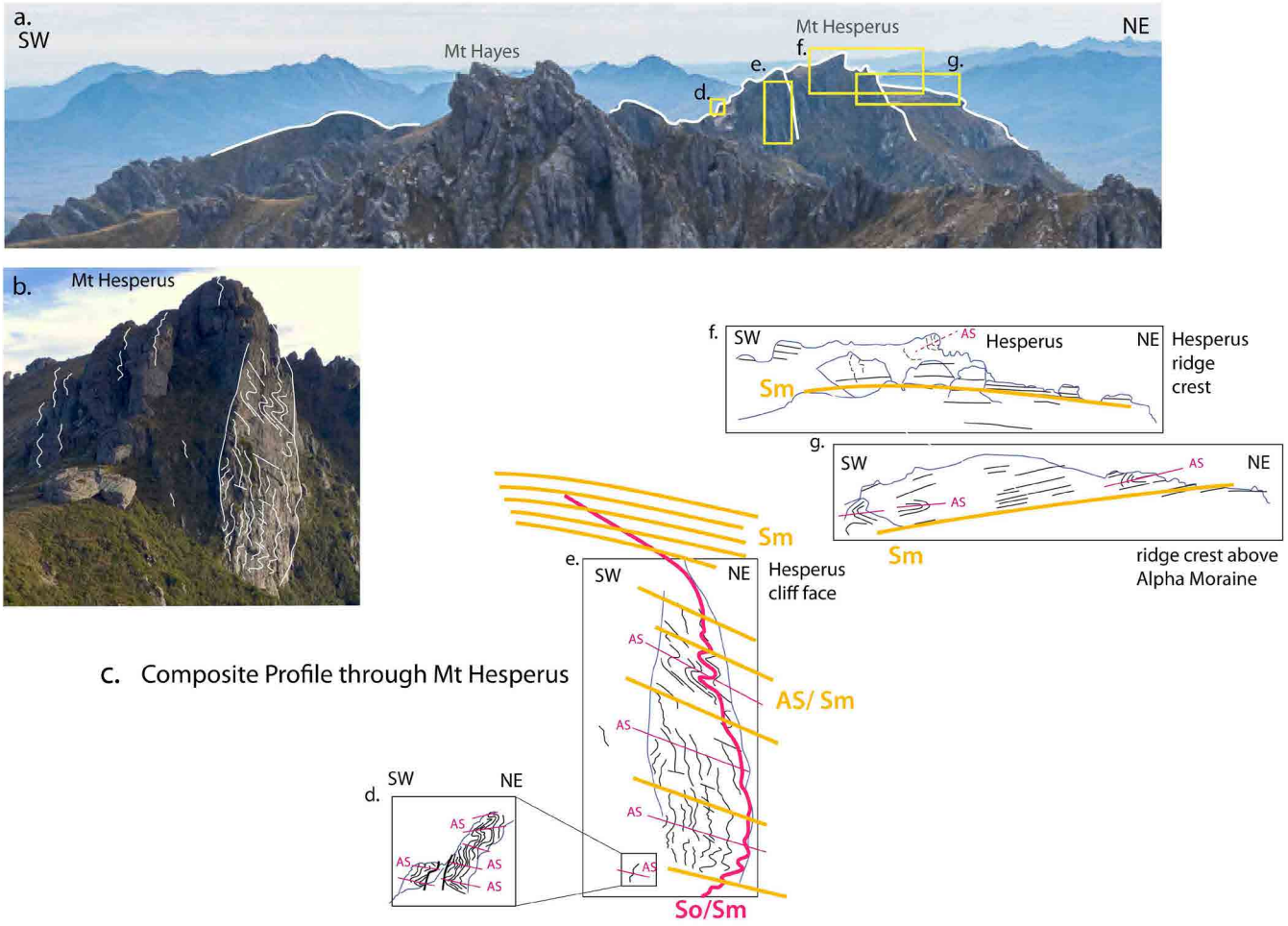

Figure 32. Mt Hesperus (1098m) structural relationships. a) View to Mt Hesperus from Mt Sirius (photo credit: Louise Fairfax). Yellow boxes highlight positions of detailed structural sketch interpretations from field photographs. b) Photo of Mt Hesperus from Capella Crags (photo by David Noble). c) formline interpretations of photos in Figures 33, 34, 35 and 36 used to construct a composite profile. Pink line: bedding foliation (So/Sm) trace. Orange lines: axial surface foliation AS/Sm transitional into zone of transposition foliation Sm at top of the range. Note profile g is down plunge from profile f (see profile locations in Figure 31).

This zone of transposition layering is at the highest structural level and sits above a northeast-closing recumbent fold hinge zone exposed in the Mt Hesperus cliff face (Figure 32b and c). The transposition layering is broadly arched across the Western Arthur Anticline (Figure 26). It contains mesoscopic fold hinges of metre- to cm-scale recumbent isoclines (Figures 6, 33a and 34).

Greater detail of the more symmetrical folds in the macro-fold hinge can be seen at the base of the Mt Hesperus ridgeline adjacent the walking track (Figure 36).

The Capella Crags (Figure 37) provides a link between the Mt Hesperus Profile (Figure 32) and the Lake Cygnus and Capella Crags Profile (see Section 3.2.2 following). Formline interpretation of the Capella Crags hillside shows another upper limb to macro-fold hinge transition (compare with Figure 35). This chevron folded transition from asymmetric folds on the upper limb to more symmetrical folds in the macro-fold hinge defines the structural character at the northwestern end of the Western Arthur Range (including Mt Hesperus-Capella Crags-Lake Cygnus). Mesoscopic fold hingelines identified in the photo (blue line segments in Figure 37c) show significant plunge and plunge direction changes through this exposure. Some of these mesoscopic fold hinges, particularly in the macro-fold hinge (designated hinge zone in Figure 37d) deviate by up to 80° from a generalised 310° trend.

3.2.2 Lake Cygnus and Capella Crags Profile (Section 2, Figure 15)

The Lake Cygnus and Capella Crags profile (see Figures 38 and 39) has been constructed using formline interpretation of photographs of the hillsides above Lake Cygnus and Capella Crags (Figure 38, 40, 41 and 42). The hillside provides on the order of 150-200m of relief.

This profile (Figure 39) contains repeated zones of chevron folding showing differences in fold asymmetry and fold tightness coupled with, or linked to, the angle between the folded layering So/Sm enveloping surface and the associated fold axial surfaces (i.e. high angles: hinge zone, whereas lower (acute) angles: limb zone). Parts of the section have been offset by late, north-trending, dextral oblique slip faults complicating the overall interpretation.

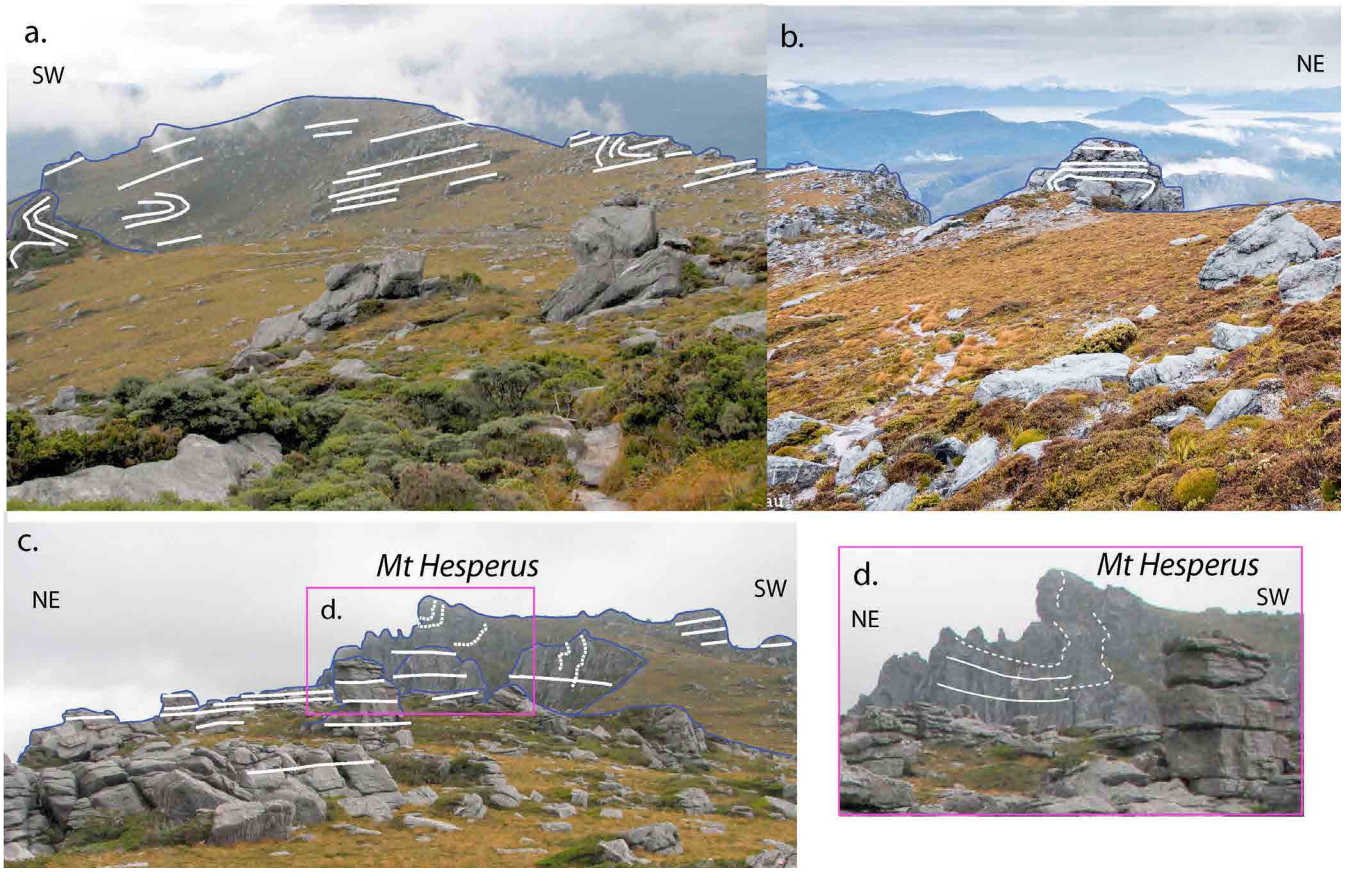

Figure 33. Flat lying foliation So/Sm dominating the North end of the Western Arthur Range. a) and b) Photos of ridgeline north of Mt Hesperus at the head of Alpha Moraine. c) and d) Views of Mt Hesperus from moor above Alpha Moraine. The flat-lying So/Sm foliation is axial surface to occasional recumbent fold closures (see photo profile from a and b at top). (photo credit: David Noble)

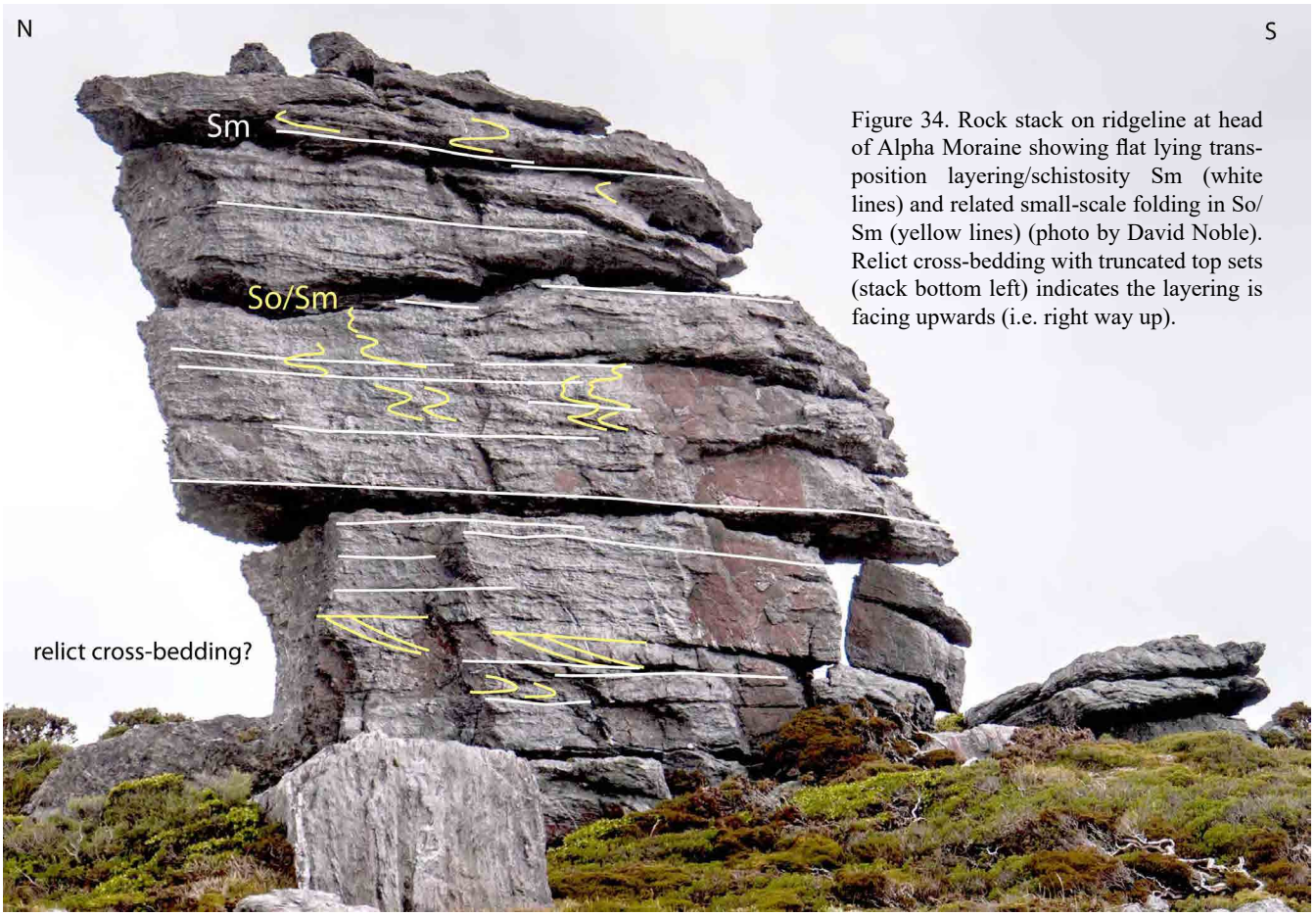

Figure 34. Rock stack on ridgeline at head of Alpha Moraine showing flat lying transposition layering/schistosity Sm (white lines) and related small-scale folding in So/Sm (yellow lines) (photo by David Noble). Relict cross-bedding with truncated top sets (stack bottom left) indicates the layering is facing upwards (i.e. right way up).

Figure 35 (left). Mt Hesperus southeast face structural interpretation. a). Cropped part of Peter Dombrovskis "Mt Hesperus in the clouds" photo [Peter Dombrovskis, National Library of Australia, nla.cat-vn680832]. b) Formline interpretation of structures within Mt Hesperus south face. The cliff section shows an upper limb with Z-vergence asymmetric folds (upper part of cliff) to an apparent hinge with more symmetrical folds in the lower part of the cliff exposure (macro-fold hinge zone).

Figure 36. Folds exposed in the hillside base of Mt Hesperus, below SW ridgeline. a) and b) bushwalking photos source unknown. c) photo by David Noble.

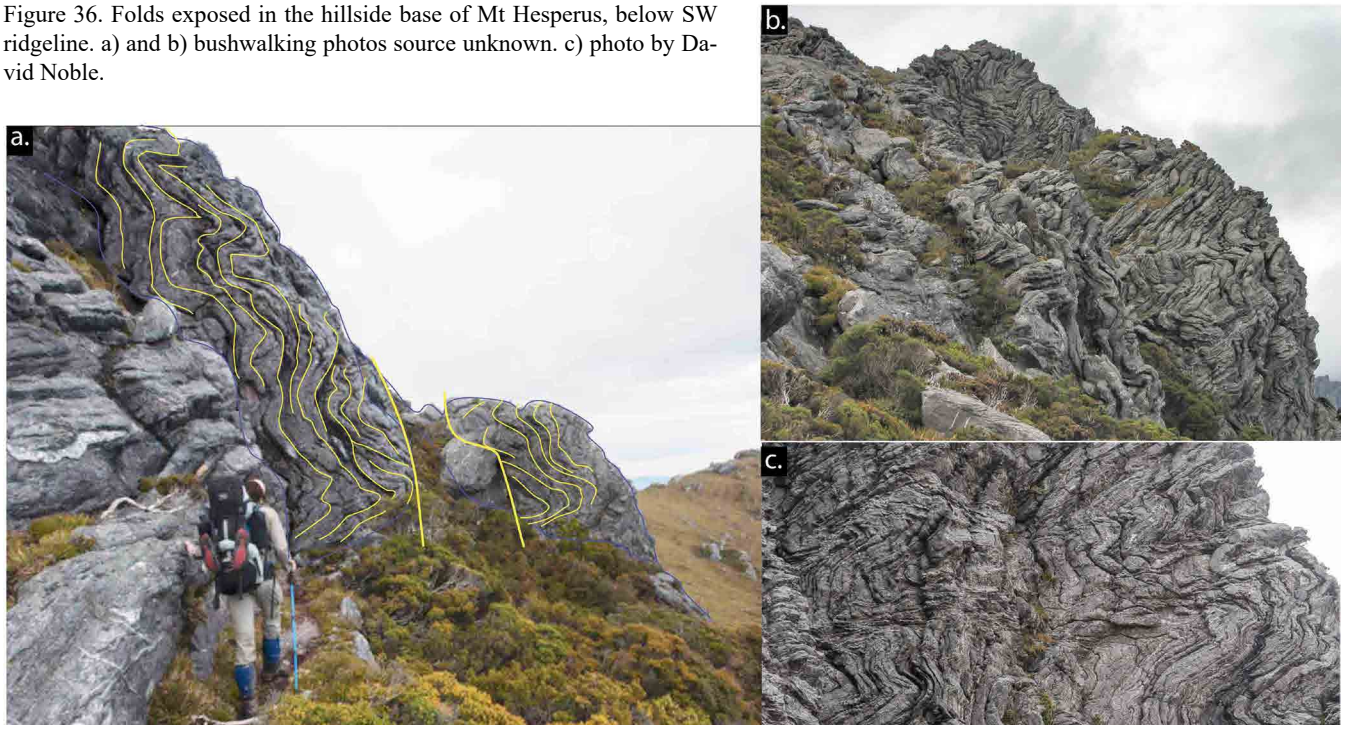

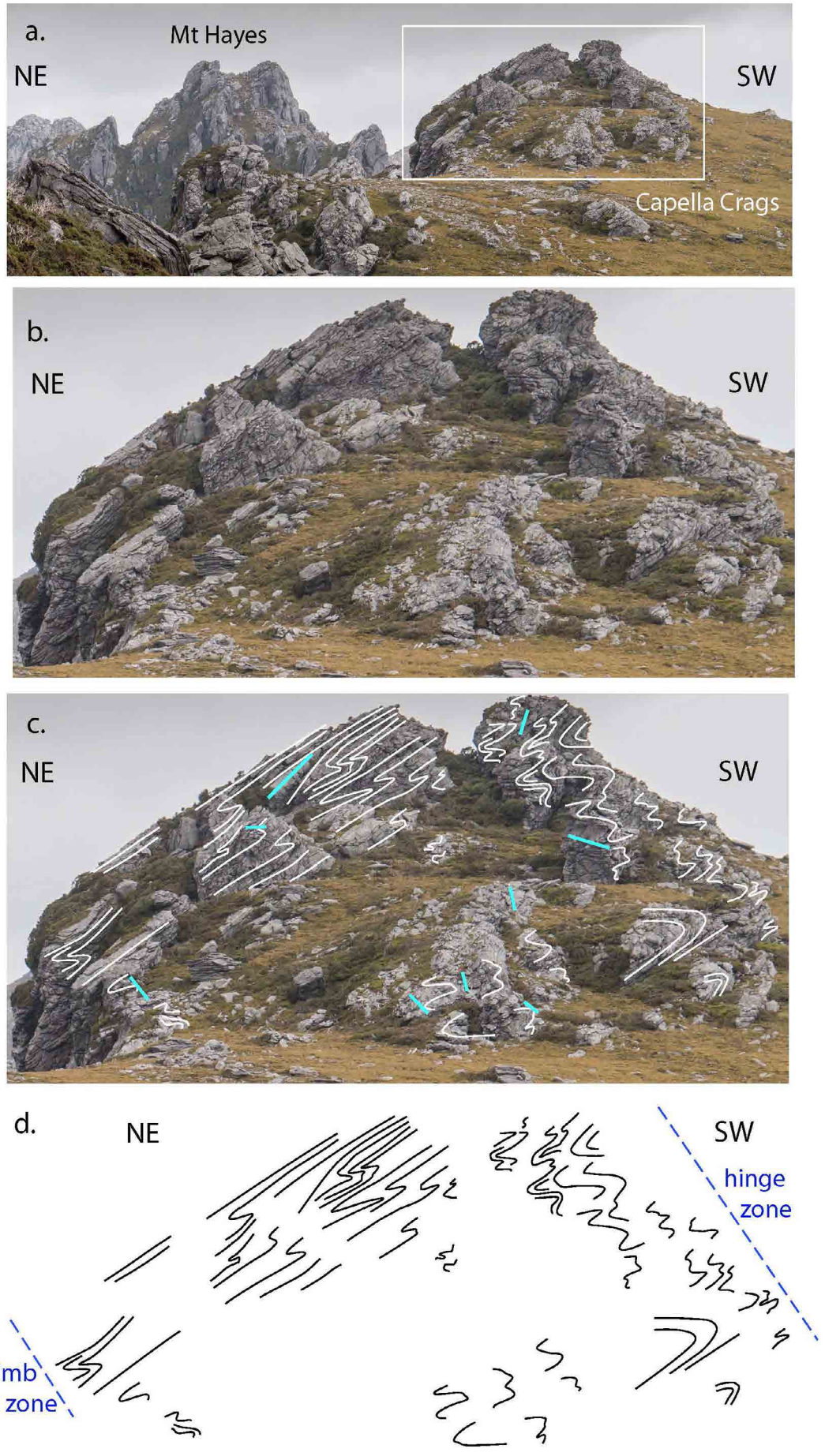

Figure 37. View of Capella Crags from base of Mt Hesperus (photo by David Noble). b) Enlargement of Capella Crags hillside, c) Enlarged view with formline interpretation (white lines: bedding foliation So/Sm traces. Light Blue: hingelines of mesoscopic folds). d) Structural profile from c) showing the chevron folded nature in the hinge zone with transition to flattened asymmetric folds towards the upper limb.

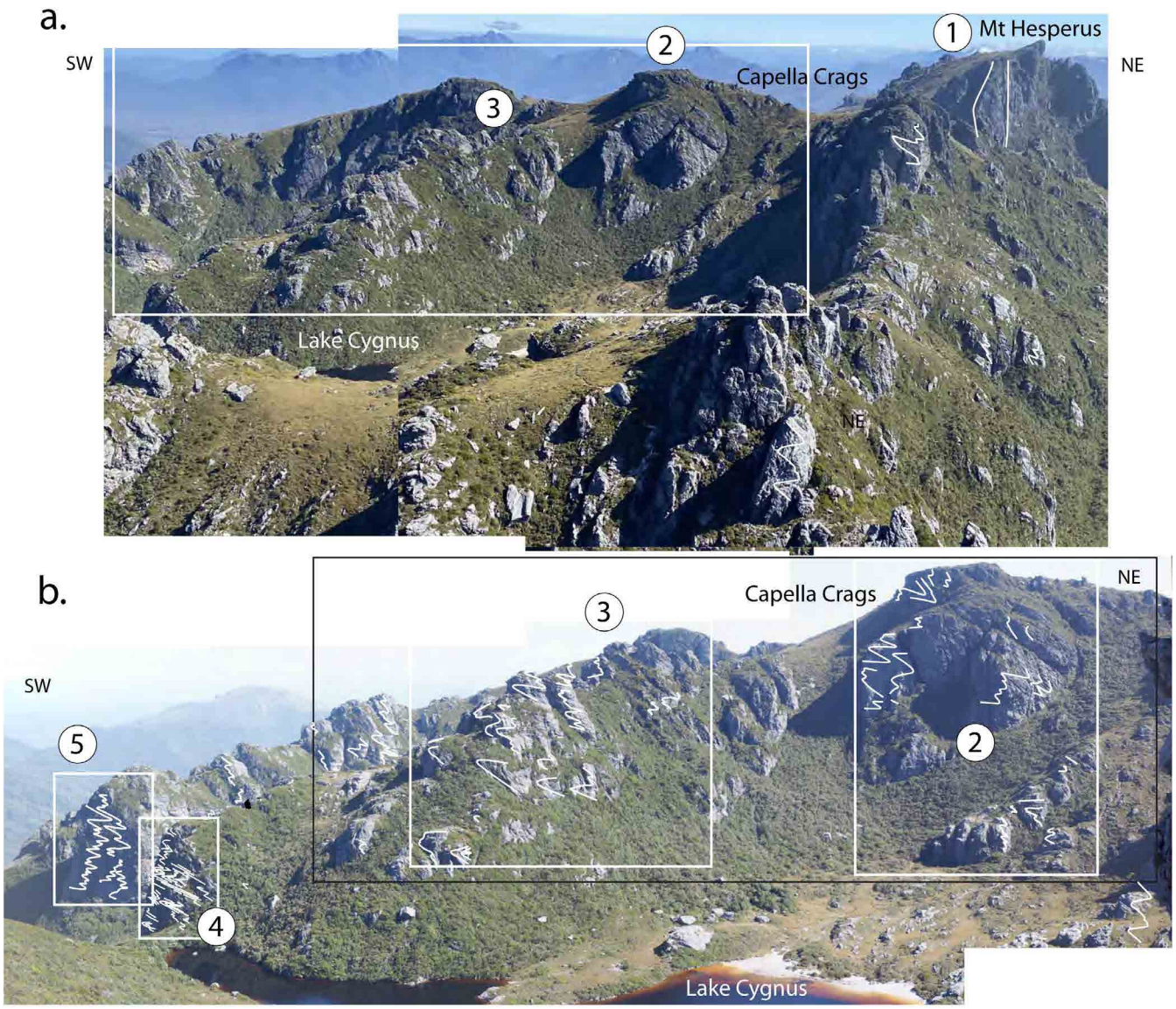

Figure 38. Lake Cygnus-Capella Crags photo collage profile used in formline interpretation to create the structural profile shown in Figure 39. Positions of the elements numbered 1 to circled 5 relate to the elements in Figure 39.

Figures 40, 41 and 42 show the formline interpretation of the individual photographs that have been assembled together given their position and elevation in the constructed profile. Each photograph can be linked back to the constructed profile using the segment given by the circled number (compare Figures 38 and 39).

In the profile, macro-scale hinge and limb zone segments have been determined by mapping out the relationships between enveloping surfaces of the chevron folded layering and the fold axial surfaces (Figure 39b). Axial surfaces of mesoscopic to larger scale chevron folds all dip moderately to the northeast across the extent of the ridgeline and the enveloping surfaces are generally steeply dipping to the southwest. Combining ridge offsets and gaps in exposure with the fault network interpreted from the aerial imagery (Figure 31), individual faults have been projected into the line of section (black dashed line traces in Figure 39b). The positions of these faults explain the offsets in the macro-fold hingeline seen in the profile. Note there is a general arching of the macro-fold hinge zone that reflects the open refolding by the Western Arthur Anticline. The actual form of the younger fold in this profile is complicated by the fact that hingeline segments in each fault hanging-wall have been displaced to the north (i.e. these faults are the oblique slip dextral-normal faults).

Without the presence of, and knowledge of the movement sense of, the steeply dipping oblique-slip faults the formline pattern has the appearance of a stacked sequence of alternating “hinge” zones (i.e. where fold axial surfaces AS and the bedding foliation So/Sm enveloping surfaces are at high angle) and “limb” zones or high strain zones showing flattened and attenuated asymmetric Z-folds (i.e. where the angle between the AS and the So/Sm enveloping surfaces are at a much lower angle).

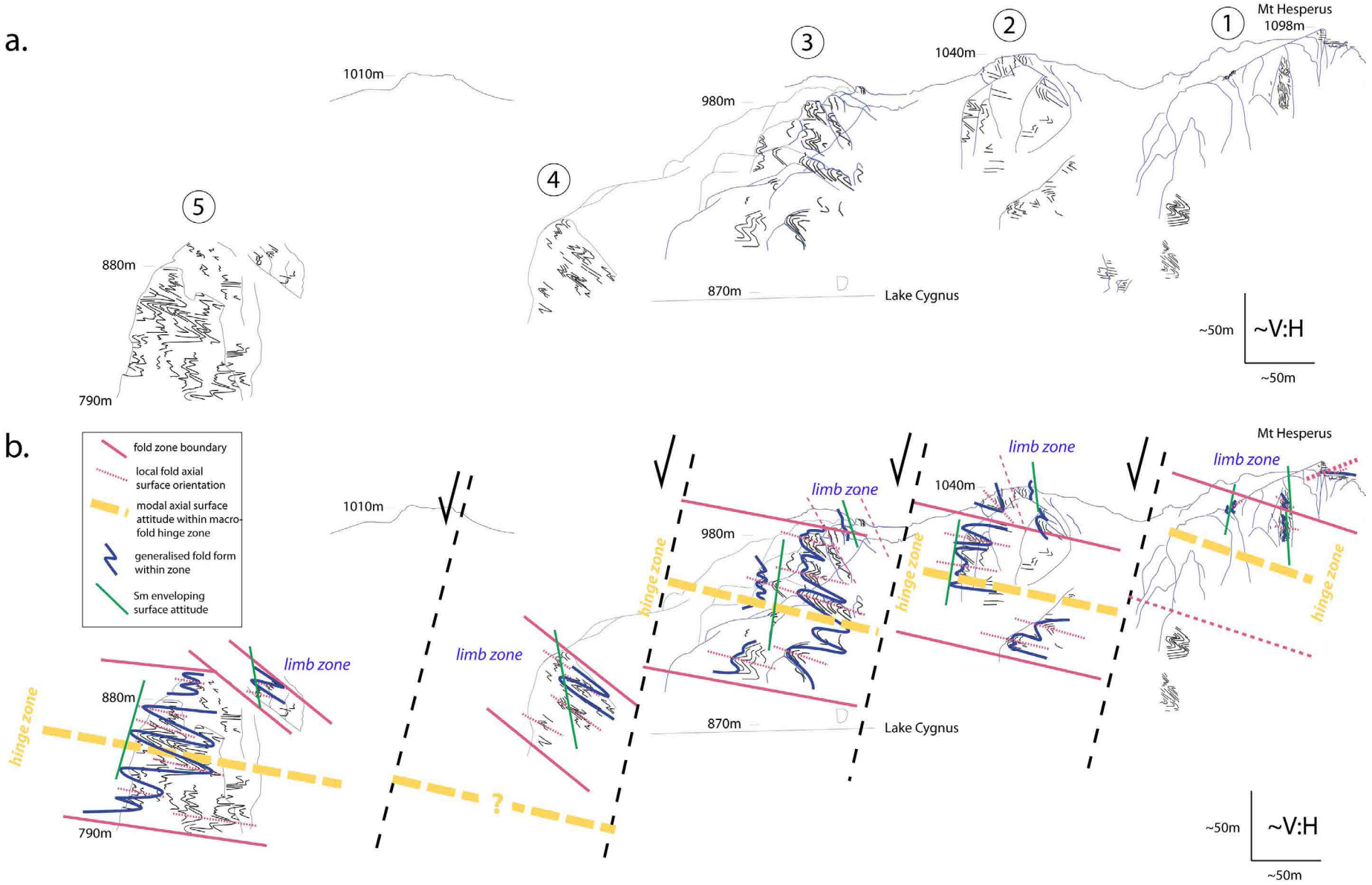

Figure 39. Structural profile 2 north of Lake Cygnus (see Figure 15 for location) a) Ridgeline trace with local elevations and formline interpretation off hillside photographs (Figures 40, 41 and 42). Positions of the hillside elements numbered 1 to 5 relate to the elements in Figure 38. b) Enhanced structural interpretation of the formline pattern in a) showing boundaries (pink lines) to the hinge zone domains, attitudes of enveloping surfaces to the bedding foliation So/Sm (green lines) and generalised axial surface attitudes (thick dashed orange lines). Black dashed lines are faults projected onto the section line from the aerial imagery interpretation (see Figure 31).

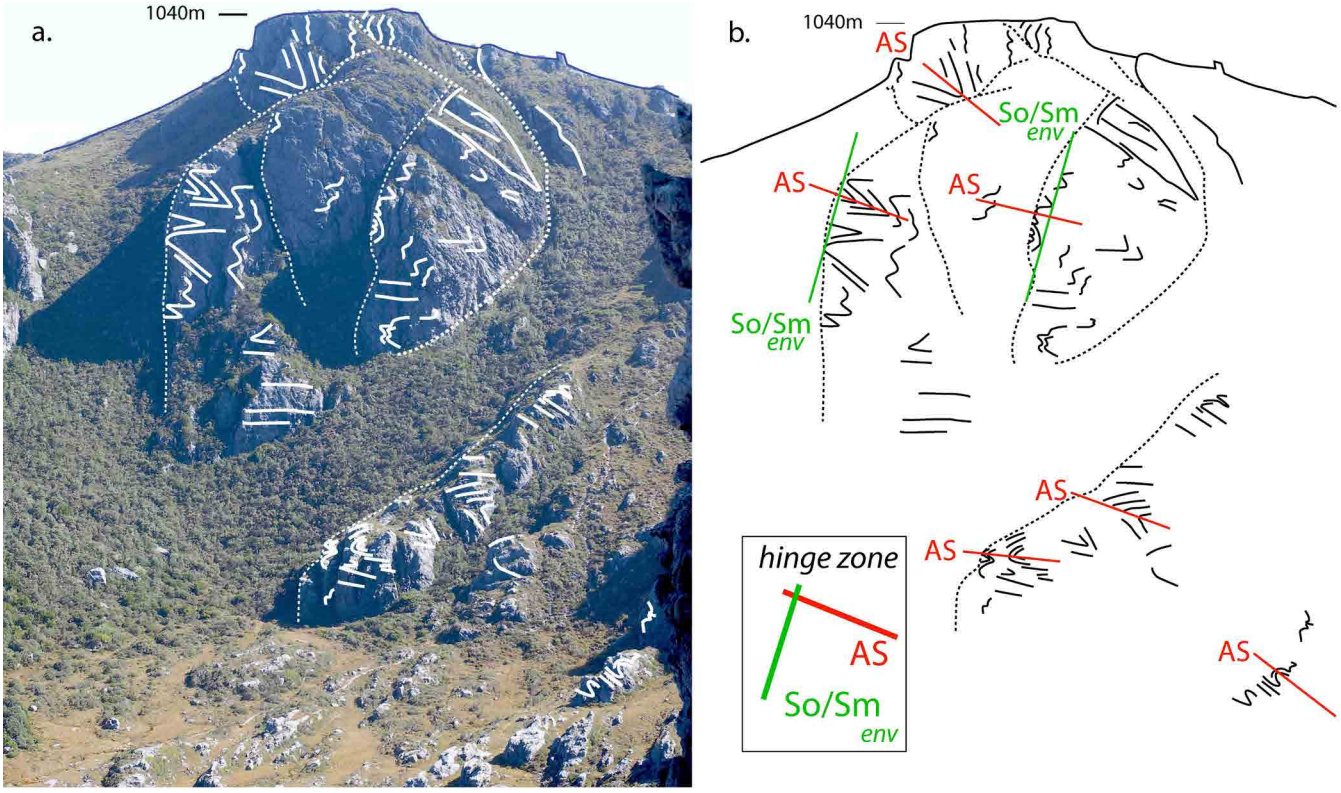

Figure 40 (above). Structural interpretation of Capella Crags above Lake Cygnus. This is Profile Segment 2 in Figure 37. Meso-fold axial surface traces AS are shown as red lines. The green line traces are the enveloping surfaces (So/Smenv) of the folded So/Sm shown by black line traces. The inset shows the generalised relationships between AS and the So/Sm . An orthogonal relationship suggests a macro- fold hinge zone.

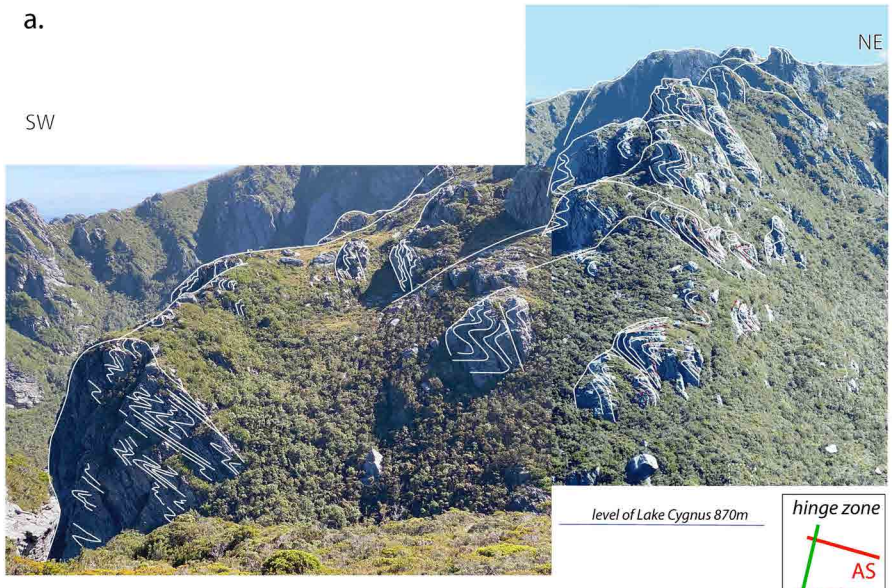

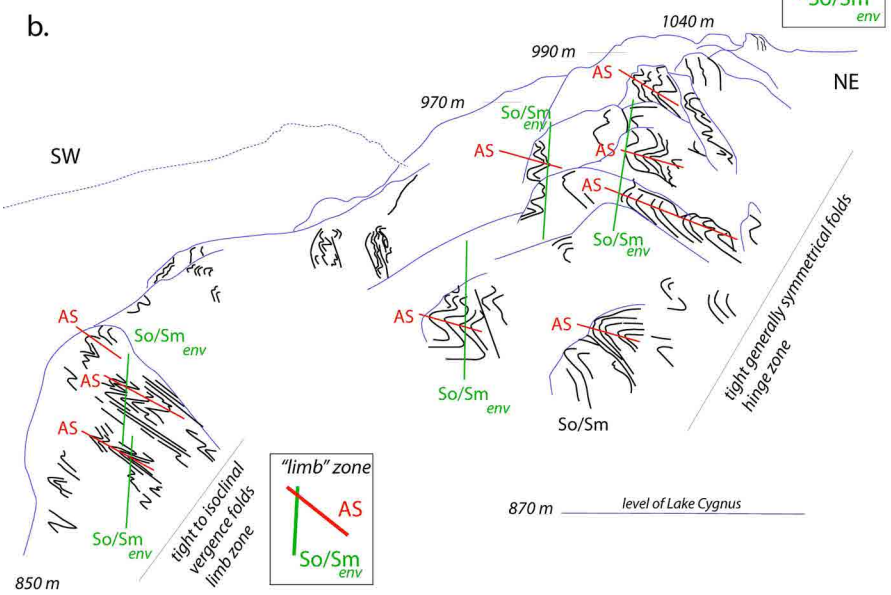

Figure 41 (left). Ridgeline extending north from Lake Cygnus to Capella Crags showing structural formlines in So/Sm (black line traces). These are Profile segments 3 and 4 in Figure 37. Meso-fold axial surface traces AS are shown as red lines. The green line traces are the enveloping surfaces (So/Smenv) of the folded So/Sm. The insets shows the generalised relationships between AS and the So/Sm .

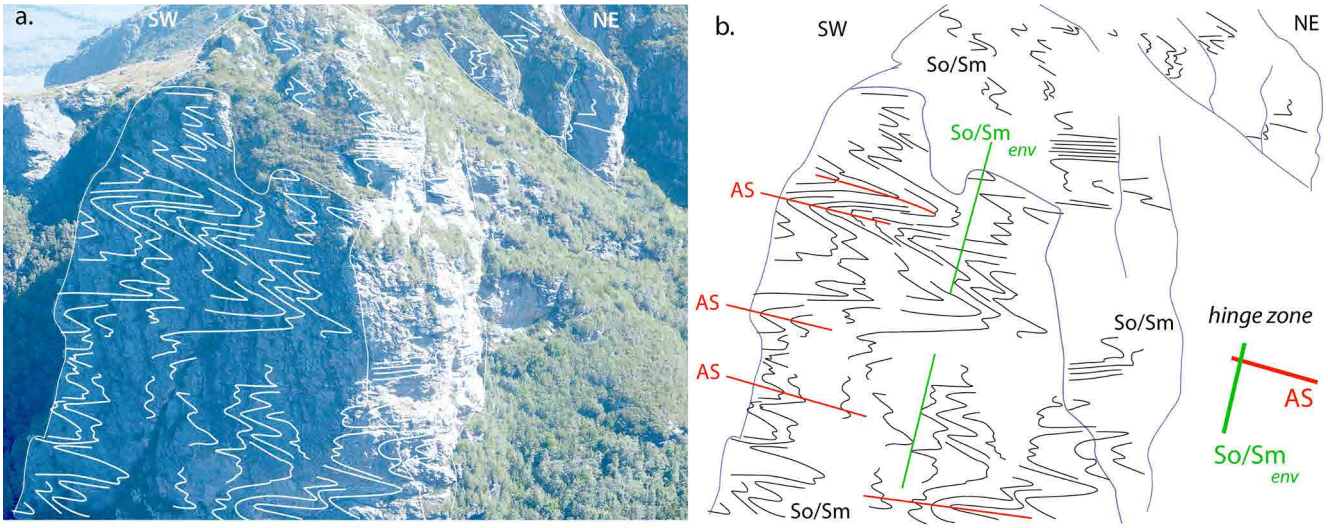

Figure 42. Cliff with chevron-folded thinly bedded quartzite west of and below Lake Cygnus. View to the northwest. a) Cliff and b) formline annotation of So/Sm on cliff face. This is Profile Segment 5 in Figure 37. Meso-fold axial surface traces AS are shown as red lines. The green line traces are the enveloping surfaces (So/Smenv) of the folded So/Sm shown by black line traces. The inset shows the generalised relationships between AS and the So/Sm . An orthogonal relationship suggests a macro- fold hinge zone.

Inspection of other structural profiles to the southeast, in particular the nearby Mt Hayes (section 4, Figure 15) suggest that the identified macro-hinge zone is the northeast-facing and closing recumbent macro-fold that dominates the ridge crest of the Western Arthur Range. The position of the axial surface trace from Mt Hayes through Lake Cygnus to Mt Hesperus is difficult to map out through the fault network shown in Figure 31.

3.2.3 Lake Cygnus southeastern ridgeline Profile (Section 3, Figure 15 and section B-B', Figure 43)

The Lake Cygnus southeastern ridgeline profile (Figure 43) is different to the northern profile (Figures 38 and 39). It shows a series of chevron folds in thinly bedded quartzite without 1) any apparent broad hinge zone(s) of an early F2 recumbent fold, and/or 2) any apparent higher strain zones (or limb zones) as in the northwestern Capella ridgeline profile. The overall generalised foliation Sm is moderately northeast dipping and shows a flattening in the middle part of the profile (Figure 44c).

Components of the Lake Cygnus Profile B-B' are shown in Figures 44, 45 and 46. Truncated cross-bedding (see Figure 7) in outcrop 3 (Figures 44a and 46) indicates that So/Sm is right-way-up in the profile.

Less cliff exposures and lack of extensive outcrop along this ridgeline southeast of Lake Cygnus provide a "narrower" sectional view (due to a relief extent ranging from ~20-100m). The generalised Sm dips at ~30° to the northeast (but flattens between Outcrops 2 and 3, Figure 44a and c), whereas the So/Sm enveloping surfaces are steeply southwest dipping (see also Figure 45). These are the same relationships observed in Profile 2 (Figure 39).

A photo profile (Figure 47) across the ridgeline contains outcrops 3 (photo left) and 4 (photo right) and provides section C-C' (see location in Figure 43). Fold hingelines in the photo, shown by the white line traces, give the local fold axis plunges and plunge direction. Fold plunge is predominantly gentle to the north (5-10°), although some folds plunge gently to the south (Figure 47).

3.2.4 Haven Lake-Mt Scorpio Profile (Profile 10, Figure 15)

The traverse from Haven Lake to Kappa Moraine via Mt Scorpio provided another structural profile (Figures 48 and 49). Section construction (Figure 49) combined with map compilation (Figure 48) suggests two oppositely closing recumbent fold hinges like those observed at Mt Hayes and the Dorado Peak area separated by a reverse fault system. Part of the major, northeast-closing recumbent fold is exposed in the cliff section near Lake Sirona (Figure 50).

Changes in bedding-cleavage angular relationships between Lake Sirona and Mt Scorpio requires the presence of the southwest-closing recumbent macro-fold. At Lake Sirona the bedding dips more steeply than cleavage (i.e. overturned fold limb) with counterclockwise rotation of cleavage back to bedding (closing the acute angle), whereas at Mt Scorpio the bedding dips less steeply than cleavage (i.e. right way up limb) with clockwise rotation of cleavage back to bedding (see Figure 49b). The change in cleavage vergence (rotation) indicates the presence of a fold hinge. The So/Sm dip changes necessitate a tighter more angular hinge at Mt Scorpio than seen at Mt Hayes and Dorado Peak (compare Figures 17, 18 and 49).

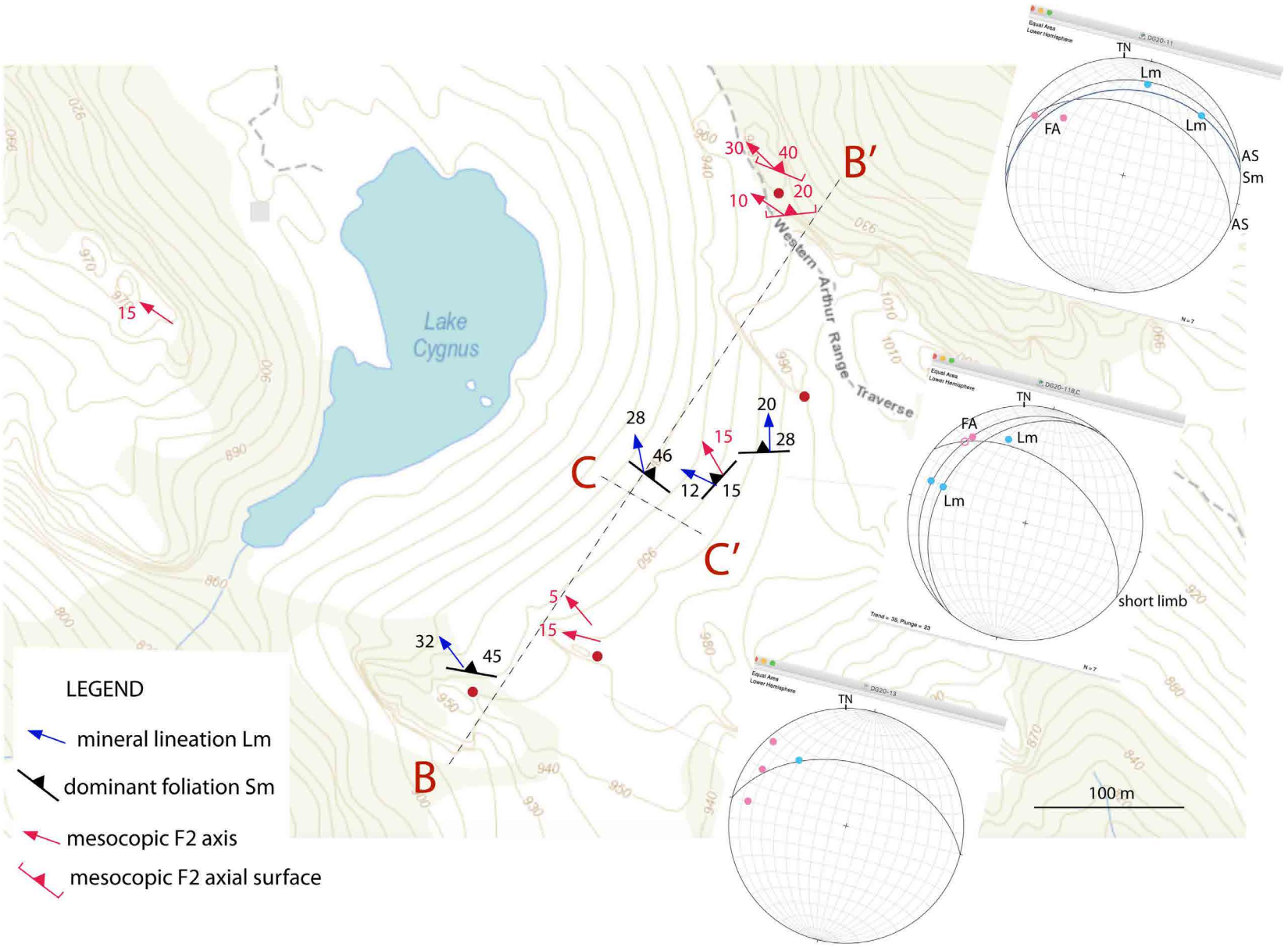

Figure 43. Structural data from ridgeline traverse on ridge southeast of Lake Cygnus. Stereonet insets show relationships between measured lineations (Lm) and fold axes (FA), and the general northeast-dipping foliation Sm. Section line B-B' is shown in Figure 44. Section C-C' is shown in Figure 47.

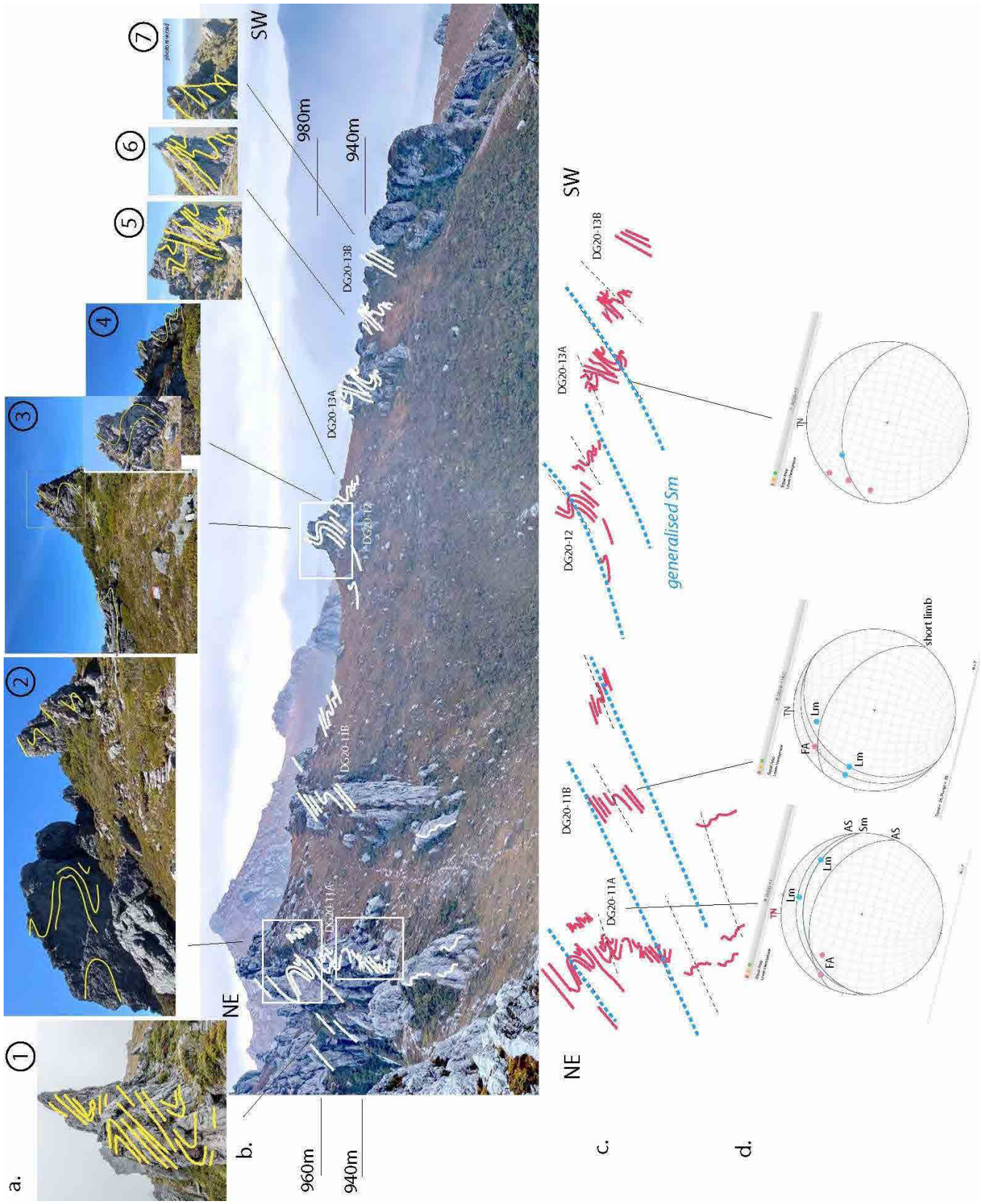

Figure 44. Structural profile construction along ridgeline southeast of Lake Cygnus. View looking to the southeast. a) Series of photos used to construct the sketch structural profile in (c). Outcrop photos are numbered 1 to 7. b) Ridgeline photo showing the locations of the outcrop photos in a). c) Sketch structural profile B-B'. Blue dashed lines define the generalised Sm attitude across the ridgeline. d) Stereonets showing relations between foliation (Sm), fold axial surfaces (AS), fold axes (FA) and the mineral lineation (Lm).

Figure 45. Rock pillar as Outcrop 1 in Figure 44a showing asymmetric S-vergence folds defined by formlines in So/Sm (white line traces). The folds are contained within a moderately northeast-dipping Sm (i.e. dipping to photo left). Note rock slab steps as part walking track on right side of photo (Photo credit: Bretto.com).

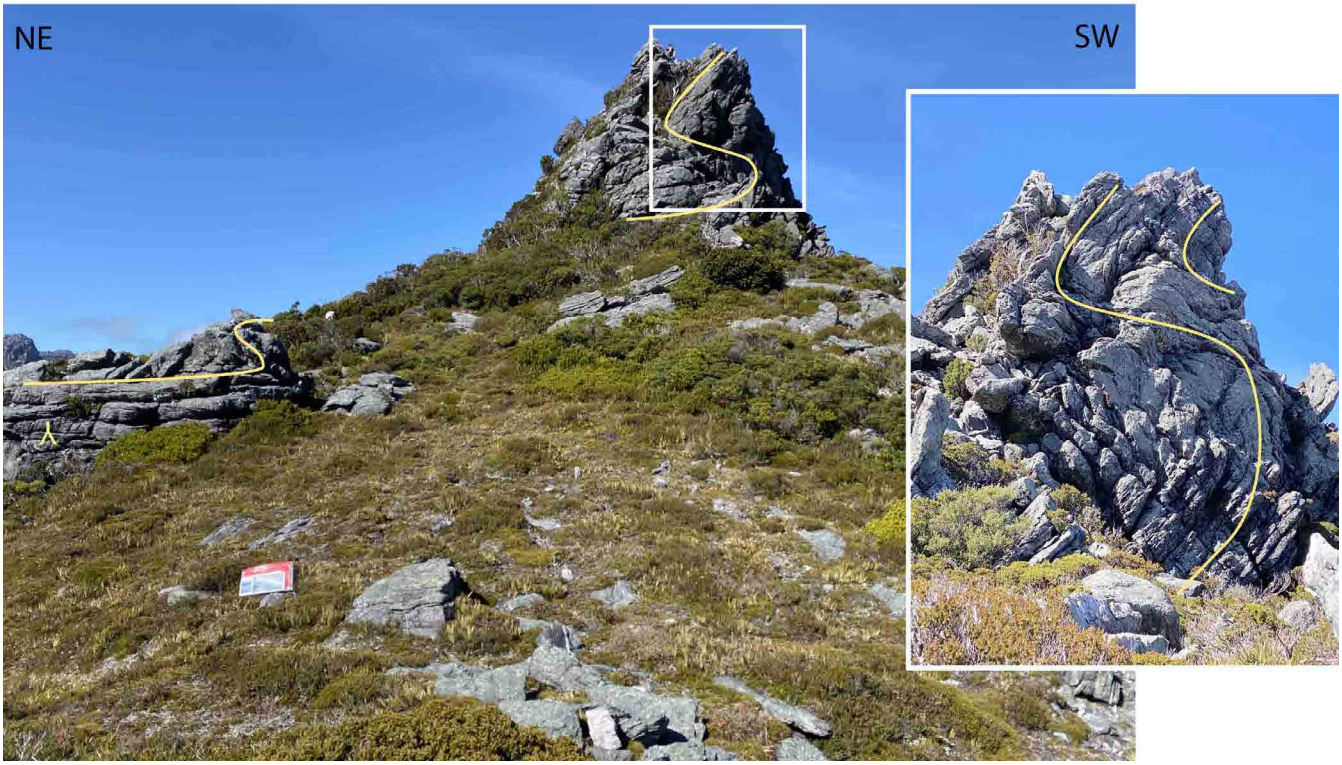

Figure 46. Asymmetric, S-vergence chevron folds (looking up-plunge) in Outcrop segment 3 in Figure 44a. The cross-bedded quartzite in Figure 7 occurs in the outcrop on the left side of the photo with flat lying Sm.

Yellow lines: bedding foliation So/Sm.

Figure 47. Fold plunge variation across the ridgeline south of Lake Cygnus. Outcrop on the left is Outcrop 3 in Figure 44a whereas outcrop on the right is Outcrop 4 in Figure 44a. View is to the northeast.

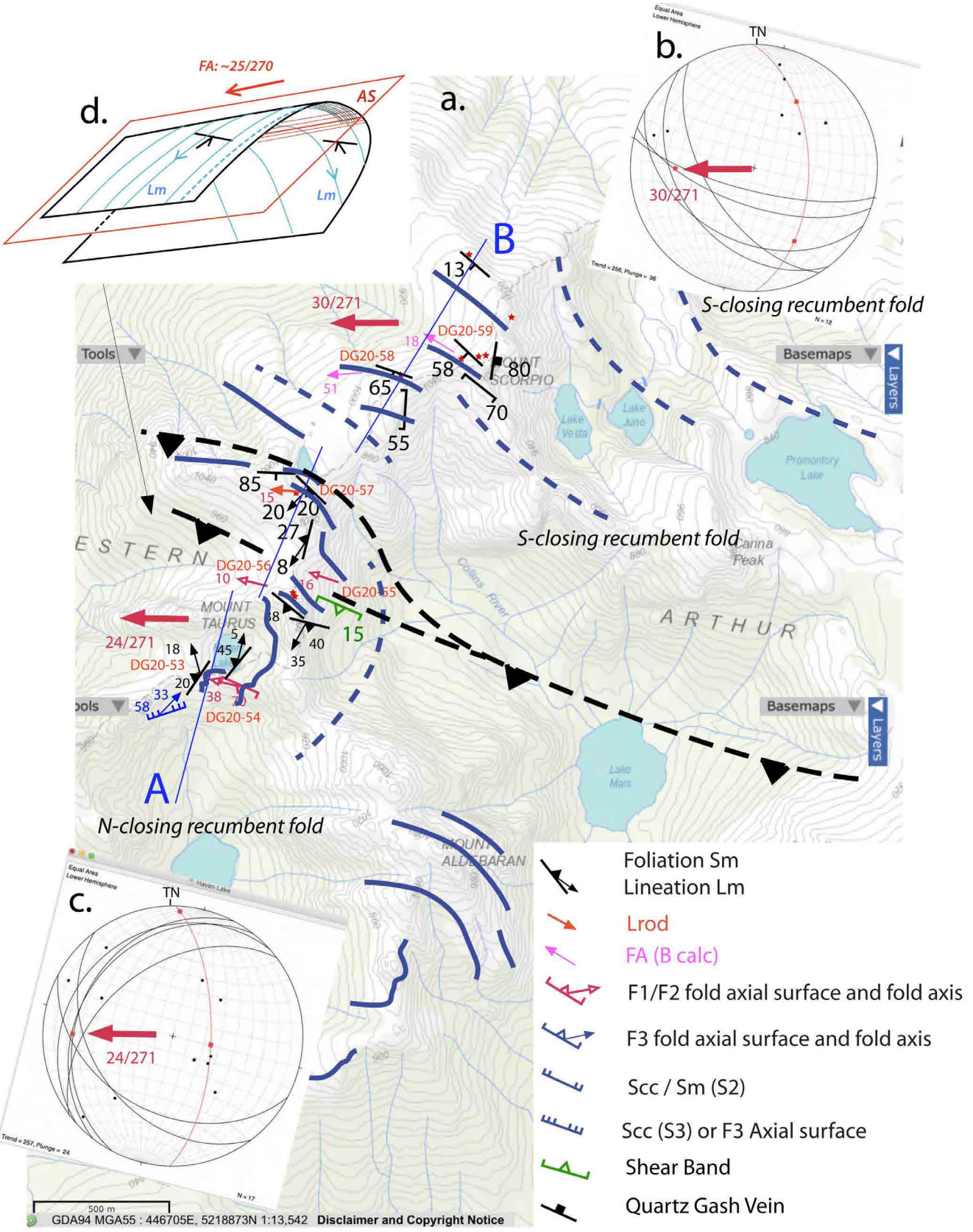

Figure 48. Structure map of the Haven Lake- Mt Scorpio traverse. a) Map on a ListMap topographic base with position of section line A-B shown. Heavy black dashed lines are inferred faults. Blue dashed lines are form-lines in the bedding-foliation So/Sm. b. Stereonet for the area north of the inferred fault trace showing a β determination fold axis of 30°/271° for the southwest-closing recumbent fold (in the fault footwall). c) Stereonet for the area south of the inferred fault trace showing a β determination fold axis of 24°/271° for the northeast-closing recumbent fold (in the fault-hanging wall). d) Schematic diagram of the recumbent fold geometry proposed to explain the lineation Lm changes observed between DG20-53 (Haven Lake) and DG20-56 across the inferred fold hinge.

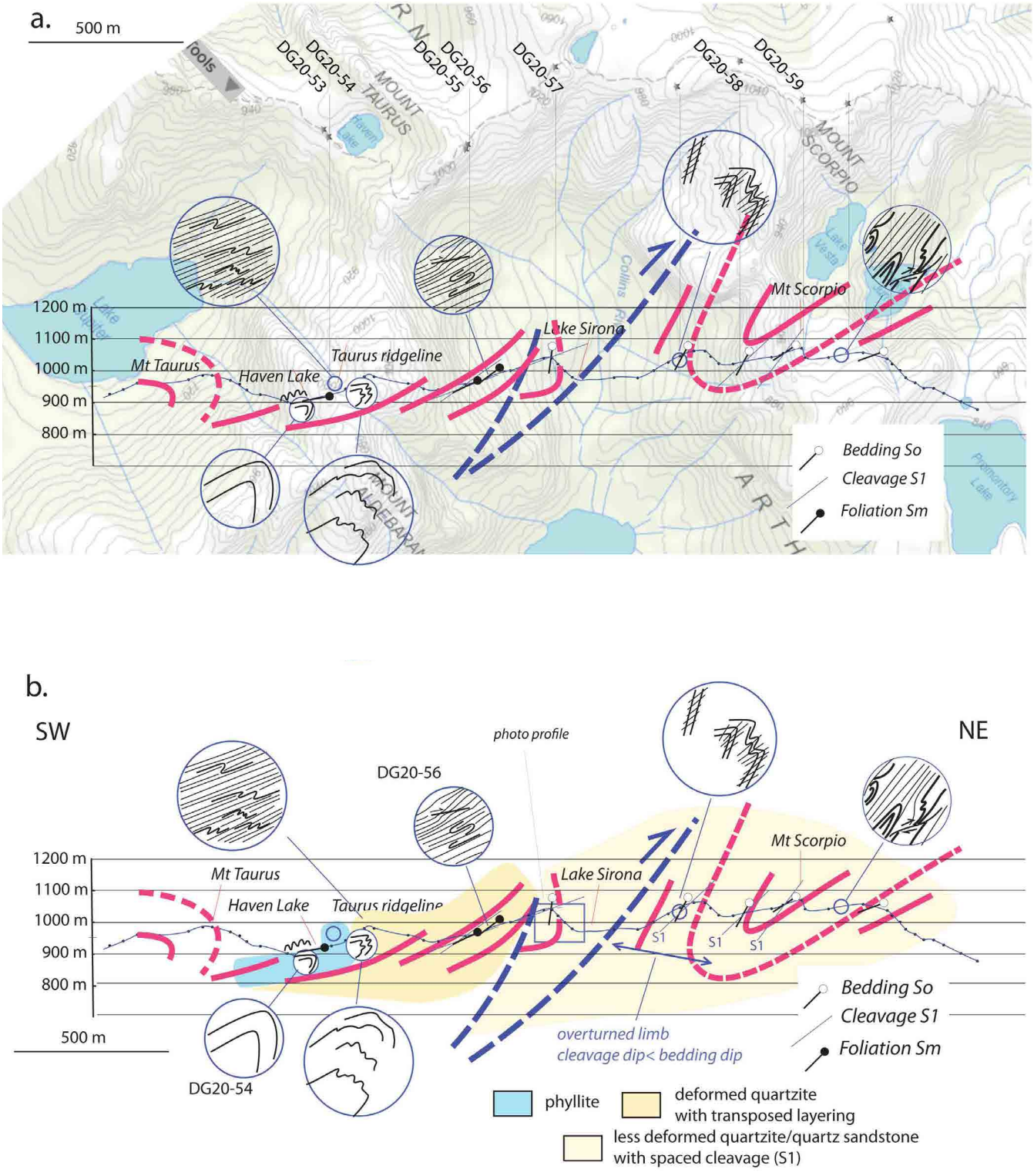

Figure 49. Haven Lake-Mt Scorpio structural profile. This is profile 10 in Figure 15. a) Profile superimposed on ListMap topographic base showing station positions on walking track (stars) and station projections to the constructed profile. b) Structural profile superimposed on lithology base and with interpreted larger scale structure (Sm/So: heavy pink lines; inferred reverse faults: heavy dashed blue lines). Insets show local structural relationships sketched or traced from outcrop photographs. Box below Lake Sirona text (centre of profile) is position of hillside photo in Figure 50.

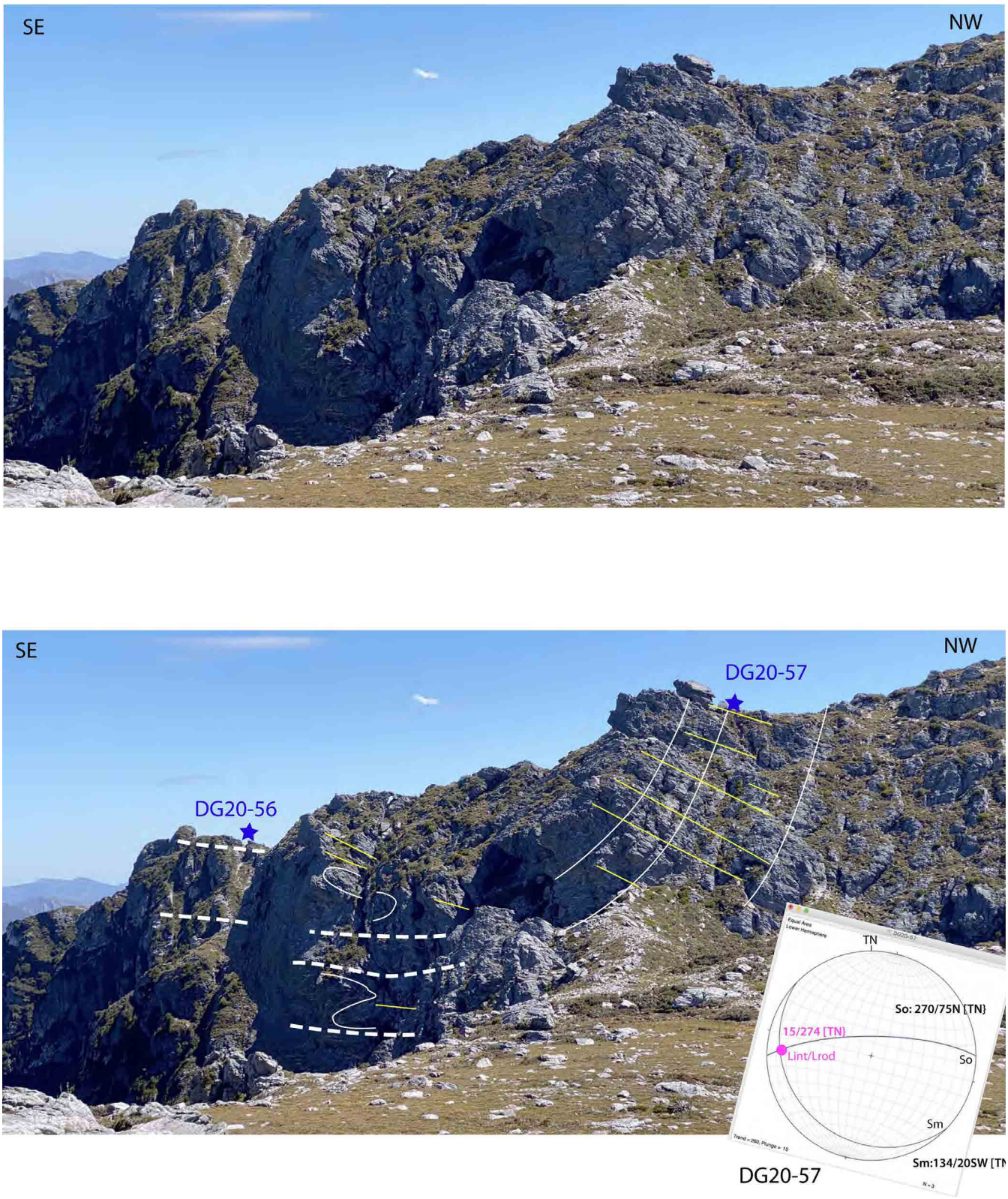

Figure 50. Oblique intersection of the northeast-closing recumbent fold in hillside at the southern end of Lake Sirona. View is to the south-west from the walking track. Inset stereonet shows structural measurements from outcrop station DG20-57 giving an inferred fold axis of 15°/274° for this closure.

The reverse fault between the northeast-closing and southwest-closing macro-folds has been inferred by a distinct change in lithology and the style and intensity of deformation (Figure 49b). The footwall consists of less deformed, lower-metamorphic grade quartzite/ quartz sandstone (Figures 51 and 52) that generally shows bedding overprinted with a spaced to slaty-type primary cleavage (Figure 51b). Cross-bedding is also relatively common (Figure 51a, b).

Most of the quartzite/quartz sandstone has very a weak or almost no mineral lineation. Quartz grains in many exposures have sub-rounded, equant to spheroidal grain form suggesting very low internal strain/deformation. The cleavage is typically a discontinuous spaced, dissolution cleavage with stylolitic character (Figure 53). The buckled vein truncations in Figure 52b are also indicative of a low-grade, dissolution-type cleavage. These spaced to slaty-type cleavages are distinct from the dominant transposition foliation Sm and the bedding-parallel foliation So/Sm that dominate the rest of the Western and Eastern Arthur Ranges.

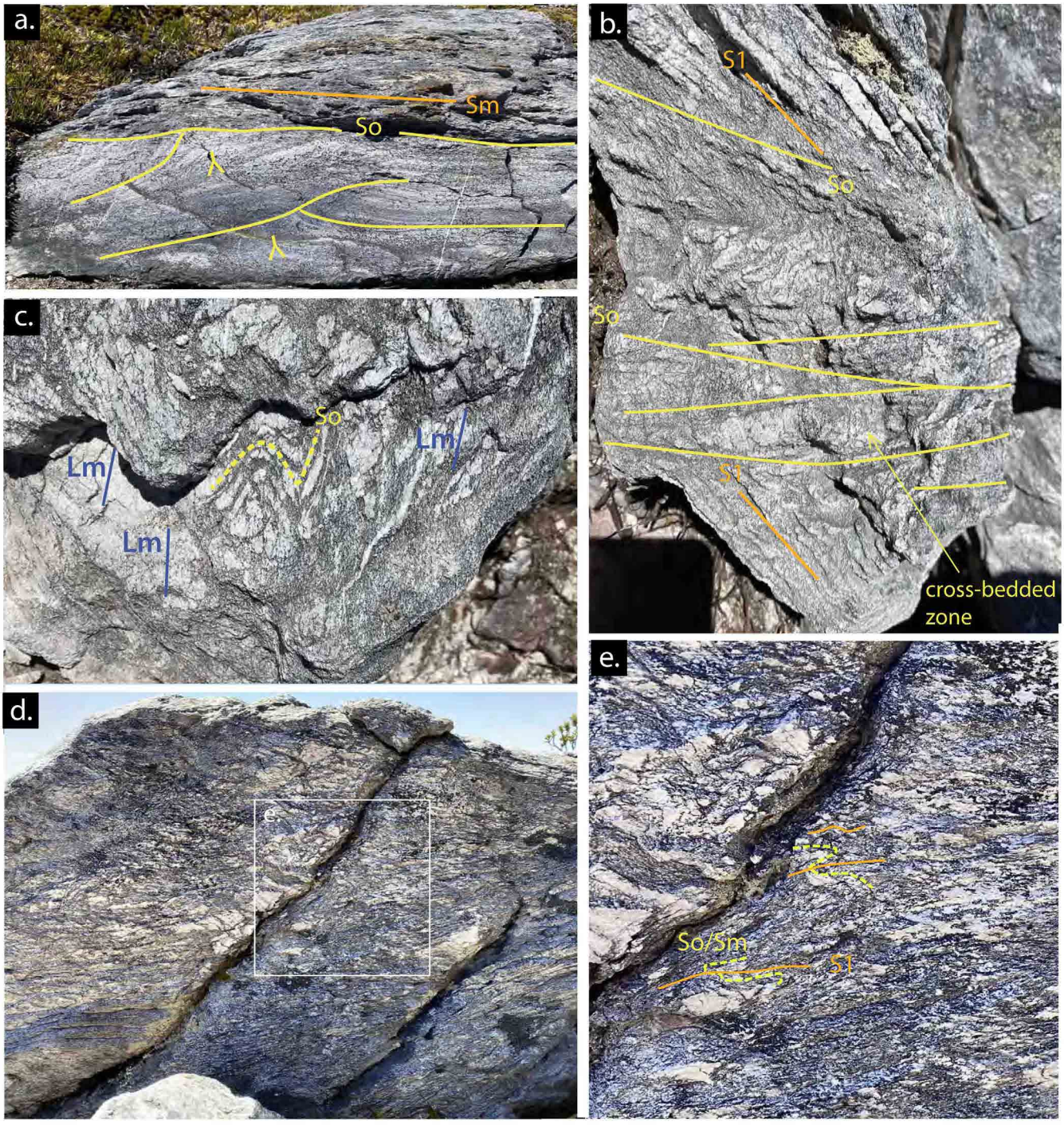

Figure 51. Photographs of bedding and deformation fabrics in low-strain quartzite/ quartz sandstone in footwall to the inferred fault north of Haven Lake. All photos are from float. a) Cross-bedded quartzite with the adjacent phyllite showing intense foliation Sm (orange line trace). b) Cross-bedded quartzite with spaced, slaty-type primary cleavage (S1: orange line traces). c). View onto foliation Sm planes in quartzite showing a strong lineation Lm (blue line traces) and curvilinear fold hinges in So (yellow dashed line traces) flattened in Sm with incipient rodding. d) Folded disrupted sedimentary layering (see folds top left), with enlargement in e) showing closer view of transposed, folded discontinuous layering and relict fold hinges (yellow dashed lines) cut and enveloped by an S1 spaced cleavage fabric.

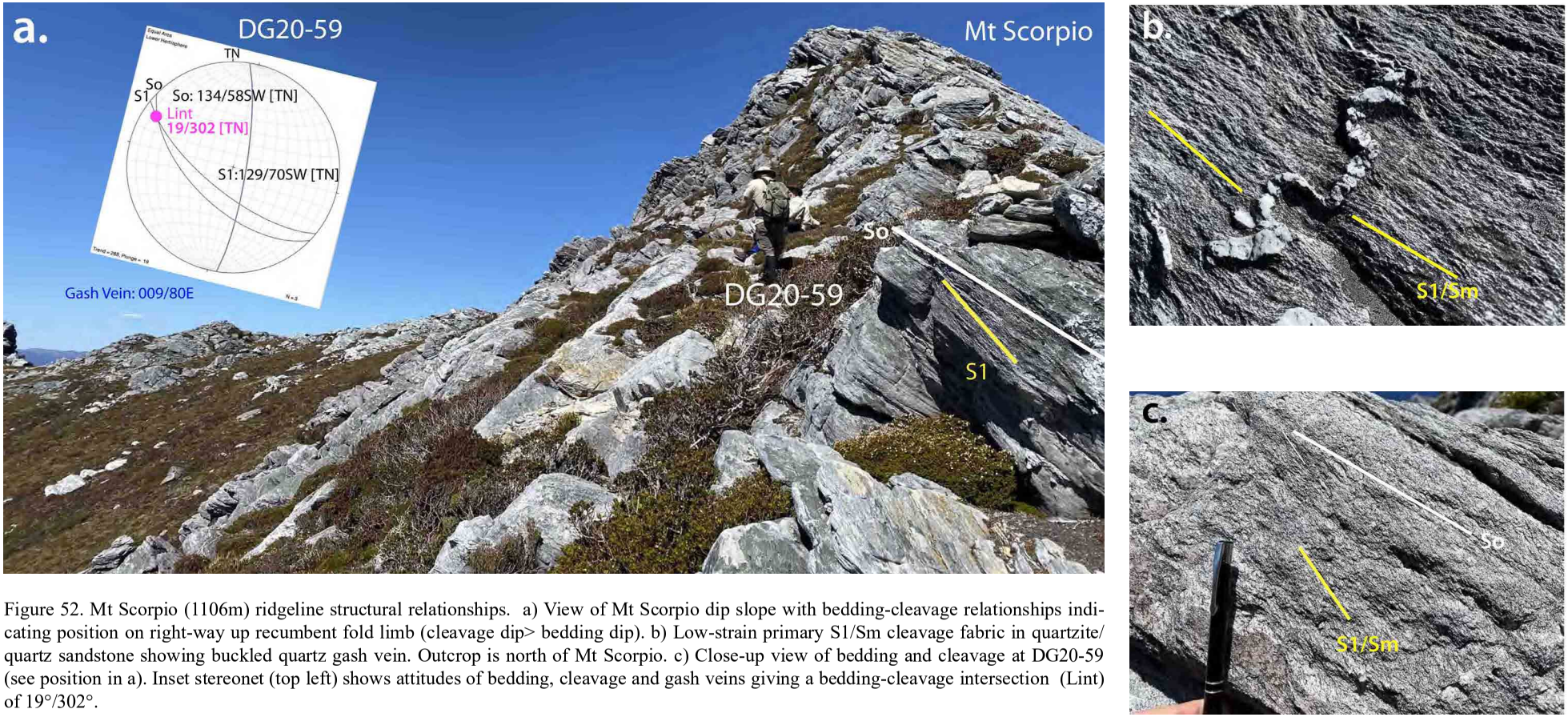

Figure 52. Mt Scorpio (1106m) ridgeline structural relationships. a) View of Mt Scorpio dip slope with bedding-cleavage relationships indicating position on right-way up recumbent fold limb (cleavage dip> bedding dip). b) Low-strain primary S1/Sm cleavage fabric in quartzite/quartz sandstone showing buckled quartz gash vein. Outcrop is north of Mt Scorpio. c) Close-up view of bedding and cleavage at DG20-59 (see position in a). Inset stereonet (top left) shows attitudes of bedding, cleavage and gash veins giving a bedding-cleavage intersection (Lint) of 19°/302°.

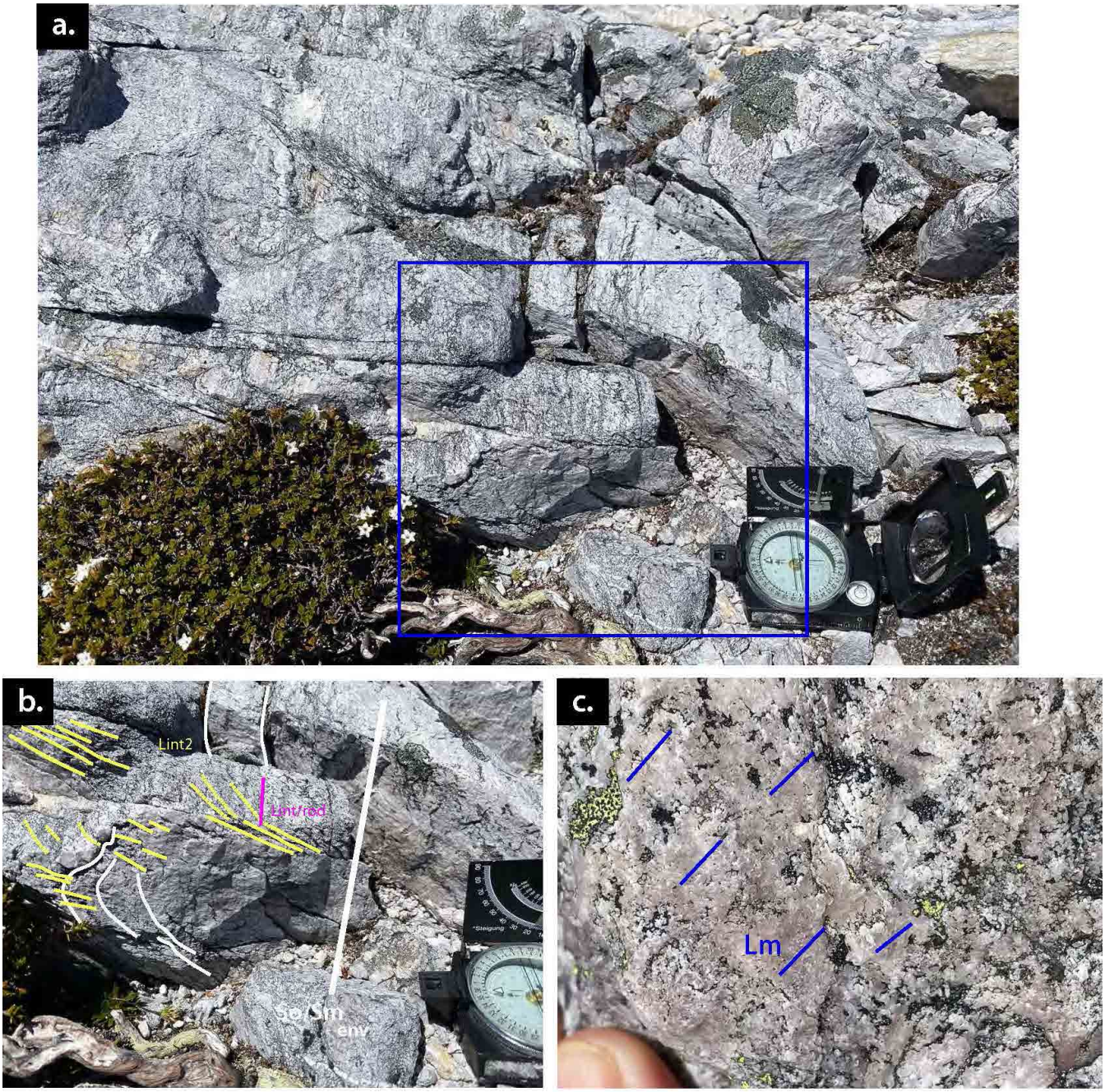

Figure 53. Quartzite and fabrics at DG20-57 (outcrop above Lake Sirona). a) Foliation in banded quartzite (steeply northeast-dipping enveloping surface: to left in photo) intersecting with sub-horizontal, short discontinuous, spaced cleavage (yellow traces in b). Marked colour banding-intersection lineation (Lint: pink line trace in b) shown on foliation surfaces. b) Annotated enlargement of part of a). c) Close view of foliation surface showing a weak Lm defined by occasional white muscovite flakes and a weak quartz grain elongation in parts. Stereonet data shown in Figure 50 inset.

Within the less deformed quartzite/quartz sandstone of the inferred south-closing fold there are some metre-scale zones of stronger deformation (Figure 54). They are characterised by more intense foliation Sm (Figures 51a, c, d and e), partial rodding fabrics (Figure 51c) and localised transposition (Figures 51d, e and 53).

The lower intensity of deformation in the Lake Sirona-Mt Scorpio closure contrasts with the intensely deformed transposition layering in the hanging wall and on the apparent lower limb of the northeast-closing recumbent macro-fold, as seen at Mt Taurus (Figures 55 and 56) and the outcrop at DG20-56 (Figure 57).

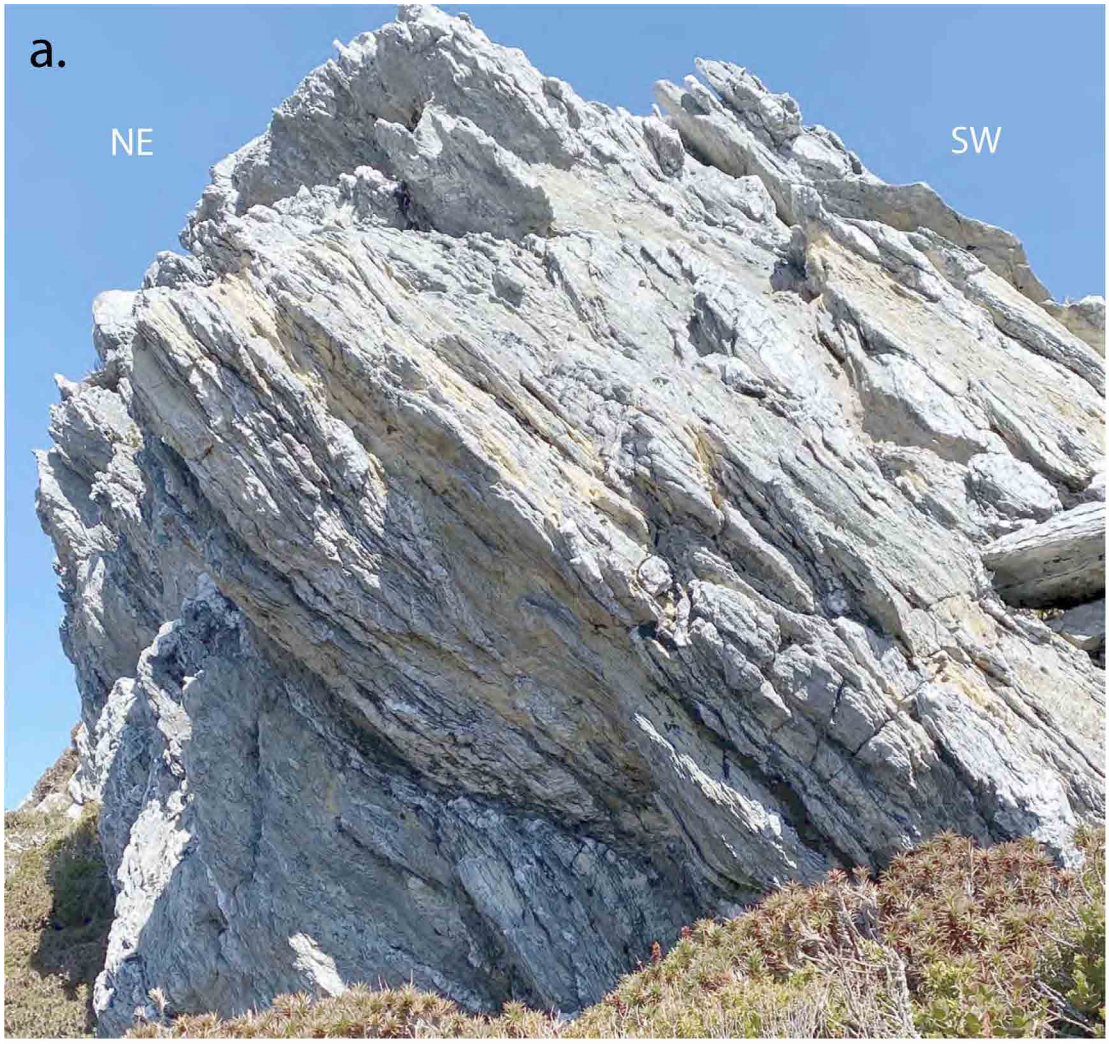

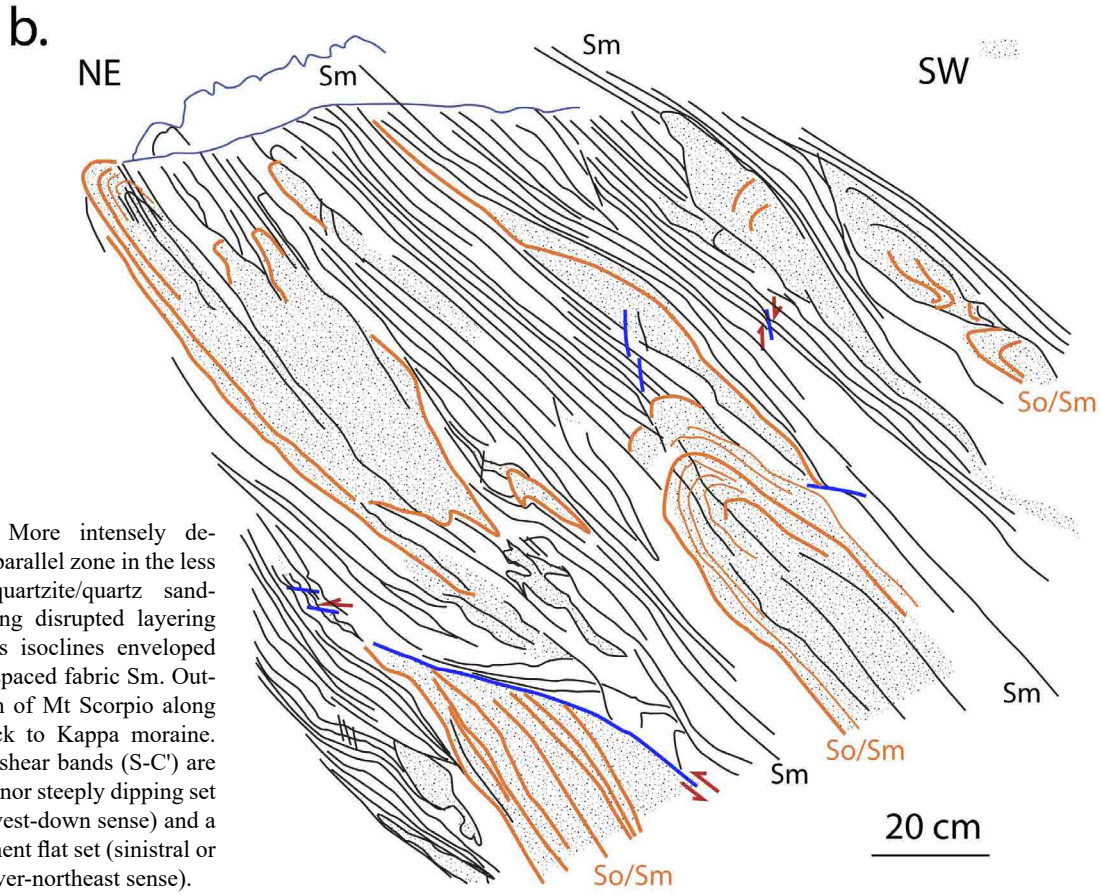

Figure 54. More intensely deformed Sm-parallel zone in the less deformed quartzite/quartz sandstone showing disrupted layering with rootless isoclines enveloped by s strong spaced fabric Sm. Outcrop is north of Mt Scorpio along walking track to Kappa moraine. Two sets of shear bands (S-C') are present, a minor steeply dipping set (dextral or west-down sense) and a more prominent flat set (sinistral or southwest-over-northeast sense).

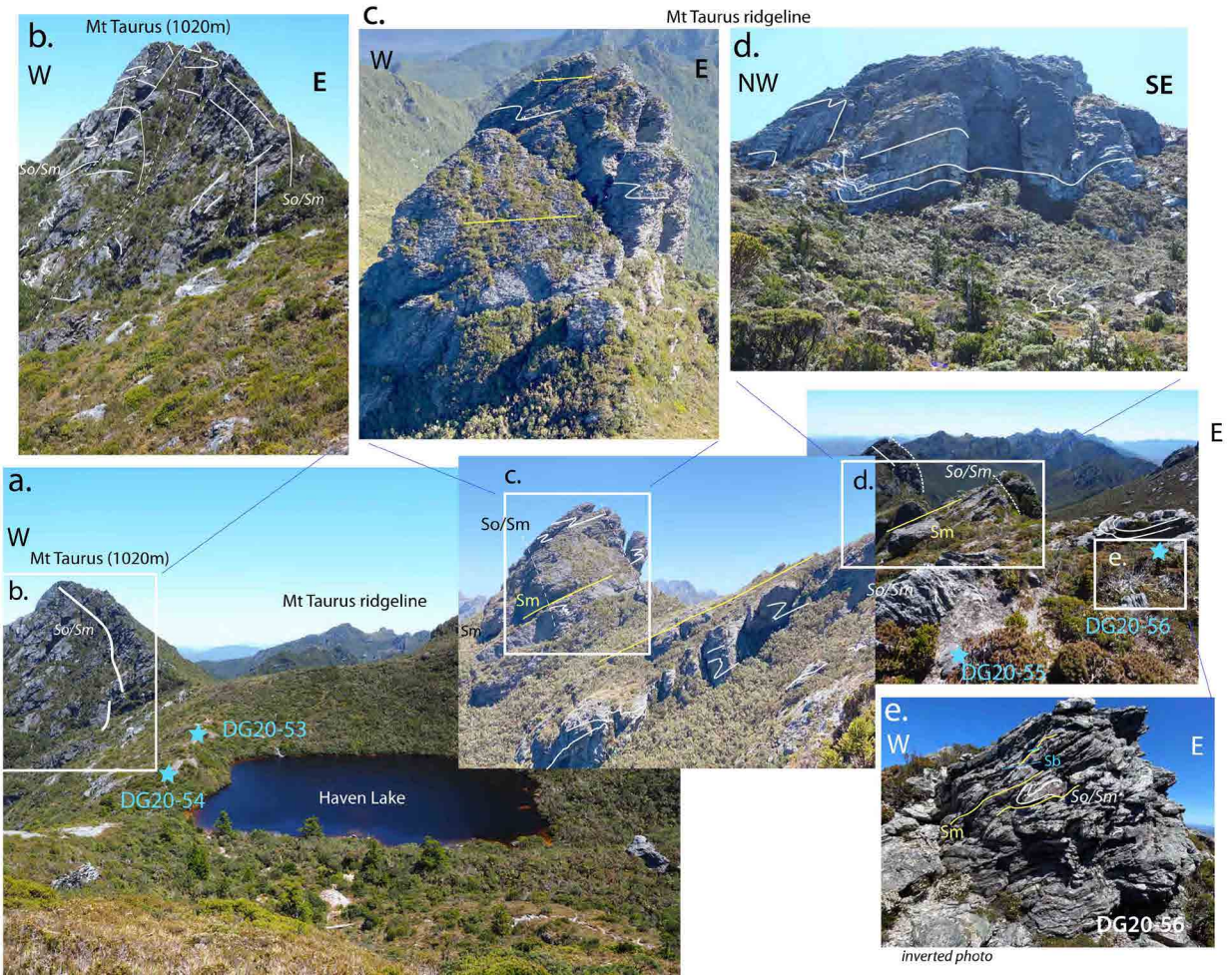

Figure 55. Composite photo along profile Taurus (1020m) ridgeline above Haven Lake. View is to north centred on "bulls head"-like part of Mt Taurus ridgeline (compare with profile in Figure 49). Recumbent macro-fold hinge in hillside (left) shows an up-plunge lower-limb transition into a zone of intense transposition layering (photo right side).

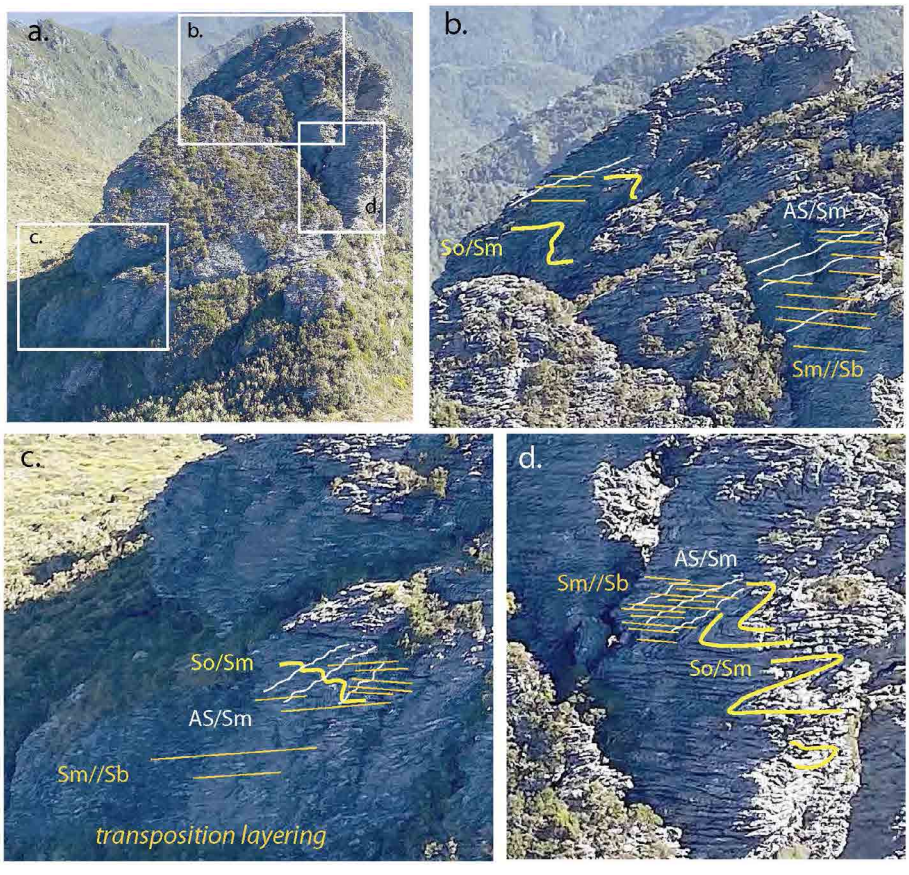

Figure 56 (left). Mt Taurus ridgeline north of Haven Lake showing intense crenulation cleavage/transposition layering development on the apparent "lower limb" of the northeast-closing recumbent macro-fold (see profile interpretation in Figure 49). Fold asymmetry has Z-form (down plunge) and is therefore considered not related to vergence folding on the macro-fold lower limb. View is to the northwest from Haven Lake.

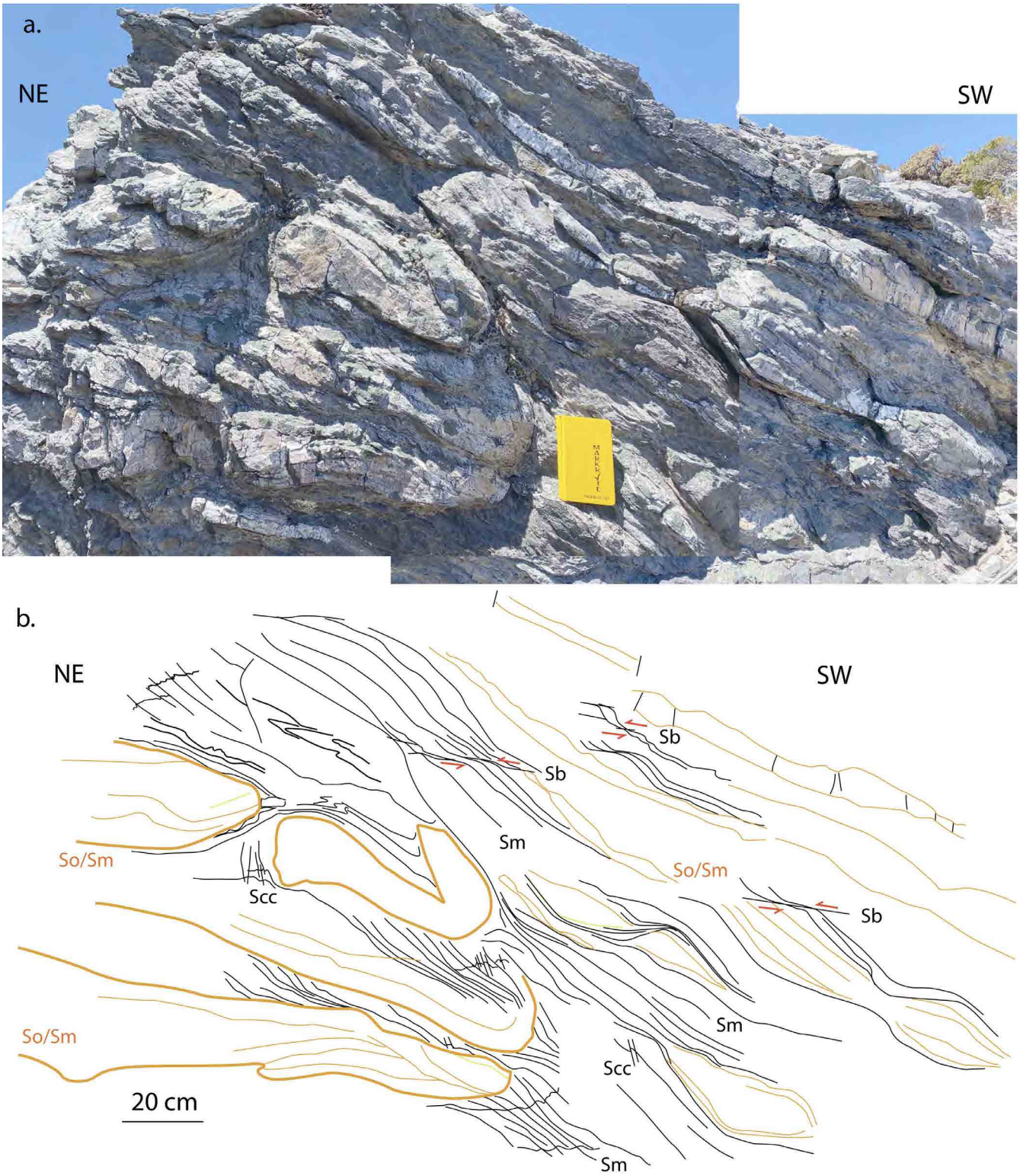

Figure 57. Outcrop DG20-56 showing rootless isoclinal folds in psammitic bands segmented and boudinaged with late shear bands (Sb) showing southwest-over-northeast shear sense. This represents an early stage in the development of transposition layering.

3.2.4.1 Geometry and Structure at the eastern end of the Western Arthur Range and transition with the Eastern Arthur Range Structure (Figure 59)

1. East of Mt Scorpio the geometry and axial surface trace position of the south-closing macro-fold have been dictated by the interpreted attitudes of, and relations between, bedding and cleavage in Figure 58. The view towards Mt Canopus over Promontory Lake suggests that the fold continues through to at least Mt Canopus (Figures 58 and 59). The fold hinge-line at Mt Scorpio is 30°/271° (Figure 48b). Pencil structure in low-grade pelite near where the photo was taken above Kappa Moraine gave Lstretch as 25°/280°, indicating that the macro-fold axis is sub-parallel to regional stretching direction.

2. The northwest-closing macro-fold axial surface trace continues through Centaurus Ridge to the West Portal with the hinge is exposed in the lower knoll south of West Portal peak (Figure 29b and c).

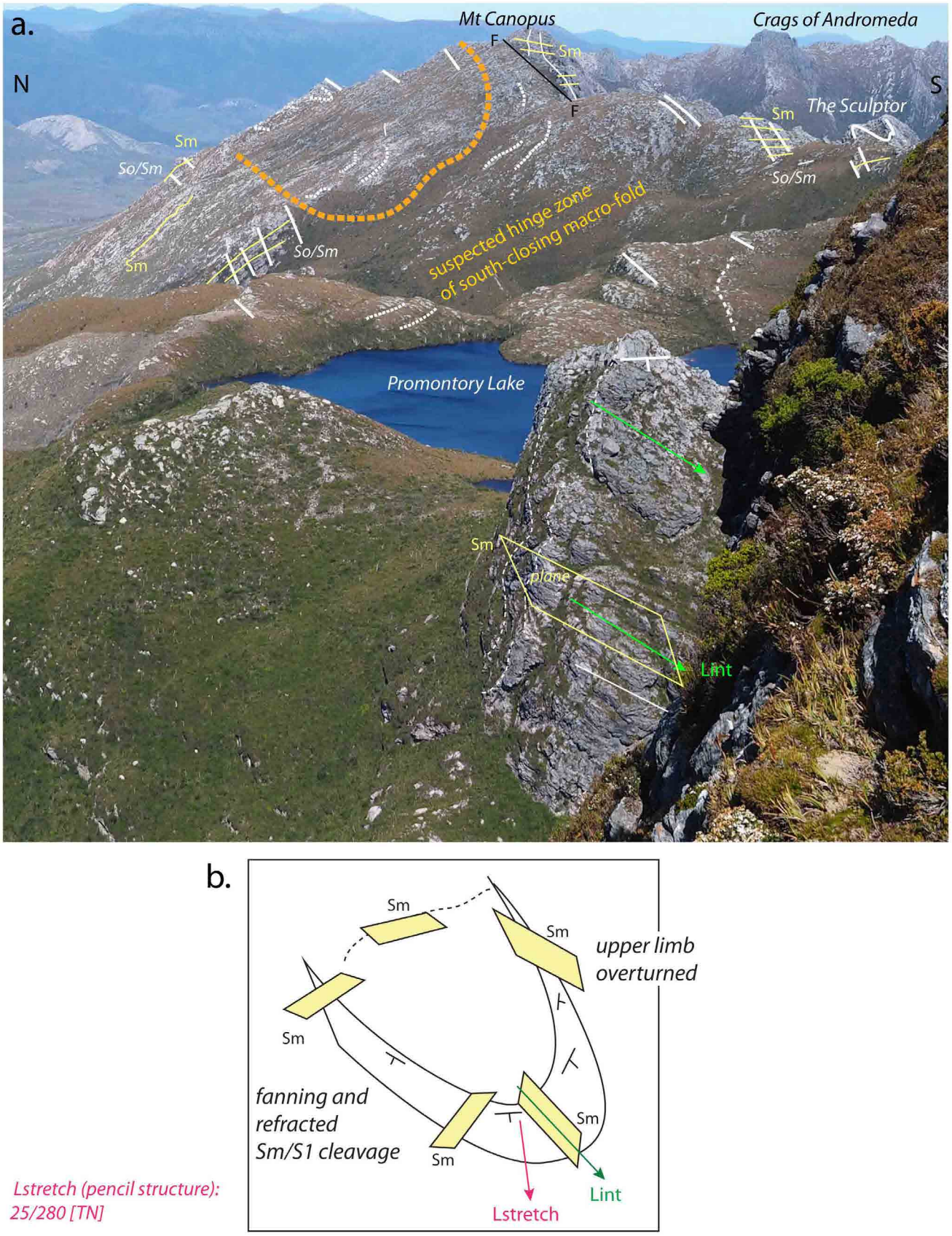

Figure 58. a) Apparent closure of the south-closing macro-fold with the hinge region enclosing Promontory Lake. The view is to the east over Promontory Lake to Mt Canopus (1060m) from the head of Kappa Moraine. The primary S1 cleavage (yellow Sm) is fanning and also appears refracted across layering defining the fold. The hinge (see knoll in right foreground) suggests Lint is west-plunging. b) Sketch of the inferred tight to isoclinal, fold geometry with the inferred west-plunge.

green line: intersection lineation between So/Sm and S1/Sm (Lint)
pink line: direction of stretching lineation (Lstretch) given by pencil fragments in pelite
yellow rectangles: local planar attitudes of the foliation Sm (S1) at different positions around the closure.

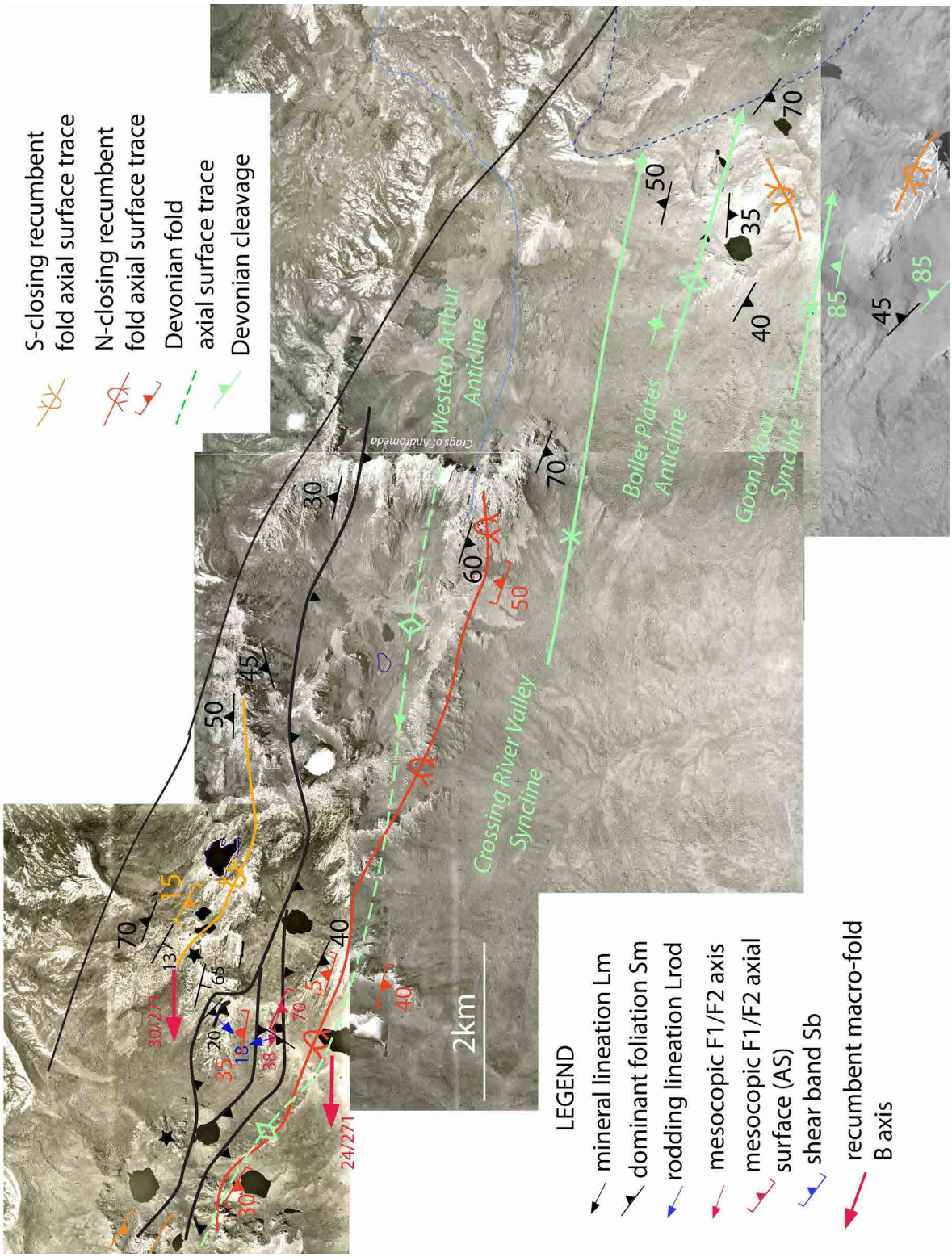

Figure 59. Structure map of the eastern end of the Western Arthur Range from Mt Capricorn to the Crags of Andromeda overlapping with the northern end of the Eastern Arthur Range. The map base is stitched, non-registered Department of Lands air photographs. The structure map shows the structural transition between the Western and Eastern Arthur Ranges. Major map structures include reverse fault traces (heavy black lines), the recumbent isoclinal macro-fold axial surface traces (red trace: northeast-closing recumbent macro-fold; orange trace: the southwest-closing recumbent fold), and the Devonian regional fold axial surface traces (green dashed line). Attitudes of the axial surfaces of the recumbent folds are shown by the red and orange barbed dip symbols. The early recumbent folds and their axial surfaces are re-folded by the younger Devonian folds.

3. The Western Arthur Anticline is dying out towards the Crags of Andromeda losing amplitude and with consequential significant broadening of the fold hinge zone as seen in the Crags of Andromeda ridgeline (Figures 29 and 30). A calculated β axis across the Crags of Andromeda is 4°/285° (Figure 59).
4. The Crossing River valley and the region between West Portal and East Portal must contain a regional scale Devonian syncline, or a faulted-out syncline, given that: 1. the positions of the Western Arthur Anticline and the Boiler Plates Anticline require an intervening syncline, and 2. So/Sm dips south from West Portal and dips north from the Boiler Plates. The inferred syncline, named the Crossing River Valley Syncline, most likely continues the length of the Western Arthur Range and occupies the Crossing River valley in the west.
5. All structures in the Western Arthur Range appear truncated by the interface "fault" against the Eastern Tyennan domain. The inferred fault runs through the Arthur Plains (Figures 4, 14 and 59).
6. The geometry of both the Devonian folds and the Cambrian macro-folds change into the Eastern Arthur Range (Figures 4 and 59). There is a slight change in strike to the east-southeast for the Devonian axial surface traces and the folds have very gentle east plunge, in contrast to the west plunge in the Eastern Arthur Range. The Cambrian fold geometry is discussed in Section 4 (Eastern Arthur Range).

4.0 EASTERN ARTHUR RANGE

The Eastern Arthur Range is broadly north-north-west-trending and consists of series of alternating north-northeast-trending and northwest-trending ridge segments (Figure 60). The north-northeast-trending ridge segments provide sectional views (red lines in Figures 60b and 61) that have enabled structural profile construction and development of a 3D understanding of the Eastern Arthur Range macro-structure. East Portal (1008m) and the Boiler Plates (1039m) define the northern end of the Range, whereas Geeves Bluff (1165m) and Federation Peak (1225m) the southern end (Figure 60a).

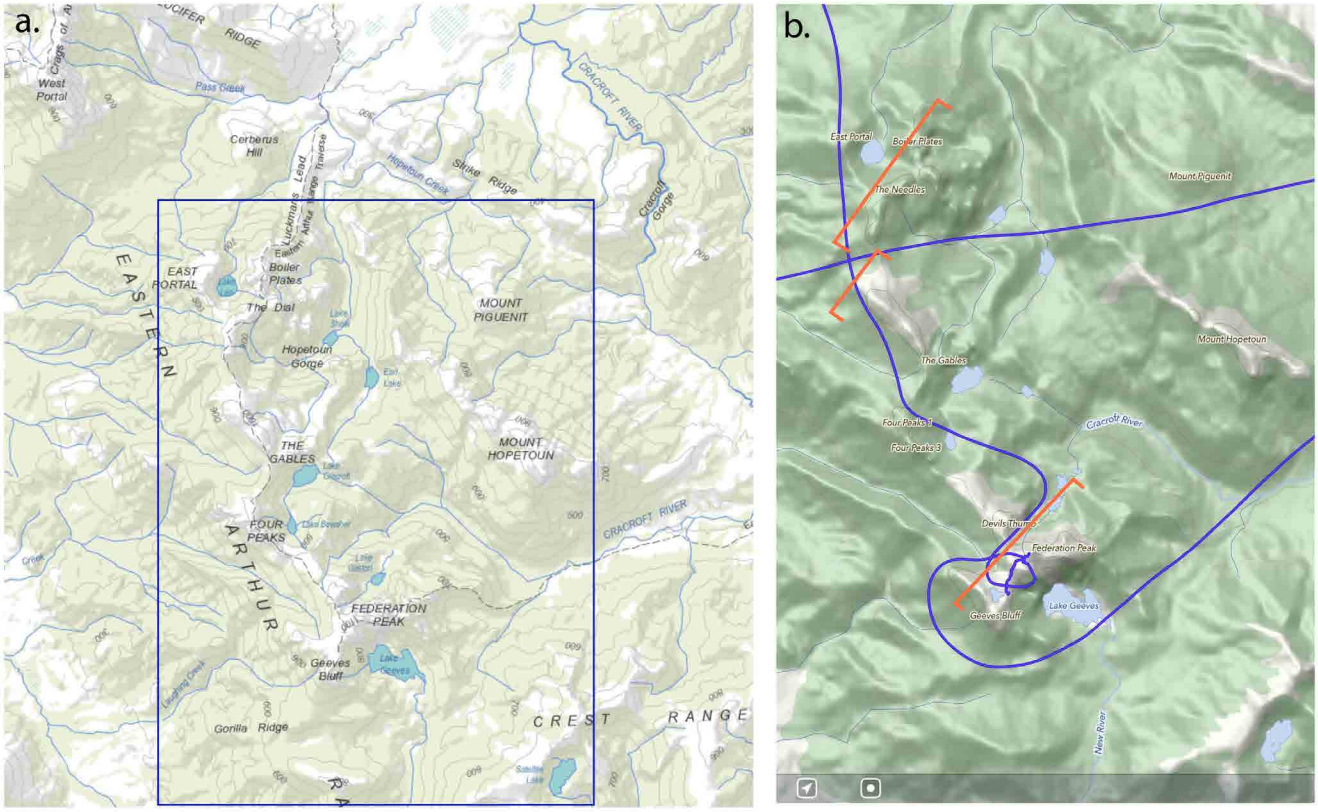

Figure 60. Topographic maps of the Eastern Arthur Range. a) LISTMap. b) MapOutTM DEM shell with helicopter flight path (blue line) and sectional views based on helicopter photographs shown by the red lines.

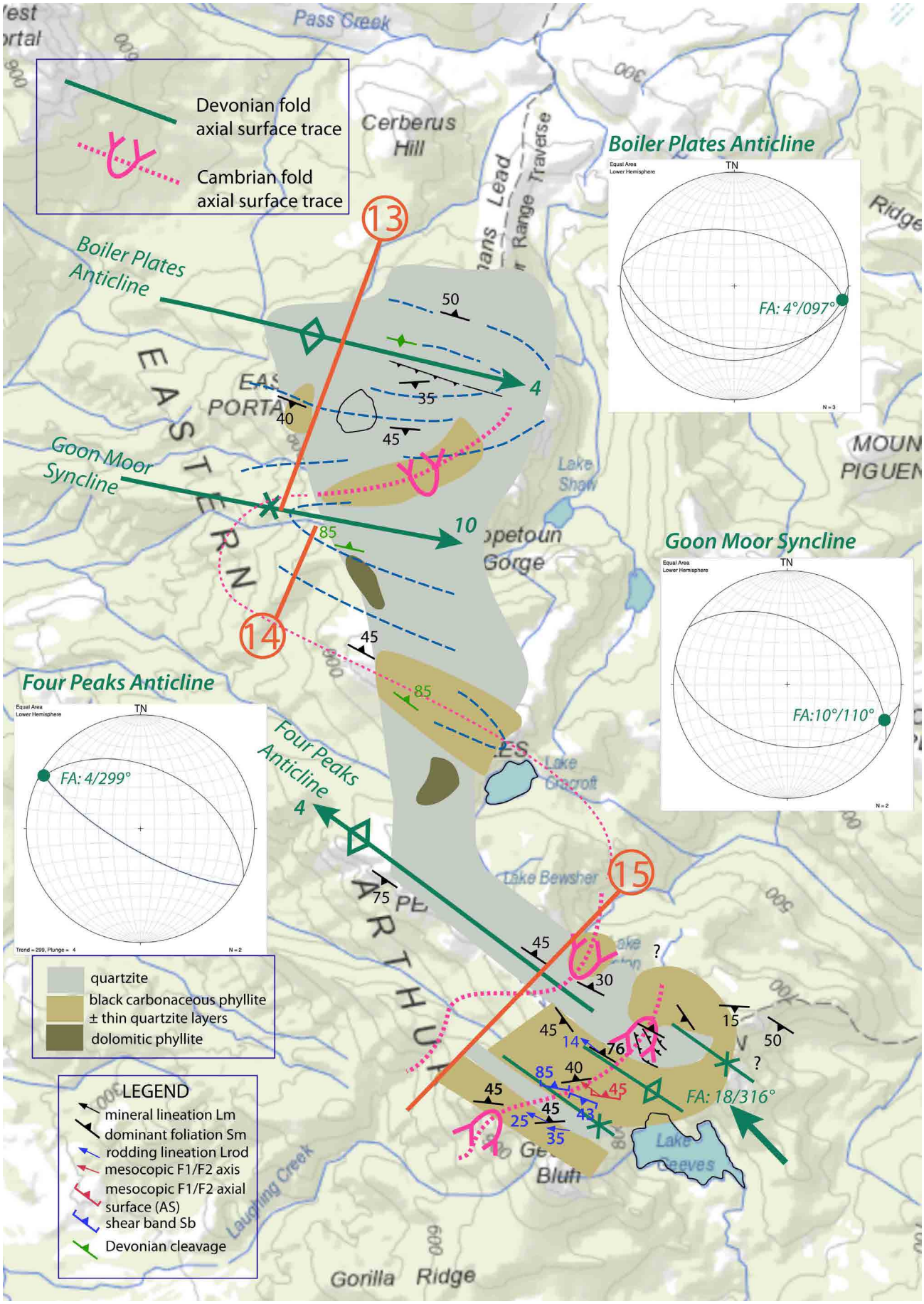

Figure 61. Structure map of the Eastern Arthur Ranges showing lithology, formline traces (blue dashed lines). and structural data. Axial surface traces of early recumbent folds are shown by the orange (southwest-closing) and red (northeast-closing) line traces and late Devonian axial surface traces in green. The positions of section line 13 (Figure 64), section line 14 (Figure 66) and section line 15 (Figure 75) are shown by the red lines with designated circled red numbers. The stereonet insets show the calculated Devonian fold (β) axes for the major Devonian folds. Lithology is based on Taylor (1959) and unpublished notes by Grant Dixon on lithology distribution through the Eastern Arthur Range.

4.1 Structure of the Eastern Arthur Range

The major structural elements incorporated in map (Figure 61) and structural profile form (Figure 62) for the Eastern Arthur Range are:

1. Two, regional-scale, Cambrian recumbent-isoclinal macro-folds as a fold-pair, with a structurally higher southwest-closing closure overlying a structurally lower northeast-closing closure. Hinge zones for these folds can be seen at The Needles and Devils Thumb (southwest-closing hinge zones) and at Geeves Bluff and Federation Peak (northeast-closing hinge zones). The interpreted folds have km-scale dimensions.
2. Three major northwest-trending Devonian folds including the Boiler Plates Anticline, the Goon Moor Syncline and the Four Peaks Anticline refold the Cambrian recumbent folds (Figure 61).
3. A series of broad warpings or undulation in the Federation Peak ridgeline indicates that the Devonian folding is dying out to the southeast (Figure 62).
4. Early-formed Cambrian fabrics including transposition layering with isoclines, rootless folds, internal boudins and shear bands that reflect a southwest-over-northeast shear related deformation.
5. A sub-vertical, northwest-trending Devonian cleavage with axial surface attitude to the anticlines and syncline. This cleavage overprints early-formed fabrics.
6. Devonian and Cambrian hinge zones show slight obliquity (Figure 61).
7. Plunge for both the Cambrian and Devonian folds is generally to the northwest (Figure 61).
8. Northwest-trending, steeply northeast- and southwest-dipping reverse faults cut both the Cambrian and Devonian fold systems.
9. A semi-imbricate, steeply northeast dipping reverse fault system, interpreted as steeply dipping back-"thrusts" cut and displace the Federation Peak macro-fold.

4.2 Eastern Arthur Profiles

4.2.1. East Portal to Goon Moor

The ridgeline from the Boiler Plates to Goon Moor (Figures 63 and 64) shows Devonian upright folds with an anticline at the Boiler Plates cut by a steeply southwest dipping reverse fault, and a syncline at the Goon Moor (Figure 64). The Goon Moor syncline shows a zone of intense cleavage cutting the southern limb (Figure 64).

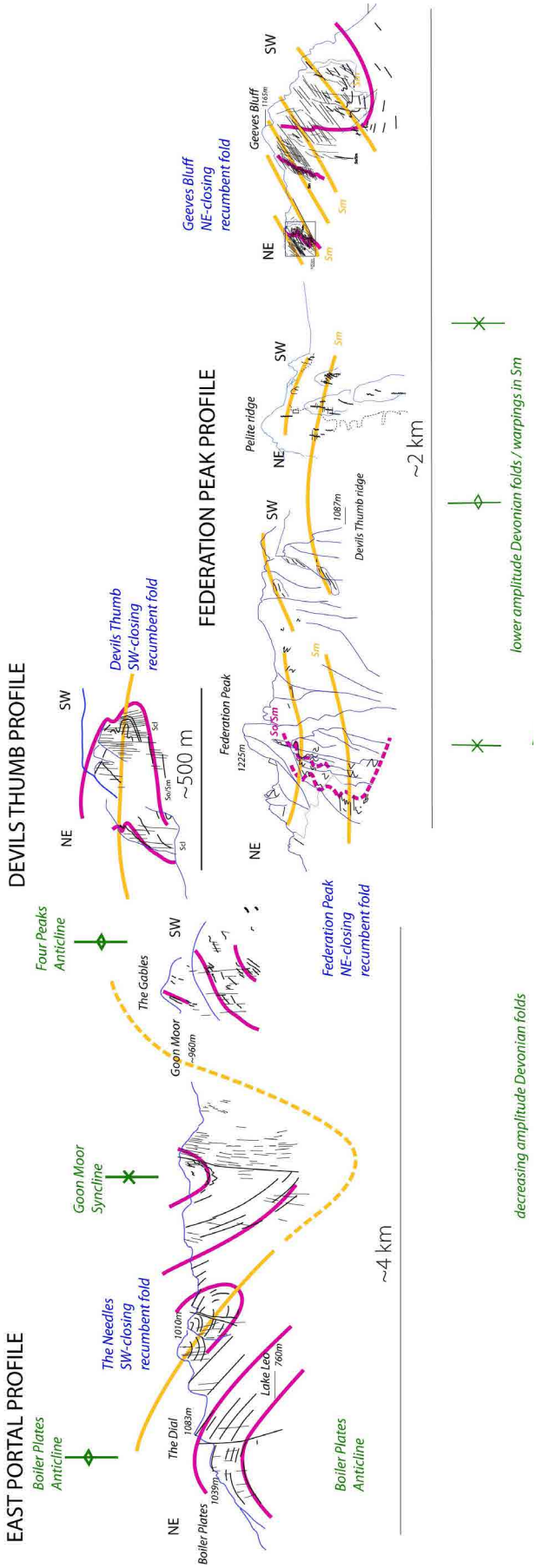

Figure 62. Composite Eastern Arthur Range structural profile based on stitching profiles 13, 14 and 15 shown in Figure 61. These include the offset East Portal profile (Figure 64), The Gables Profile (Figure 66), the Devils Thumb profile (Figure 69) with the Federation Peak profile (Figure 75). The plunges of the folds were used to position the various profile segments in the resultant composite profile (see Figure 76).

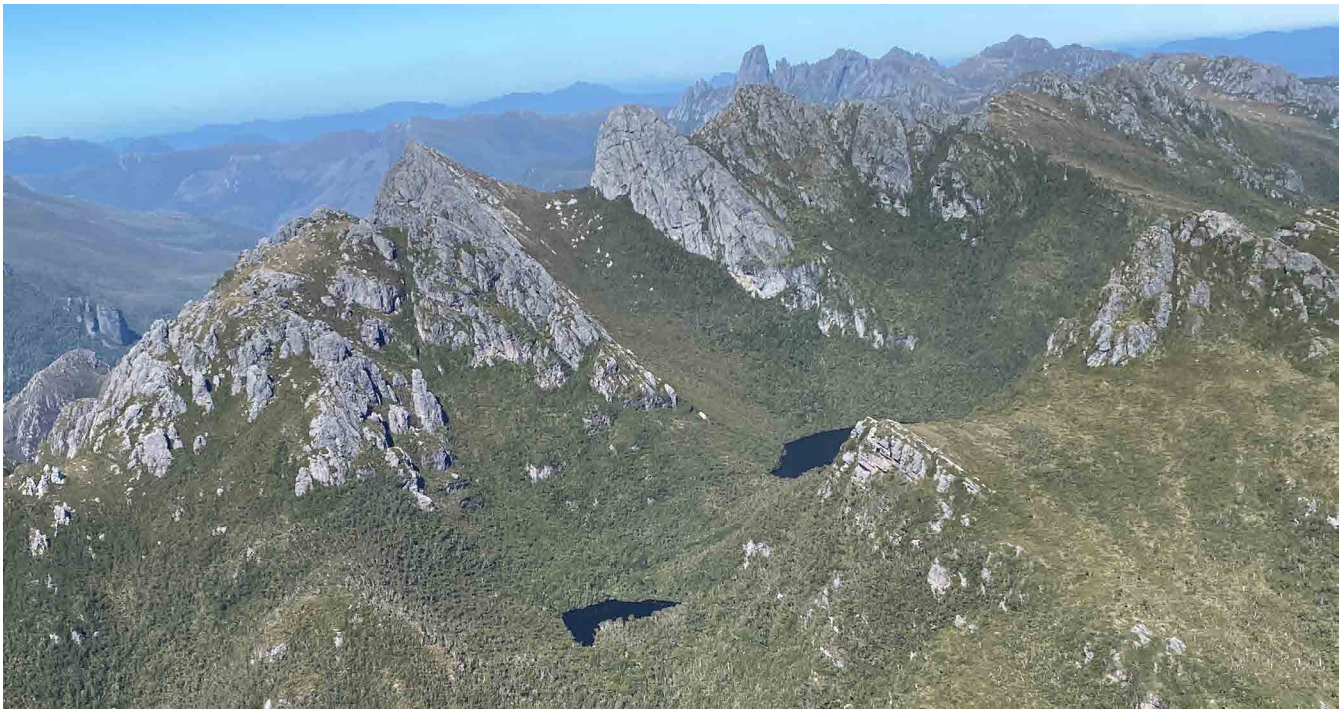

Figure 63. Aerial view of the quartzite ridgeline at the northern end of the Eastern Arthur range showing East Portal (bottom right), the Boiler Plates (photo left) and "The Needles" (upper right) with Federation Peak in the back ridgeline. Lake Leo in photo centre.

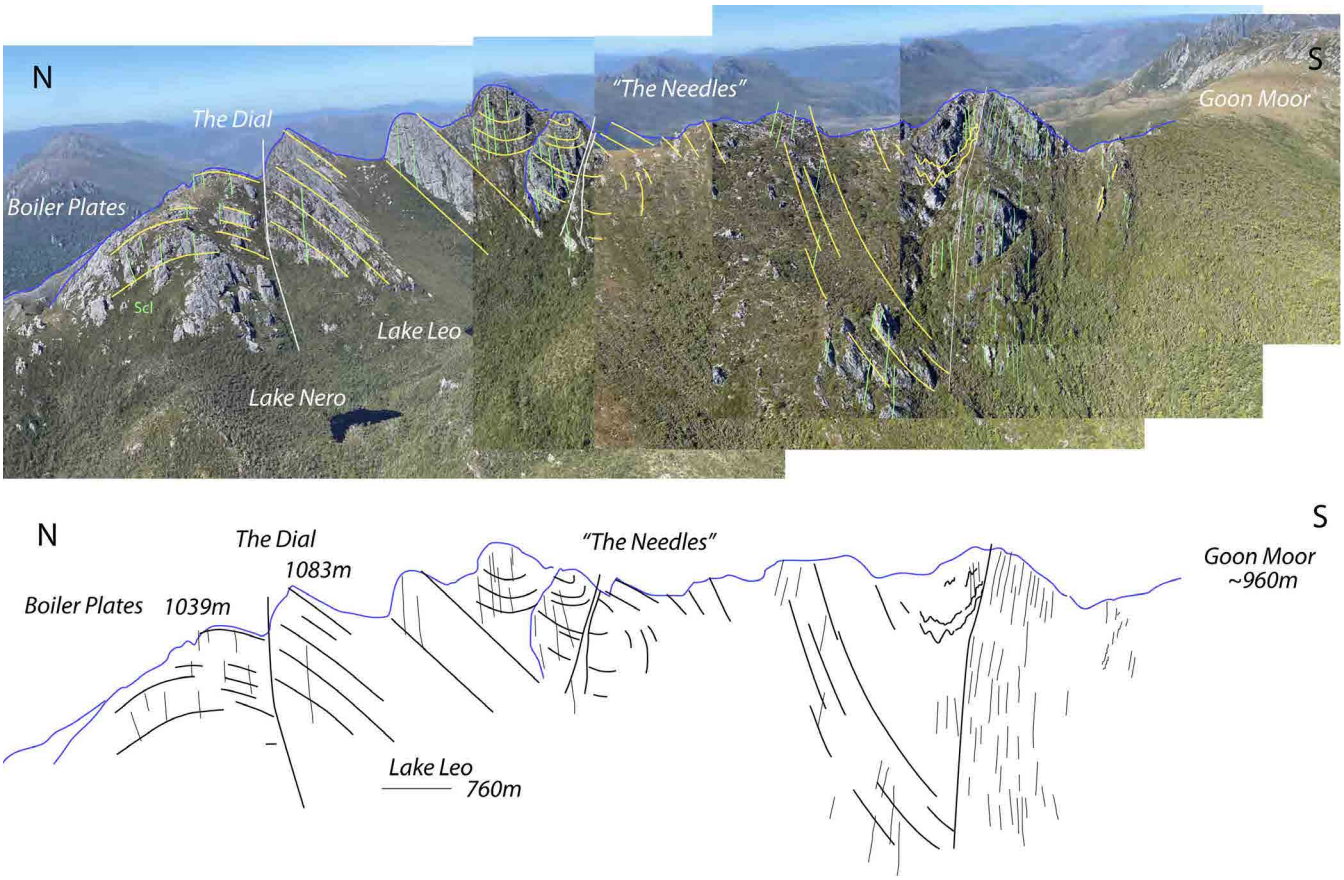

Figure 64. Structural profile (profile 13 in Figure 61) at the north end of the Eastern Arthur Range from The Boiler Plates to Goon Moor. a) Stitched photo base (top) and formline interpretation (bottom). The folded layering is So/Sm and the depicted upright Devonian folds have a sub-vertical cleavage (fine black lines).

"Hidden" within the regional folded So/Sm layering is an early recumbent southeast-closing isoclinal macro-fold at "The Needles" (Figures 64 and 65). This hinge is cut and offset by a series of steeply dipping faults.

4.2.2. Goon Moor to the Gables

Across Goon Moor through to the Gables (Figure 66a) there is a continuation of northeast-dipping So/Sm (see end of profile in Figure 66b and formline interpretation in Figure 67). These photos provide profile 14 in Figure 61. The Gables strike ridge is cut by a steeply dipping foliation (Devonian Scl) with So/Sm defining the northeast-dipping limb of the Devonian Four Peaks Anticline. Taylor (1959, figure 9) identified a recumbent fold through Lake Cracoft below the Gables. Projection of the "Needles" south-closing macro-fold axial surface trace across the Devonian Goon Moor Syncline suggests that the Lake Cracoft hinge is part of the folded, regional scale "Needles" - Devils Thumb south-closing recumbent isoclinal macro-fold (see axial trace interpretation in Figure 61).

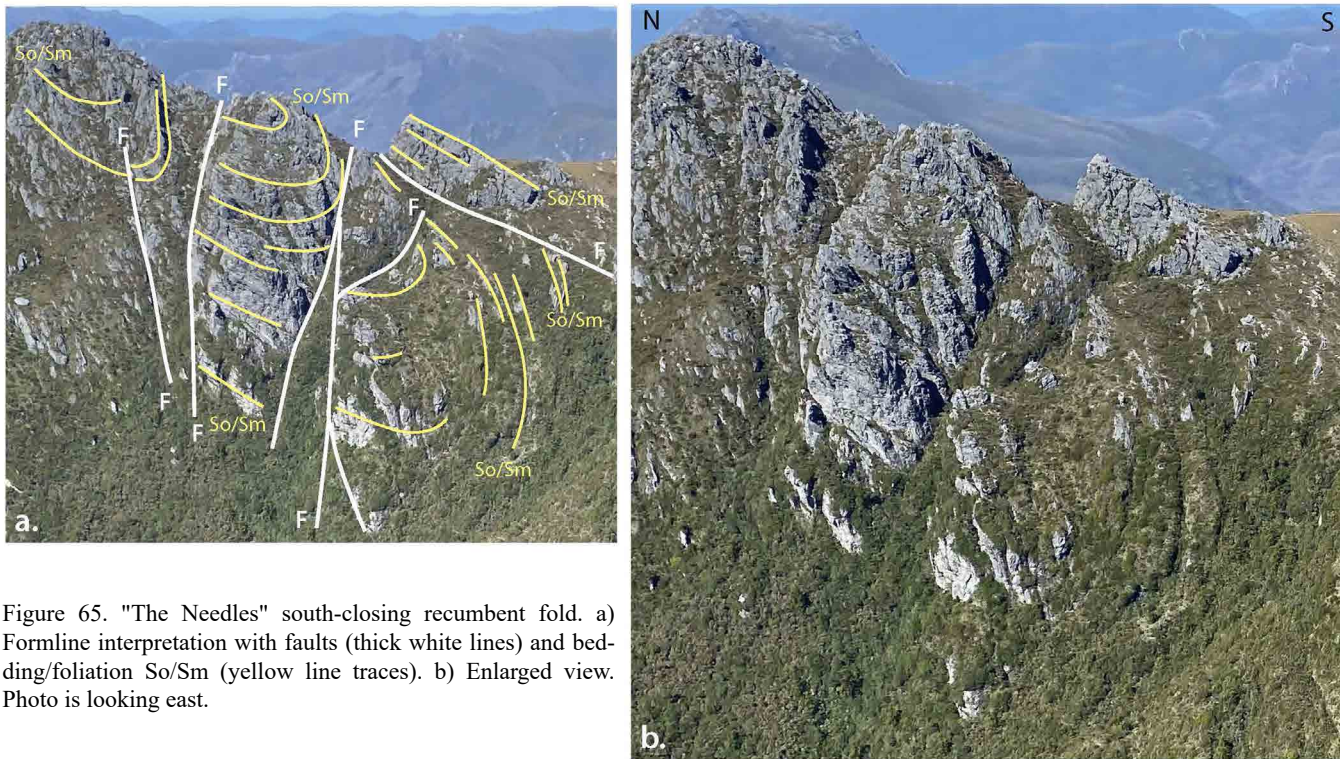

Figure 65. "The Needles" south-closing recumbent fold. a) Formline interpretation with faults (thick white lines) and bedding/foliation So/Sm (yellow line traces). b) Enlarged view. Photo is looking east.

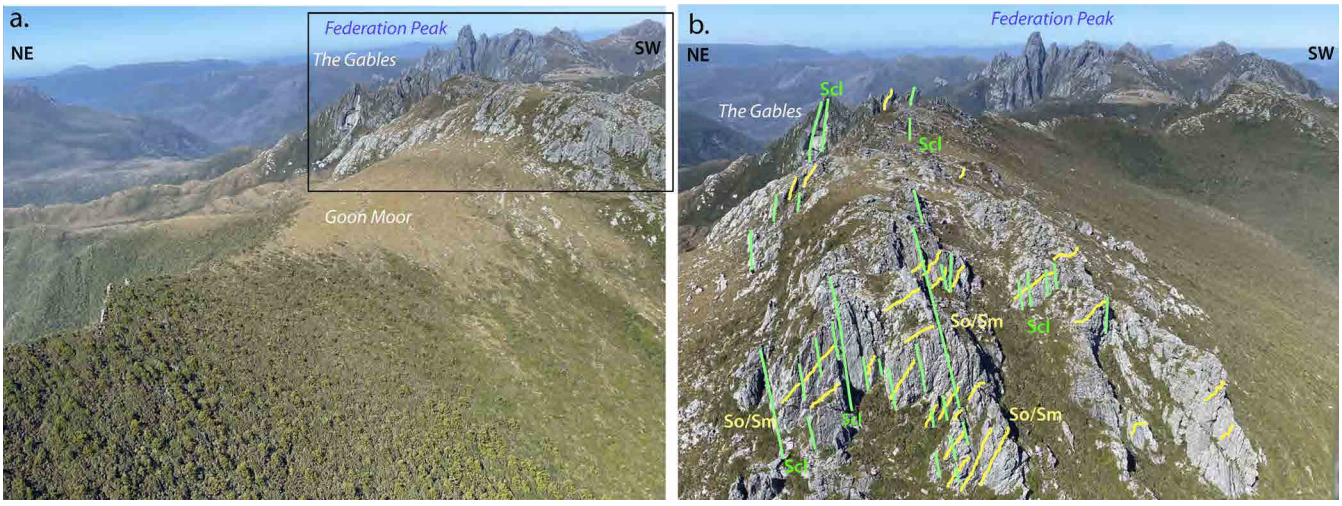

Figure 66. Aerial views from Goon Moor to the Gables ridgeline in a). b) Annotated photo to give structural profile across The Gables. Photo is along strike ridgeline to the Gables from position adjacent to Goon Moor. Yellow: So/Sm; White: overprinting foliation/ Devonian cleavage. This is profile 14 in Figure 61.

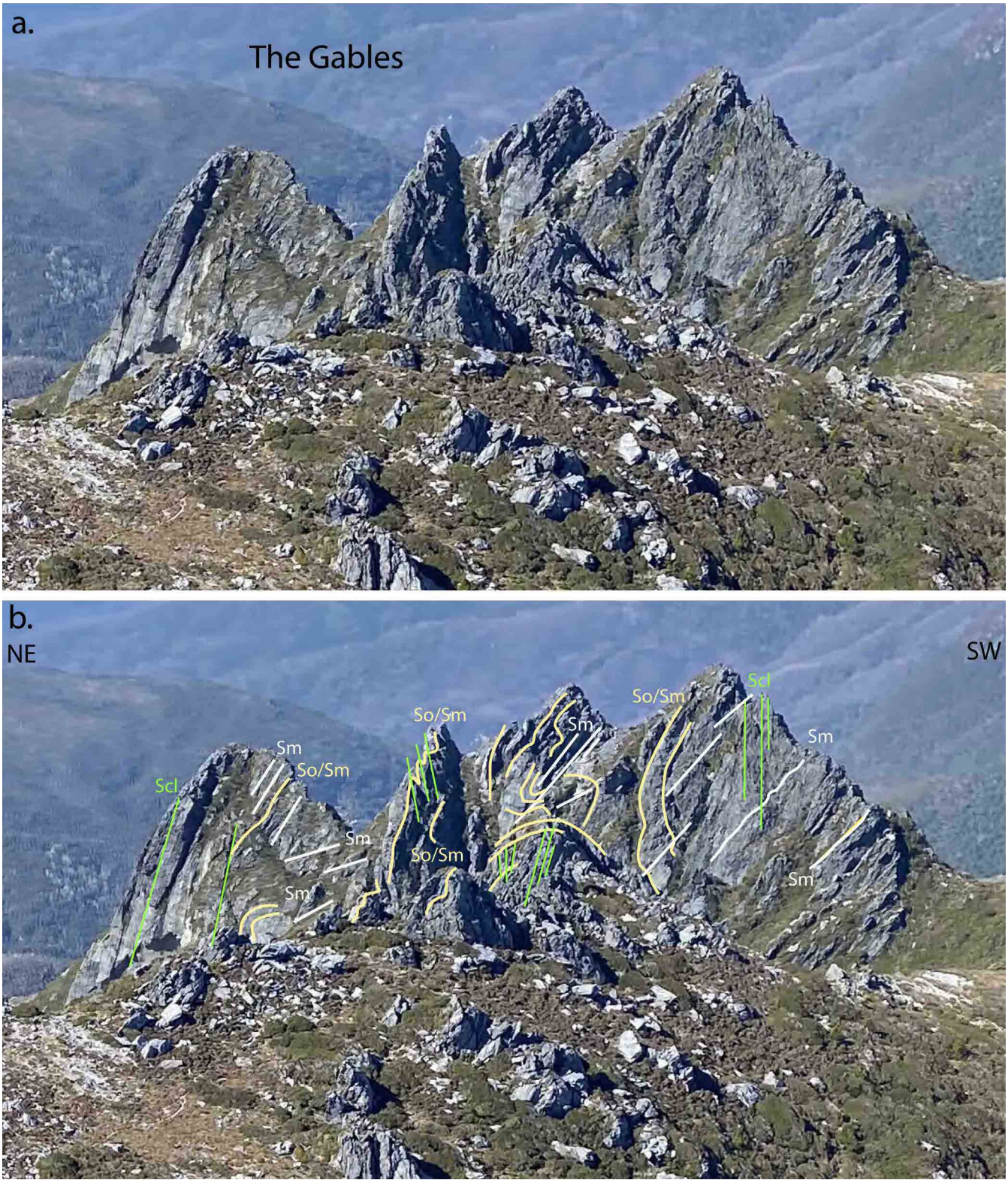

Figure 67. Oblique aerial view of the Gables showing steeply northeast-dipping So/Sm (yellow lines) cut by the dominant foliation Sm (white lines) and by a sub-vertical Devonian cleavage (Scl: green lines).

4.2.3 Four Peaks to Devils Thumb

The Four Peaks photo profile (Figure 68) has undulating sub-horizontal regional Sm that is part of the hinge zone of the Devonian Four Peaks Anticline with a sub-vertical axial surface cleavage(Scl).

The generalised Sm layering contains early recumbent isoclinal hinges that are folded about the Four Peaks Anticline (Figure 68). The steeply southwest-dipping So/Sm enveloping surface in layering in the foreground of Figure 68 suggests the presence of an early-formed, southwest-closing recumbent fold closure. This larger regional scale southwest-closing recumbent fold is apparent in the profile through Devils Thumb (Figure 69, 70 and 71). The hinge zone is visible in both the northeast flank of the Devils Thumb ridgeline (Figures 69 and 70) and in the southeast cliff face of the Devils Thumb (Figure 71). It extends along Thwaites Plateau to the Four Peaks as a zone where the So/Sm enveloping surface in layering is steeply southwest-dipping (see the

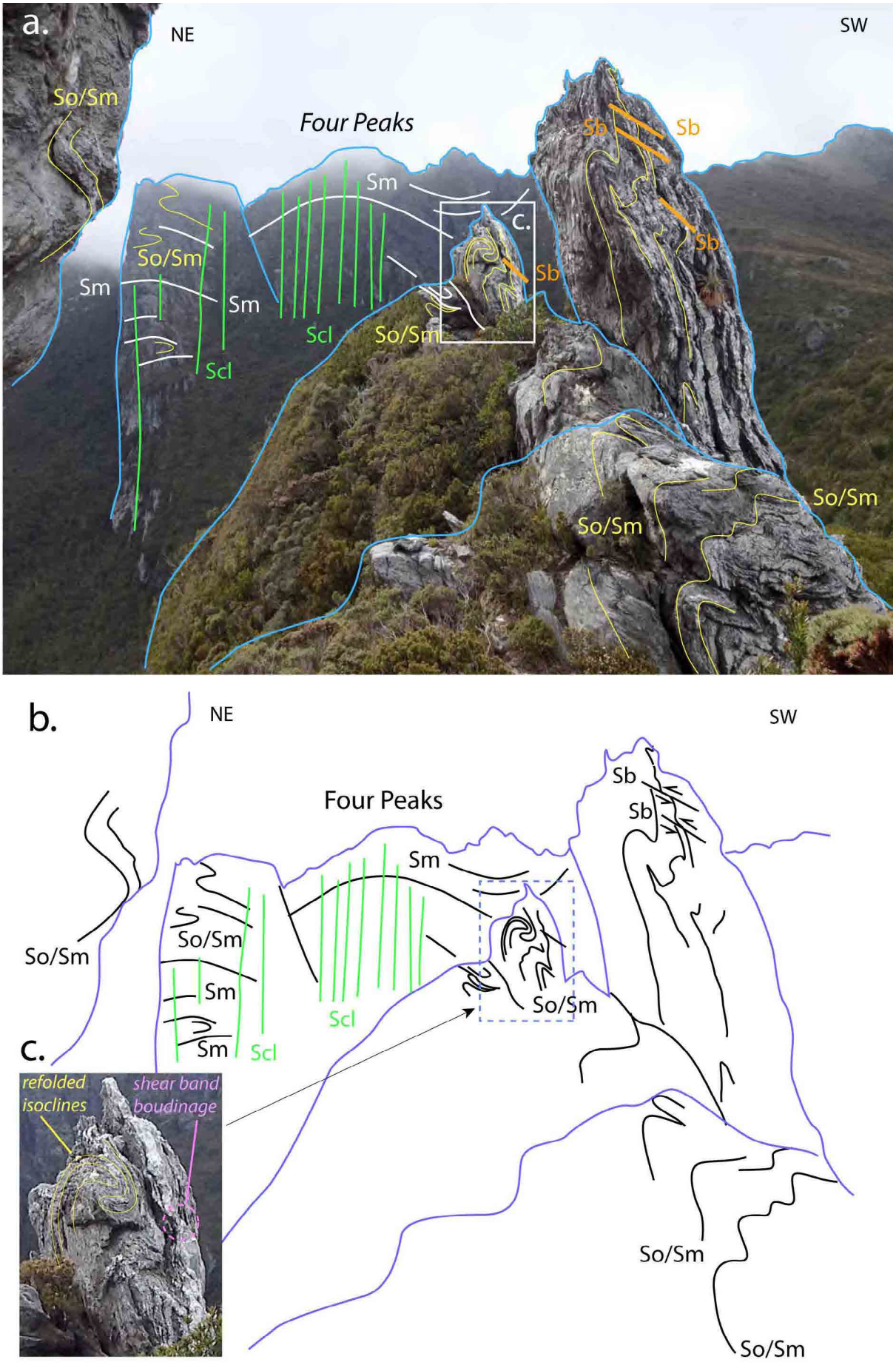

Figure 68. View of Four Peaks (ridgeline at back) showing gently undulating Sm defining the Four Peaks Anticline hinge and So/Sm rollover to the southwest in the foreground as part of the south-closing macro-fold hinge exposed at Devils Thumb. Note early recumbent isoclinal closures within the So/Sm. The rock spire in the foreground shows folded boudinaged So/Sm layering (yellow lines), some rare refolded early isoclines, overturned asymmetric folds with axial surface fabric and shear bands (Sb: orange) with southwest-over-northeast shear sense. (Photo credit: RockMonkey Adventures). b) Formline interpretation of the Four Peaks. c) Enlarged view of refolded folds and shear band boudinage.

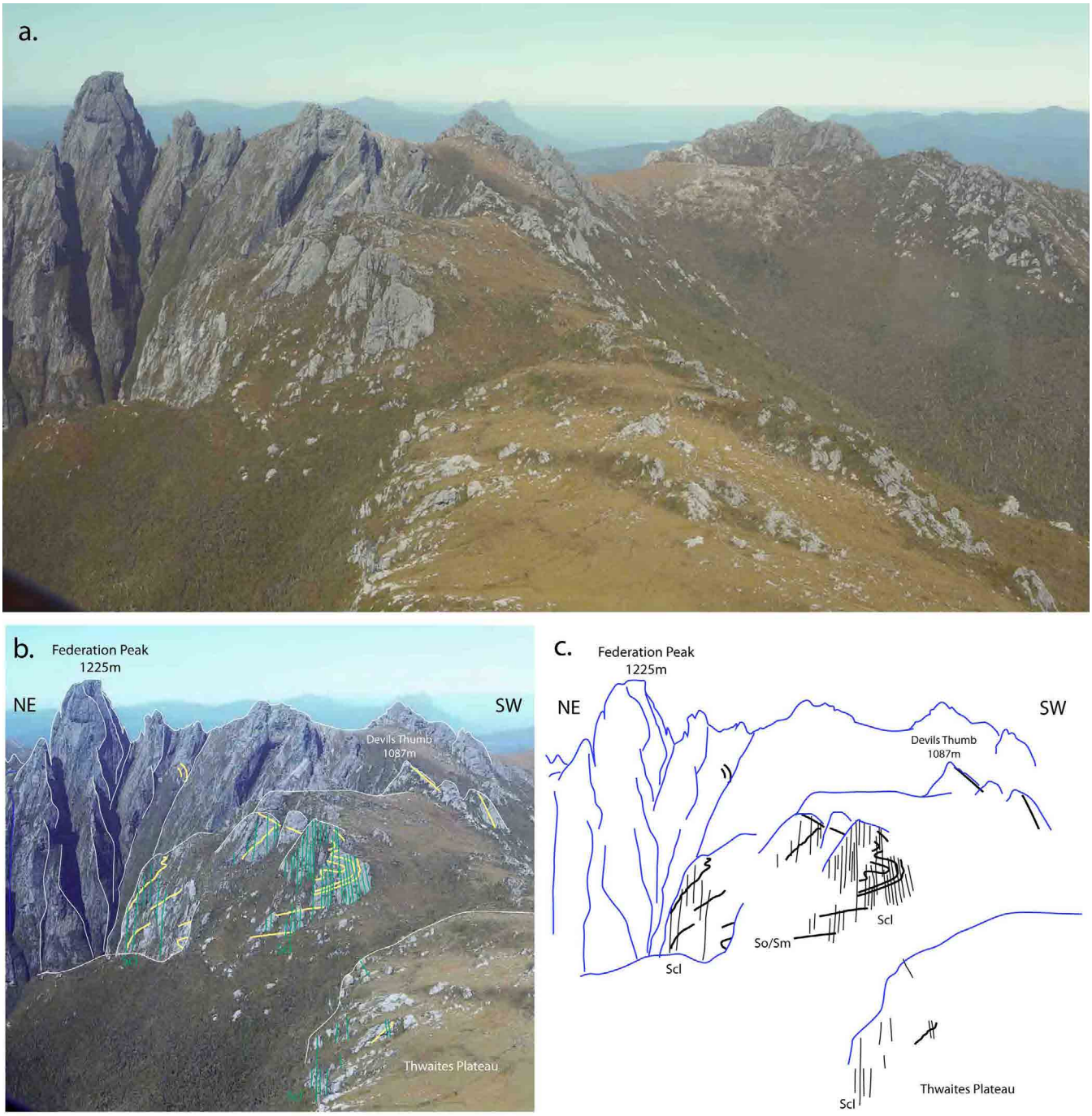

Figure 69: a) View of Thwaites Plateau, Devils Thumb and Federation Peak on ridgeline left and Geeves Bluff on ridgeline right. b) Photo base with formline interpretation of Devils Thumb through Thwaites Plateau. Blue line traces: topographic profile. Yellow lines: So/Sm; thin green lines: Devonian cleavage Scl traces. b) Formline interpretation. Blue line traces: topographic profile. Heavy black lines: So/Sm; thin black lines: Devonian cleavage traces. Compare with Figure 70.

foreground in Figures 68 and 70). A series of smaller, symmetrical recumbent folds occur within the broader southwest-closing macro-fold hinge (Figures 70b and 71).

4.2.4 Federation Peak to Geeves Bluff

Federation Peak (Figure 72) consists of an "upstanding block of quartzite the northern face of which drops almost sheer into a large cirque containing the Northern Lakes" (Taylor, 1959, p.36). The cirque is bounded on the northwest by Thwaites Plateau and on the east by Bechervaise Plateau (Figures 73 and 74). The Geeves cirque on the southeast side forms a 608m back-wall to Federation Peak (Collins, 1999, p.100).

Taylor (1959) identified phyllite in the southeast slopes of Federation Peak in the valley occupied by Lake Geeves. Beyond Federation Peak towards Geeves Bluff the ridgeline is made up of bands of black pelite (carbonaceous phyllite with minor thin quartzite bands) and thin-bedded, white quartzite (Figure 81). Grant Dixon (2021, pers.com.) on numerous climbing expeditions

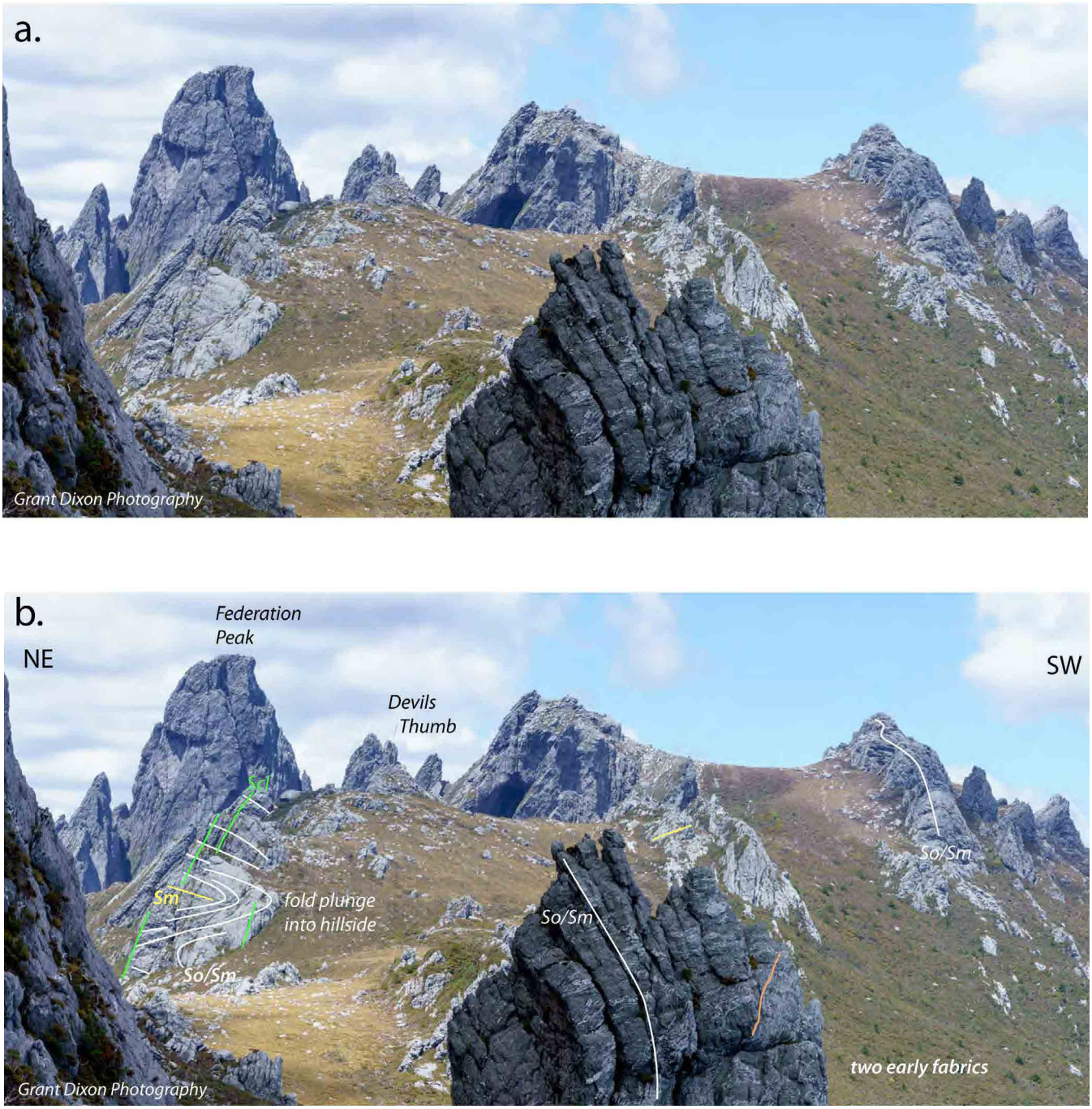

Figure 70. a) View to the southeast of Thwaites Plateau showing Devils Thumb ridgeline in front of Federation Peak. (photo credit: Grant Dixon). b) Formline interpretation of the northeast side of Devils Thumb ridge (photo left) showing macro folds that are part of a major south-closing fold hinge exposed in Devils Thumb (see also Figure 71).

at Federation Peak has identified lithology differences between the upper summit tower quartzite and more phyllitic foliated lithology towards the base of Federation Peak, including Blade Ridge and below on the northwest side. The phyllite lithology also occurs on the spurs running east from Devils Thumb and Thwaites Plateau (Figure 61).

The Federation Peak ridgeline between Geeves Bluff and the Bechervaise Plateau (Figure 73) is cored by a northwest-plunging, north-closing, isoclinal macro-fold that can be seen in the Federation Peak cirque walls (Figures 74 and 75). The ridgeline is also is cut by a series of northwest-trending, steeply northeast-dipping reverse faults (Figures 72 and 73) that form a semi-imbricate fan centered on Federation Peak. This fault set is interpreted as a steeply dipping back-"thrust" system related to the Devonian thrust and reverse faults mapped out in the Western Arthurs.

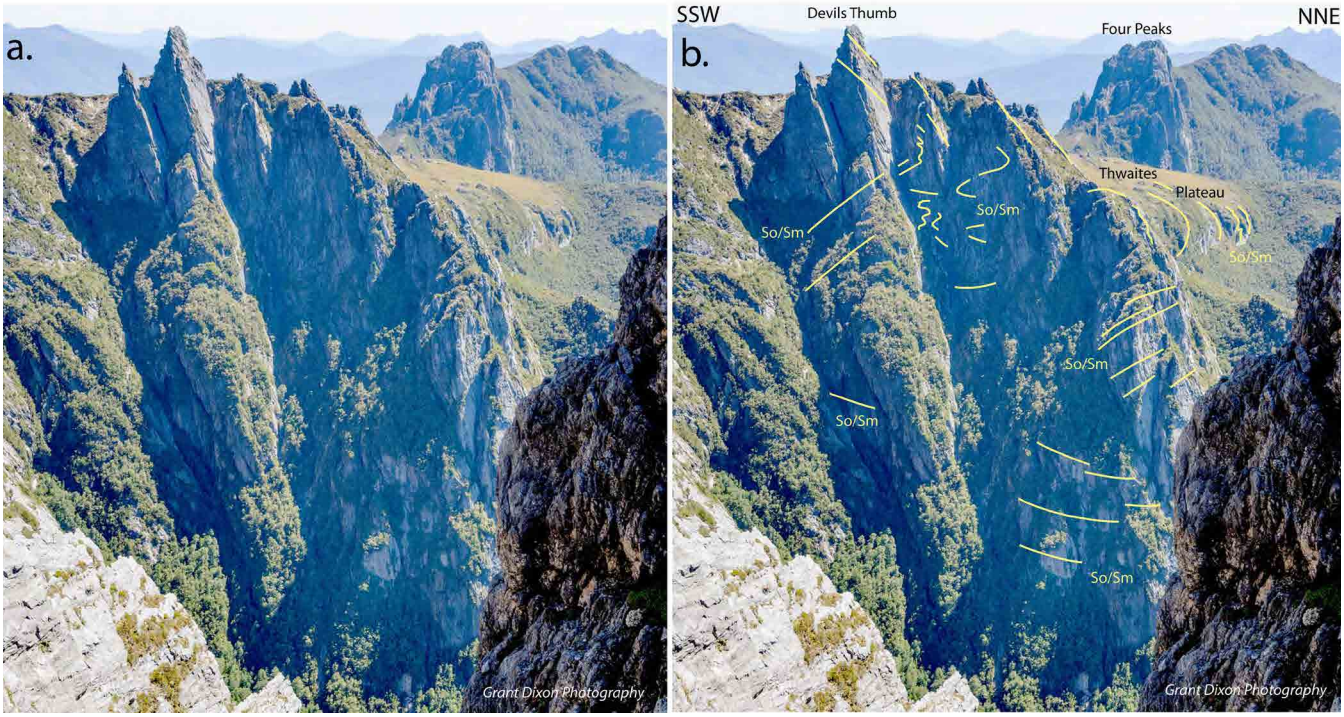

Figure 71. View of Devils Thumb (1087m) with formline interpretation in b) showing a smaller, structurally higher northeast-closing hinge as part of the broader major southwest-closing recumbent fold. View to the west. Compare with Figures 69 and 70. (Photo credit: Grant Dixon)

All the structural elements are west-northwest trending (Figure 74) with ridgelines defining the regional north-west-trending strike. The mineral/stretching lineations at Stations DG20-14, DG20-15 and DG20-16 are all west-northwest trending with gentle west plunges (blue lines on stereonet insets, Figure 74). Variations in Sm across part of the Federation Peak ridgeline provide a Devonian β axis of 28°/316° (Figure 74).

The Federation Peak to Geeves Bluff structural profile (profile 15 in Figure 61) is shown in Figure 75a. It is also based on formline interpretation of oblique aerial photographs taken from a helicopter (Figures 75b, 77, 78, 80 81 and 87) as well as photographs taken along the ridgeline (Figures 79, 82, 83, 84 and 86). The profile shows broad warping or gentle undulations in the regional Sm (orange lines in Figure 75a) that is axial surface to a series of recumbent isoclinal macro-folds in So/Sm (pink lines in Figure 75a). These have km-scale hinge dimensions. The undulations in Sm are due to lower amplitude younger Devonian folding at Federation Peak, suggesting that the northwest-trending Devonian folds that define the Arthur Ranges are dying out to the southeast.

The two major, oppositely closing Cambrian macro-folds in the profile (Figure 75) are constructed from superposition of the Devils Thumb photo profile with the Federation Ridge profile that sits approximately 1km northwest of the main ridgeline (Figure 73 and compare with Figure 69). Due to a ~25° plunge of the folds in the Federation Peak ridgeline (Figure 76) the Federation Peak-Geeves Bluff north-closing macro-fold plunges beneath the Devils Thumb south-closing macro-fold (Figure 76) and is therefore structurally lower as shown in Figure 62.

The Federation Peak - Geeves Bluff ridgeline profile (Figure 75) is made up of several components that have been used to construct the profile. These include from northeast to southwest:

1) Northeast-closing Federation Peak recumbent macro-isocline (Figure 77)

Another part of the Eastern Arthur Range fold-nappe geometry is a So/Sm formline interpretation of the north and south faces of Federation Peak (Figures 77, 78 and 80). These suggest the presence of a northeast-closing recumbent macro-fold. The interpretation will require closer inspection and field checking, due to the effects of the Pleistocene glaciation, as well as jointing, faulting and vegetation (see Figure 72). All these make structural interpretation of the cirque wall-faces of Federation Peak difficult (Figures 77, 78 and 80).

The summit also contains a smaller, northeast-closing recumbent fold hinge (Figure 79) with a gently north-east-dipping axial surface foliation Sm. Close up views of the summit lithology shows a strong overprint by the younger Devonian cleavage (green lines traces Scl in Figure 79d). This cleavage is axial surface to the regional folds such as the Four Peaks Anticline.

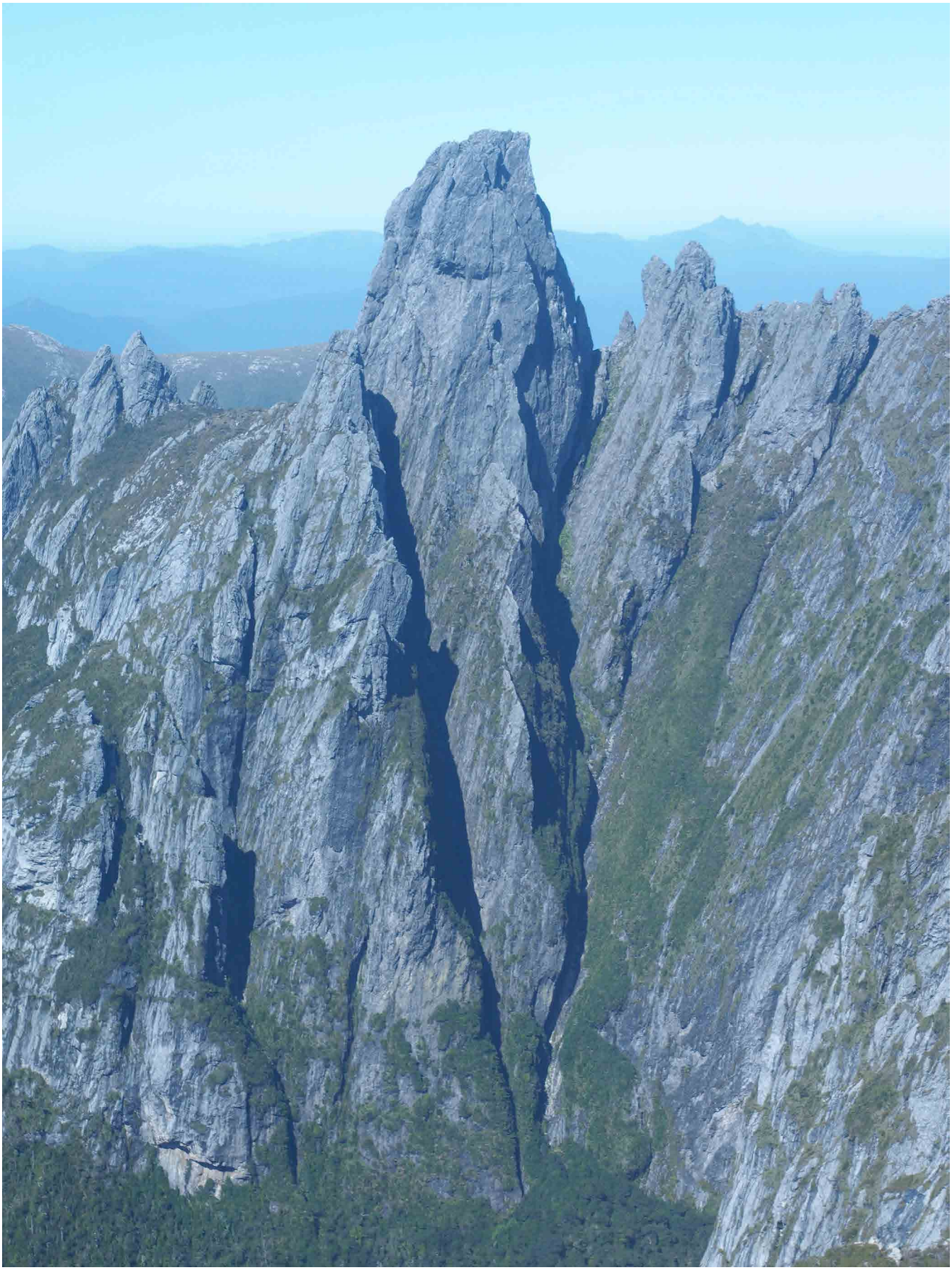

Figure 72. The ice-sculptured, northwest face of the iconic Federation Peak (1225m) showing the jagged and rugged nature of the quartzite ridgeline and the sheer drop into the Northern Lakes cirque (including Lakes Gastens, Payens and Dragonfly). The ridgeline is cut by a steeply east-dipping fault system. No apparent macro-structure is readily discernable, apart from the second- or third order, north-closing recumbent in the summit tower peak. View is to the southeast.

"...The great fang of Federation Peak sighted from near or distant mountains is the sentinel mountain of the South-West....It is a spectacular peak cut back to its massive horn shape by deep cirque glaciers- flint hard in its grey quartzite" (Collins, 1990, p.286).

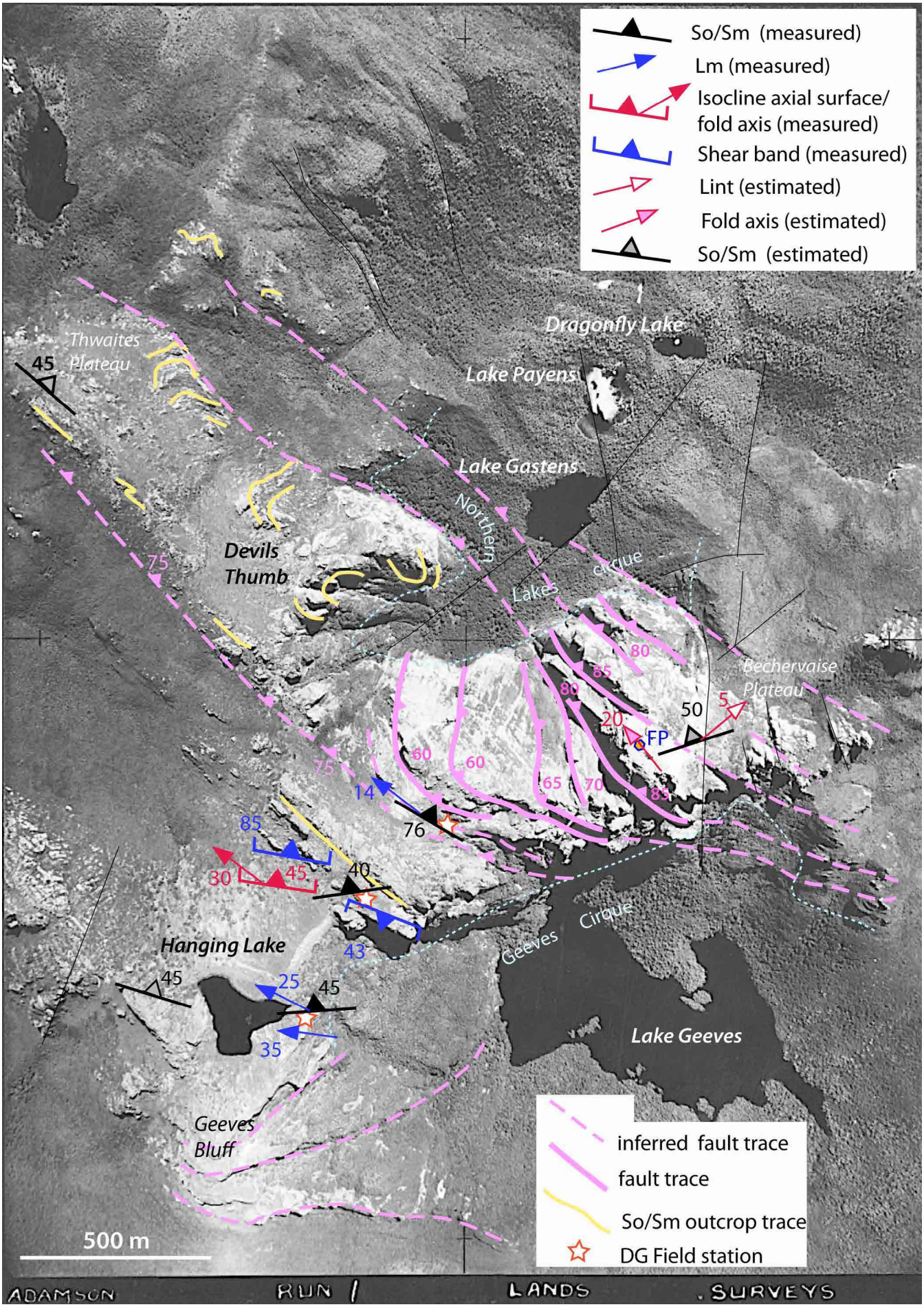

Figure 73. Structure interpretation map of the Federation Peak region showing measured and estimated structural data, formlines in So/Sm (yellow traces) and steeply east-dipping reverse faults (pink traces). Map base is a 1948 Lands Department aerial photograph. The position of Federation Peak summit is shown by the blue outlined orange polygon labeled FP. The positions of the Northern Lakes and Geeves glacial cirque walls that bound the Federation Peak ridgeline are shown by the light blue dashed lines.

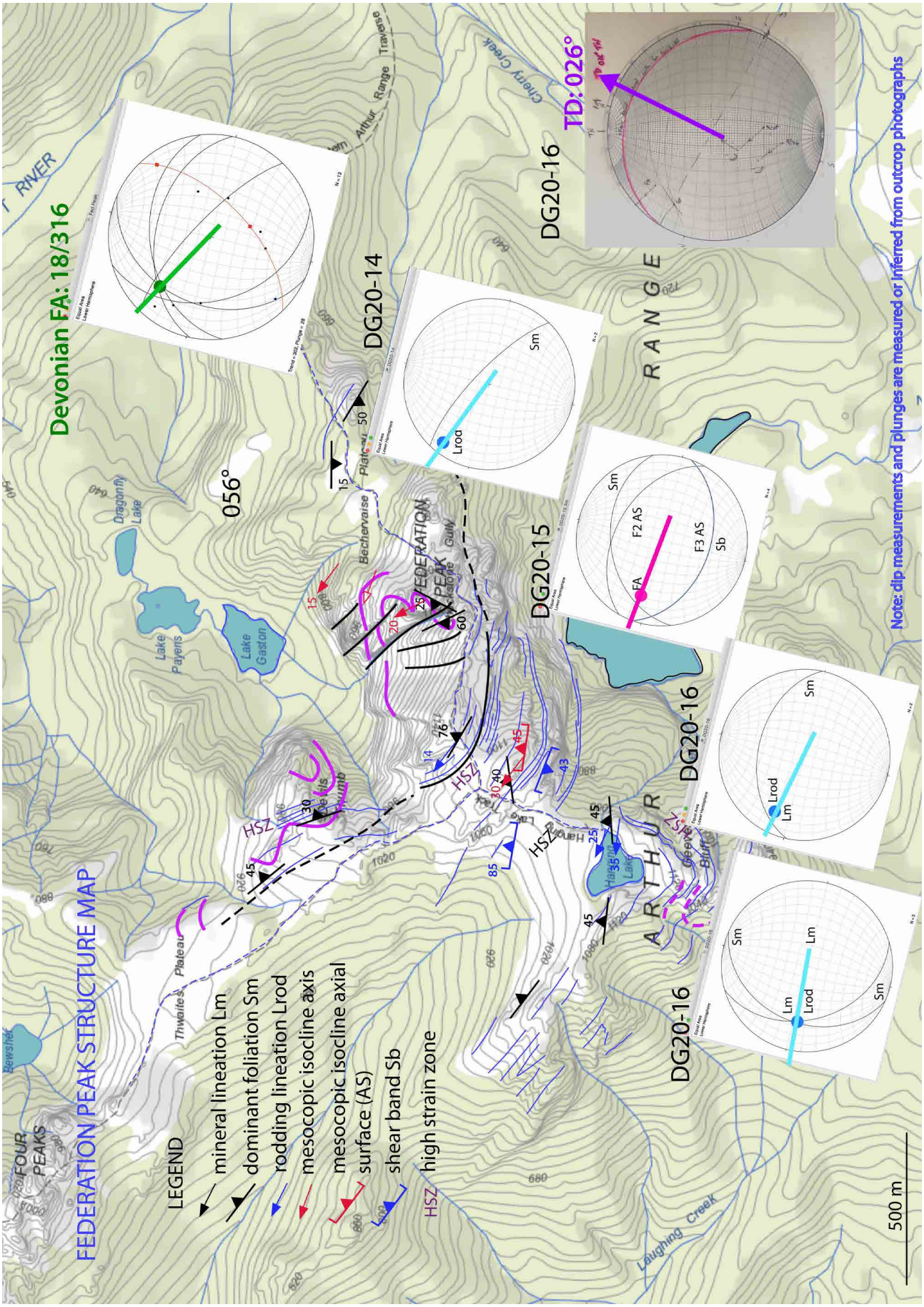

Figure 74. Federation Peak structural map based on measurements collected by the authors and photo interpretation. The thick purple line traces are formlines in So/Sm that define the northwest-plunging, isoclinal macro-fold hinges at Devils Thumb, Geeves Bluff south-west face and in the Federation Peak cirque walls.

Stereonet annotation: blue lines are Lm; pink lines are fold axes; green line is Devonian fold axis trend 28°/316° and lower right the purple line with arrow is the transport direction (TD) towards 026°.

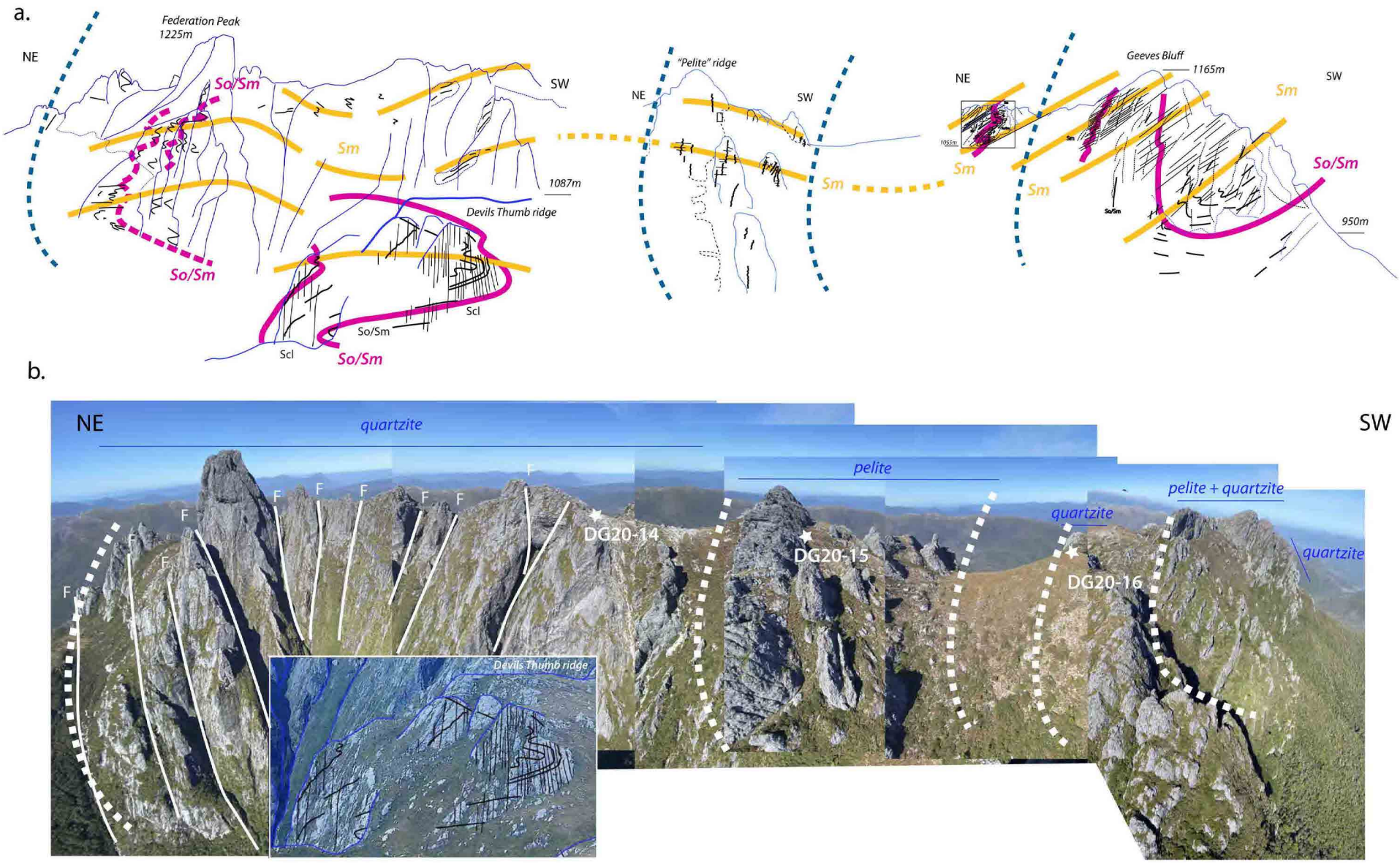

Figure 75. Federation Peak ridgeline formline profile in (a) showing the recumbent isoclinal macro-folds at Geeves Bluff and the Devils Thumb, and b) the distribution of quartzite and pelite (black carbonaceous siliceous phyllite) in the ridge photo collage. The locations of field stations DG20-14, DG20-15 and DG20-16 are shown. Pink formlines highlight the So/Sm layering that defines the closures whereas the orange lines depict the axial surface Sm foliation. Profile location is shown as profile 15 in Figure 61. Note the apparent northeast-closing Federation Peak recumbent macro-fold plunges at ~25° beneath the southwest-closing Devils Thumb recumbent macro-fold and is therefore structurally lower (see Figures 62 and 76).

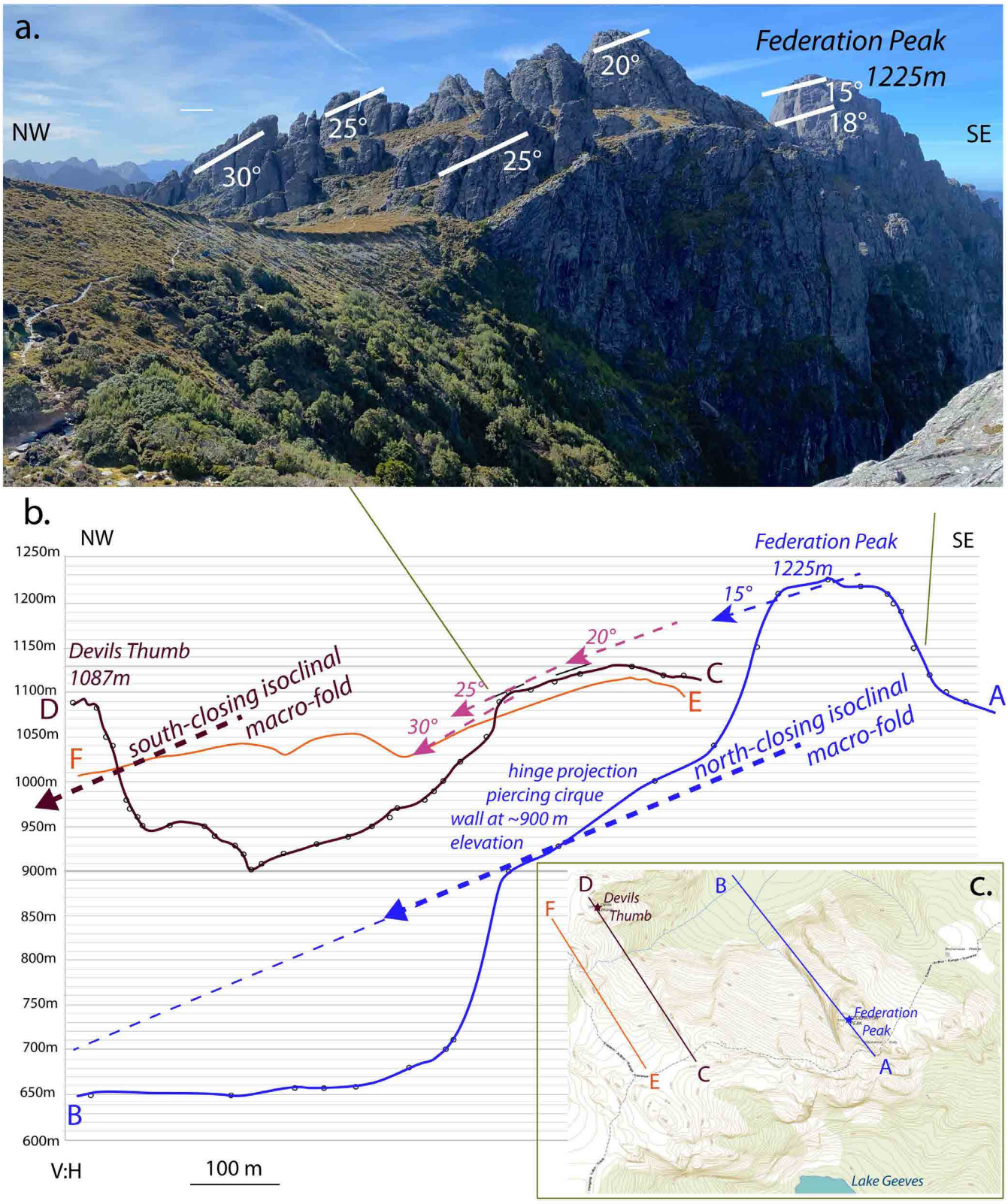

Figure 76. Federation Peak ridge profiles. a) View of ridgeline taken from just below Geeves Bluff looking to the north-northeast. The intersection traces of So/Sm on the sub-vertical Devonian cleavage are shown by the white line segments (Lint). These traces indicate the plunge of the Cambrian north-closing macro-fold. b) Serial, stacked topographic profiles A-B, C-D and E-F with superimposed Lint/fold plunge data from (a). c) ListMap topographic map showing the positions of the profiles in (b).

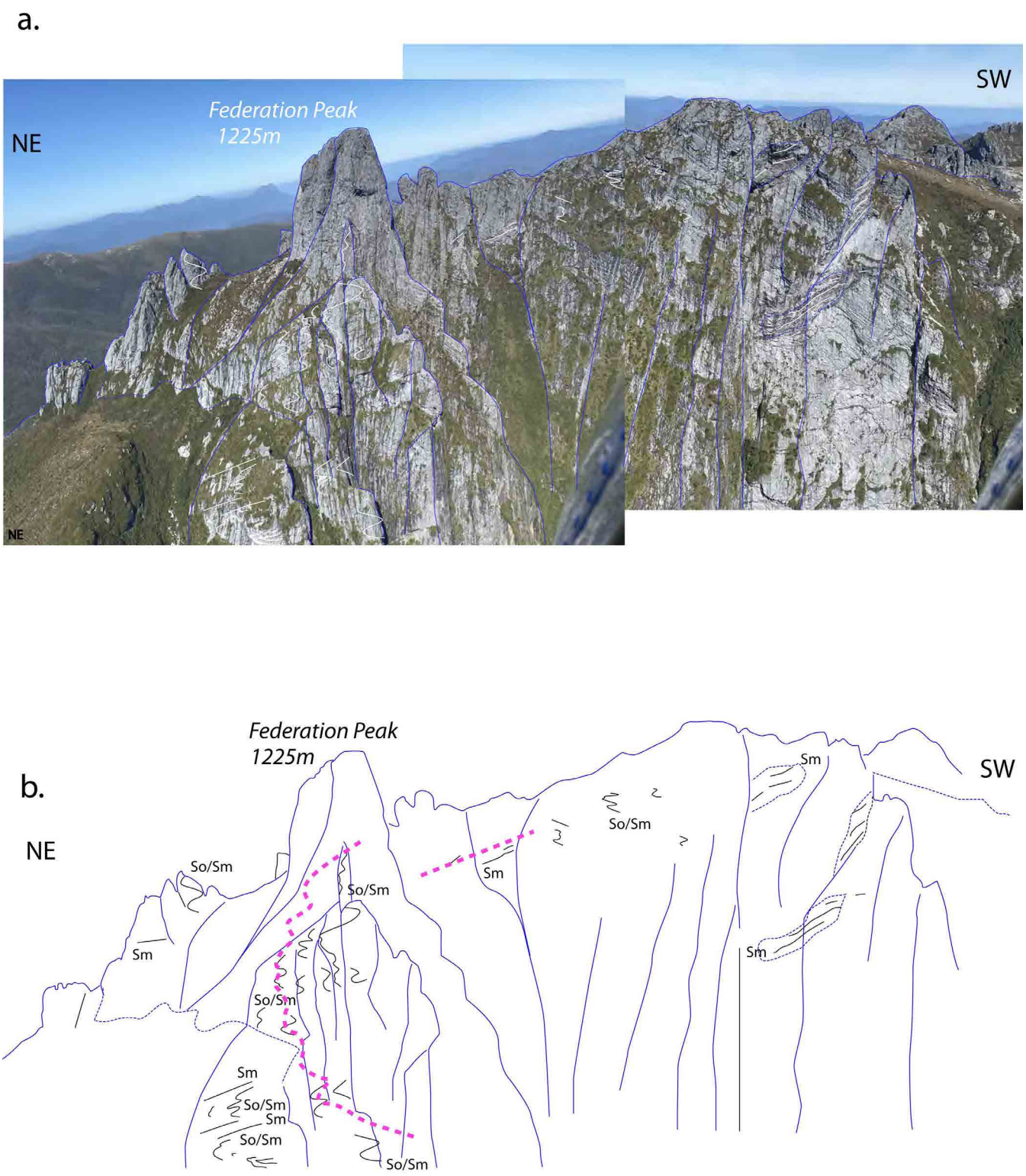

Figure 77. Federation Peak structural interpretation. a) Photo mosaic of ridgeline and (b) formline traces of So/Sm and Sm (black lines), summary formlines (pink dashed lines) and topographic features (blue lines).

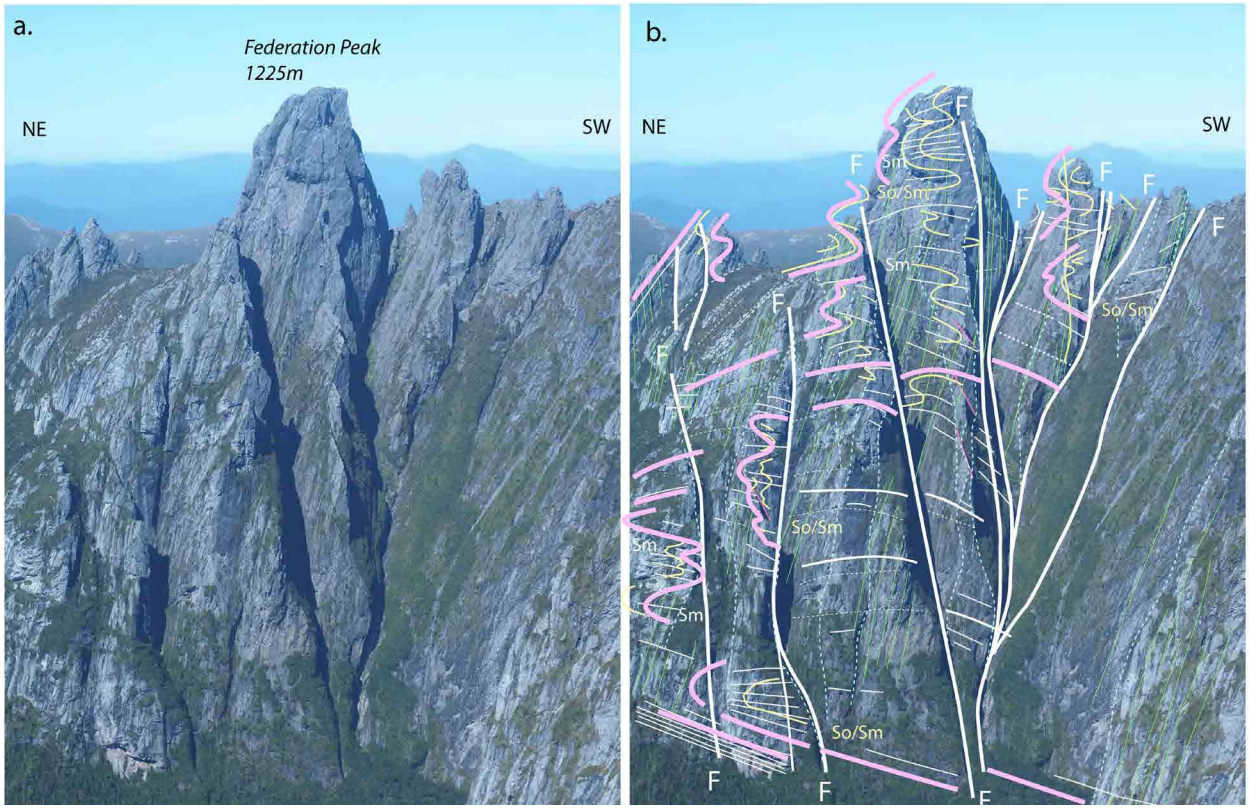

Figure 78. a) Federation Peak northwest-facing ridgeline with an apparent north-closing macro-fold hinge suggested in the north-east part of the photo. b) Formline interpretation of ridgeline showing steeply east-dipping faults (white line traces), So/Sm formlines (yellow traces and the overprinting sub-vertical Devonian cleavage (green line traces). The thick pink lines attempt to show the generalised geometry of the north-closing, isoclinal macro-fold. Fold plunge is towards the camera at ~20-30°. Note some faults have an apparent west-dip due to the camera angle but are all steeply east dipping (see Figures 72 and 73). Movement on the faults is unknown, but the faults are considered to be an originally steeply east-dipping, semi-imbricate reverse fault system.

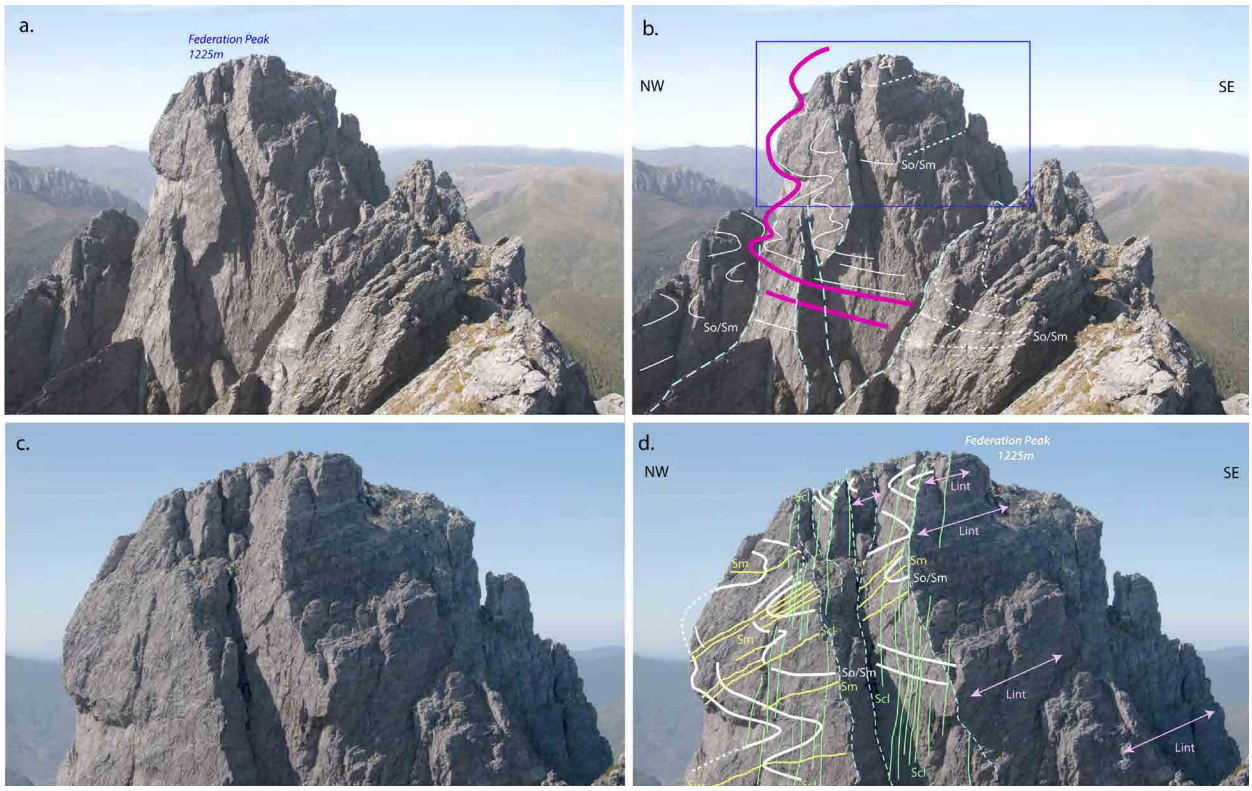

Figure 79. a) Summit tower of Federation Peak taken looking northeast along ridgeline (Photo credit: Rodney Smith). b) Formline interpretation of (a) showing isoclinally folded So/Sm (white traces). The thick pink lines define the generalised geometry of a second- or third-order north-closing recumbent fold sitting in the summit peak. c) Enlargement of summit crest with formline interpretation in d) showing isoclinally folded So/Sm (white traces), an axial surface foliation Sm (yellow traces) all overprinted by a strong sub vertical Devonian spaced cleavage Scl (green traces). Lint traces (fine pink lines with arrowheads) are sub-parallel to meso-fold hinges in the upper part of the summit tower and show 15°-20° NW plunge.

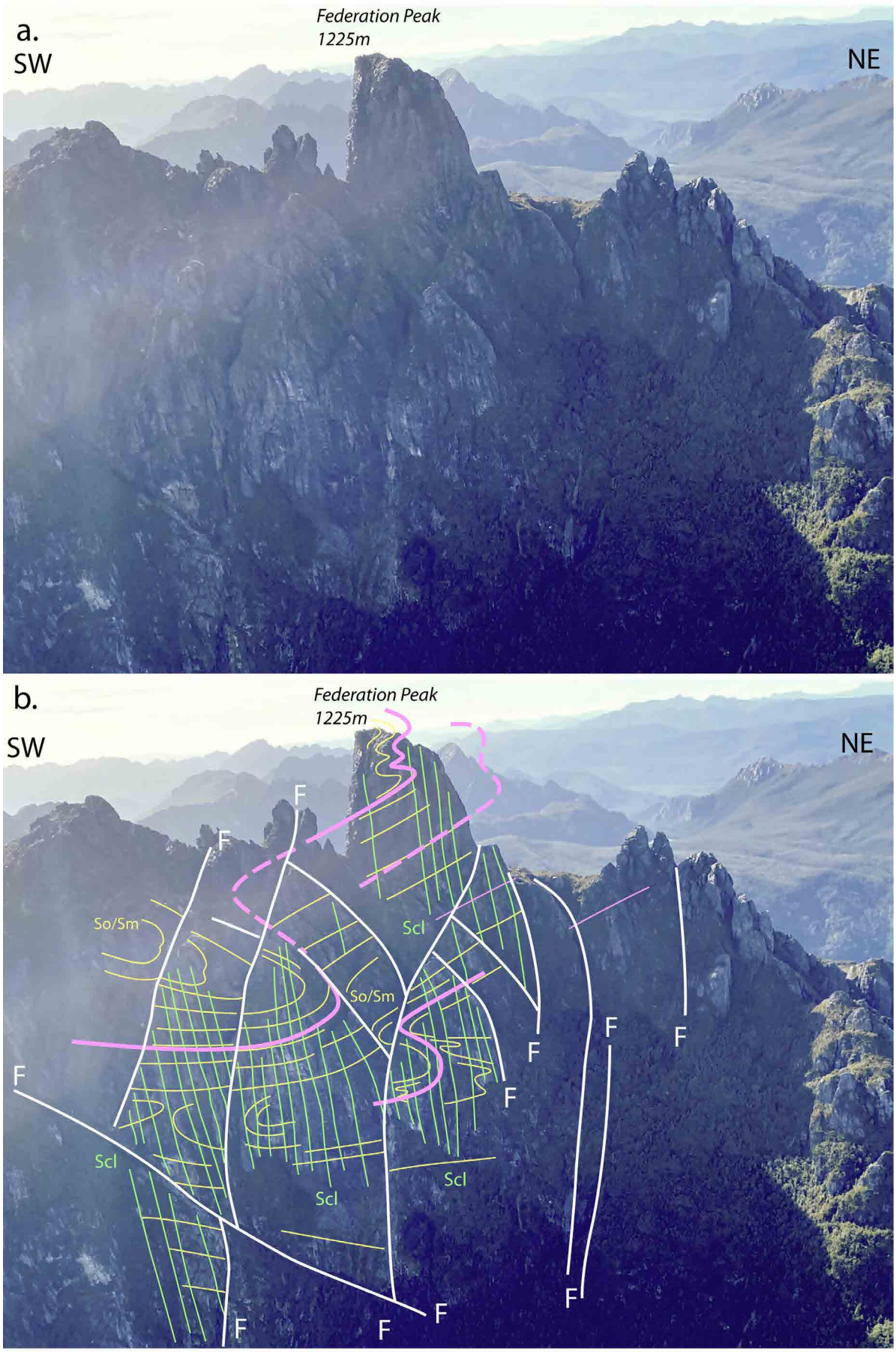

Figure 80. a) Federation Peak southeast face in shadow towering over Lake Geeves at base of cliff (not shown in photo). b) Formline interpretation showing faults (heavy white lines with F designation), formlines in So/Sm (yellow lines) and over-printing Devonian cleavage Scl (green lines). Pink lines show generalised north-closing fold form.

2) Pelite band with complex structural relationships along ridgeline between Federation Peak and Hanging Lake-Geeves Bluff (Figures 81, 82, 83 and 84).

A major zone of black, thin-banded siliceous pelite with occasional thin quartzite layering occurs just north of Hanging Lake (Figure 81a, 82a and 83). Three fabrics are common in the pelite unit along this part of the ridgeline. These are the dominant foliation Sm (pink), the So/Sm layering (orange) at low angles to Sm (both steeply northeast-dipping) and a flat lying axial surface foliation (blue dashed lines) transitional into shear band-like zones (Figures 81b).

The spaced transposition layering/"banding" that defines Sm dominates the ridgeline. This cuts and deflects the So/Sm observable in the zones between the spaced Sm with a shear band character. This also gives northeast-over-southwest shear sense like the Hanging Lake folded zone (see Element 3 following).

The complexity of these meso-scale structures is also shown in thin-bedded quartzites within the main pelite band (Figures 84). These show isoclinal folds (purple dashed circles in Figure 84b: F1/F2 isocline hinges) associated with rootless isoclines in quartz veins within the generalised Sm. The isoclines reflect intense transposition of the original So/Sm layering. Late shear bands are also common showing the general southwest-over-northeast shear sense (Figures 73 and 84b).

These mesoscale structures incorporating the intense transposition layering as well as the Hanging Lake folded zone (Element 3) reflect overturning on the NE limb of the Geeves Bluff synformal recumbent fold (Element 4). It is suggested that these are early southwest-over-northeast shear-related structures that have been subsequently folded during fold-nappe development (see Figure 85).

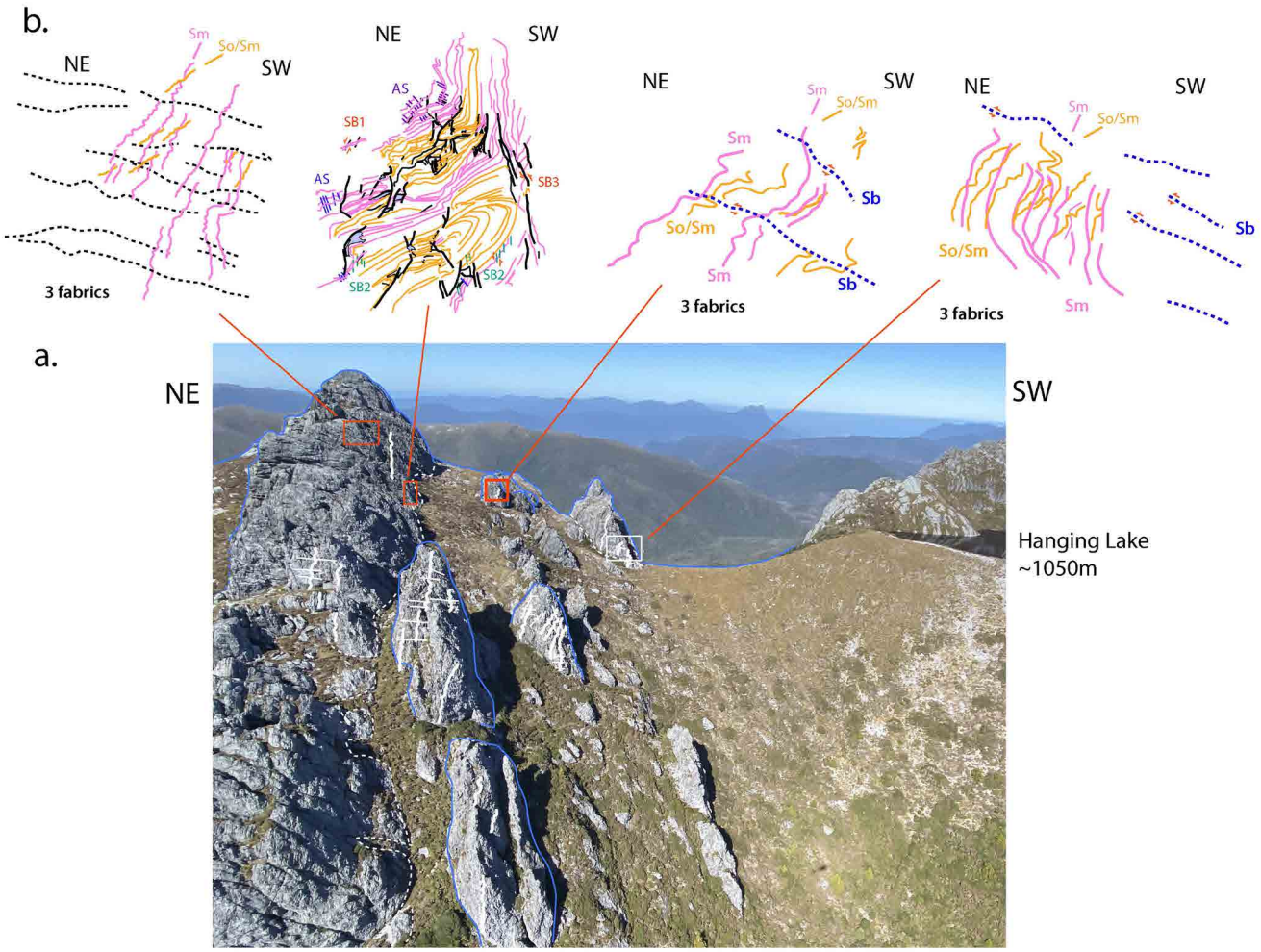

Figure 81. Structural relationships in pelite-dominated outcrops north of Hanging Lake and Geeves Bluff with formline structural interpretations at top of figure. Photographs and photo enlargements used to derive these formline interpretations are shown in Figures 82, 83 and 84.

Figure 82. Photographs showing detailed structural relationships in pelite-dominated outcrops along Federation Peak ridgeline to Geeves Bluff. These were used to show the structural relationships in Figure 81b. Three fabrics are shown: a steeply northeast-dipping So/Sm (white formlines) folded by, and at low angle to, a banded Sm also steeply northeast-dipping (orange formlines). Both are folded by open small-scale undulations with flat axial surfaces (blue dashed lines).

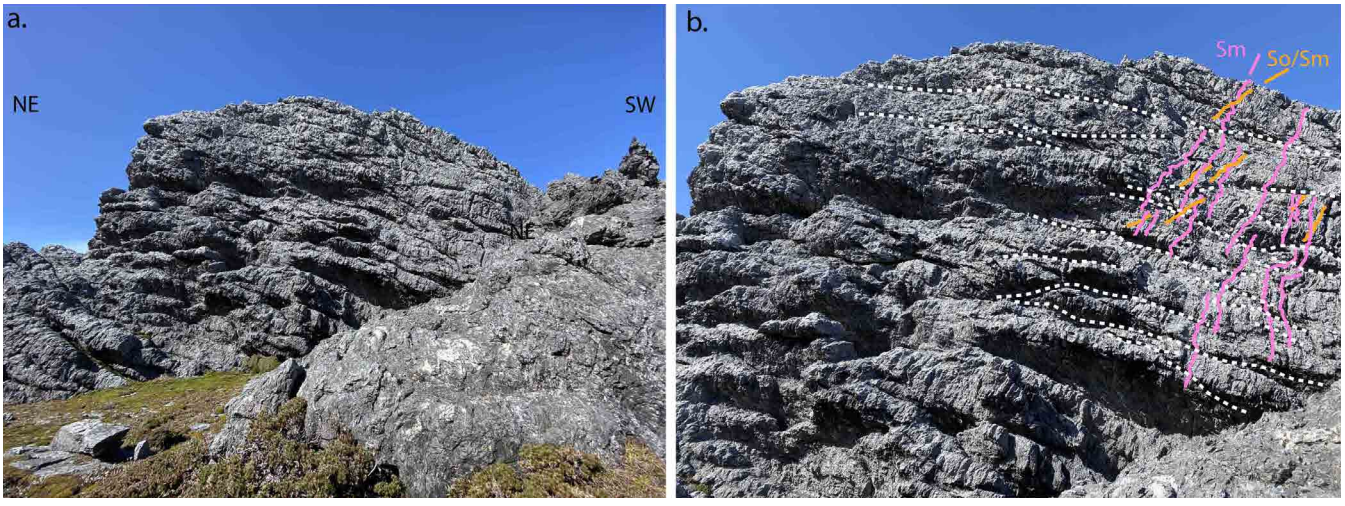

Figure 83. Structural relationships in the dominant pelite band along the Federation Peak ridgeline. Three fabrics are shown: a steeply northeast-dipping So/Sm (orange formlines) folded by, and at low angle to, a banded Sm also steeply northeast-dipping (pink formlines). Both are folded by open small-scale undulations with flat axial surfaces (dotted white formlines). This constitutes fabric relationships shown in Figure 81b.

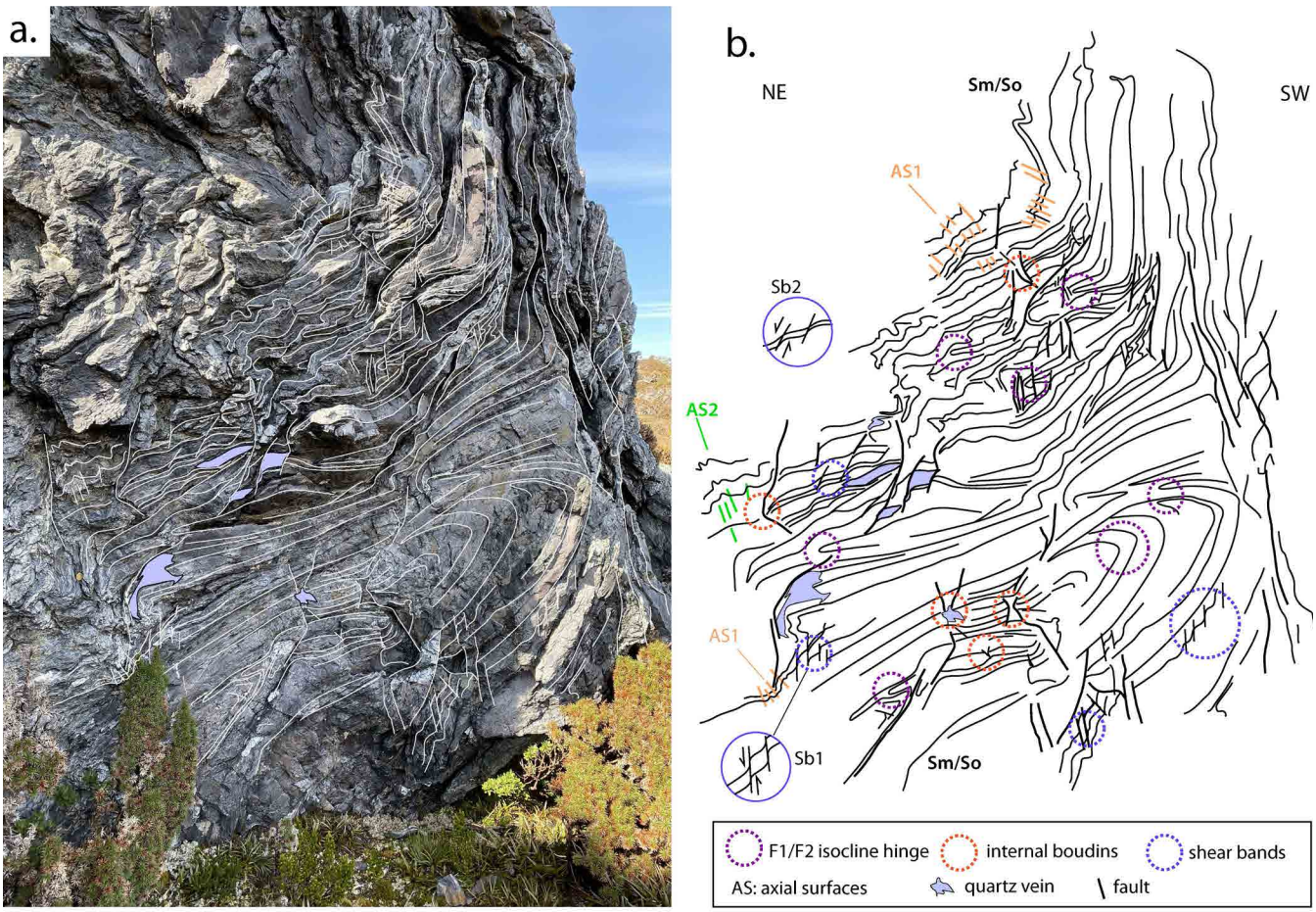

Figure 84. Structural relationships at DG20-15 (for location see Figure 84b) showing isoclinal folds within thicker beds of white quartzite (lower part of cliff) interbedded with dark siliceous pelite/phyllite (for location see Figure 82). b) Formline interpretation of the outcrop in (a) showing So/Sm formline traces (black lines), positions of F1/F2 isoclines (dashed purple circles), internal boudins (dashed orange circles) and shear bands (dashed blue circles). Orange line traces (AS1) and green line traces (AS2) are sets of overprinting crenulations cleavages.

3) Hanging Lake folded zone with asymmetric chevron folds in thinly bedded quartzite (Figure 86).

The folded zone is northeast-dipping and is bounded by higher strain Sm-parallel transposition layering in pelite (Figure 86). Cascading chevron folds in the folded zone have a northeast-dipping enveloping surface in So/Sm. Inferred fold limb attenuation transitioning into the higher strain Sm at the zone boundaries suggests S-vergence (viewed down plunge or to the northwest). The zone occurs on the northeast limb of the Geeves Bluff recumbent fold (Figure 87) and should have the opposite vergence to that observed in the zone if the folds are macrofold-related vergence folds. This requires the Hanging Lake folded zone to be part of a larger, early shear-related zone not unlike the folds and transposition layering at Lake Haven near Mt Taurus in the Western Arthur Range (see Figure 56).

4) The northeast-closing Geeves Bluff synformal, recumbent, isoclinal macro-fold within a banded pelite-quartzite-pelite quartzite sequence (Figure 87).

The northwest face of Geeves Bluff shows an apparent northeast-closing recumbent fold closure (Figure 87b). Quartzite occupies the synformal -hinge core with a black phyllitic unit on Geeves Bluff (Figure 87b). Another thin-bedded quartzite unit sits above the Geeves Bluff phyllite band and is exposed in the cliff behind Hanging Lake (Figure 86).

5.0 TRANSPORT DIRECTIONS FOR THE CAMBRIAN DEFORMATION

The Cambrian deformation TD vectors for the Arthur Ranges are shown in Figure 88. The south-southwest-over-north-northeast transport direction is approximately orthogonal to both the Cambrian and Devonian fold axial surface traces.

5.1 Western Arthur Range

Shear bands identified from bushwalker's photos with attitudes of Sm and shear bands estimated, were used to determine transport directions at Lake Oberon and Lake Mars.
Lake Oberon: towards 013°
Lake Mars: towards 003°

5.2 Eastern Arthur Range

Shear bands calculated (Four Peaks) and measured (Federation Peak ridgeline) were used to calculate transport directions.
Four Peaks: towards 022°
Federation Peak: towards 026°

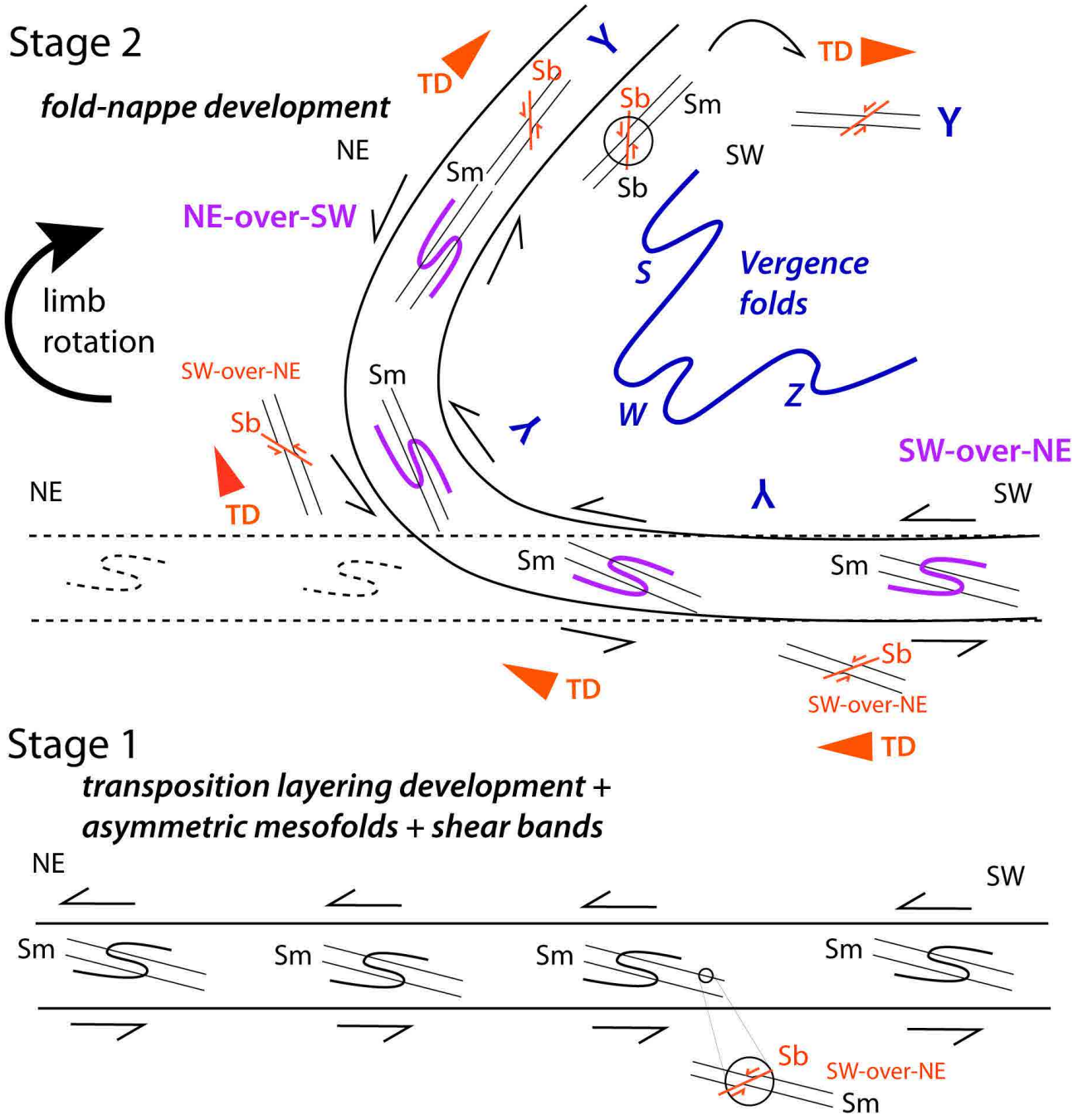

Figure 85. Schematic illustrating refolding (Stage 2) of early formed transposition layering +asymmetric isoclines +shear bands (Stage 1).

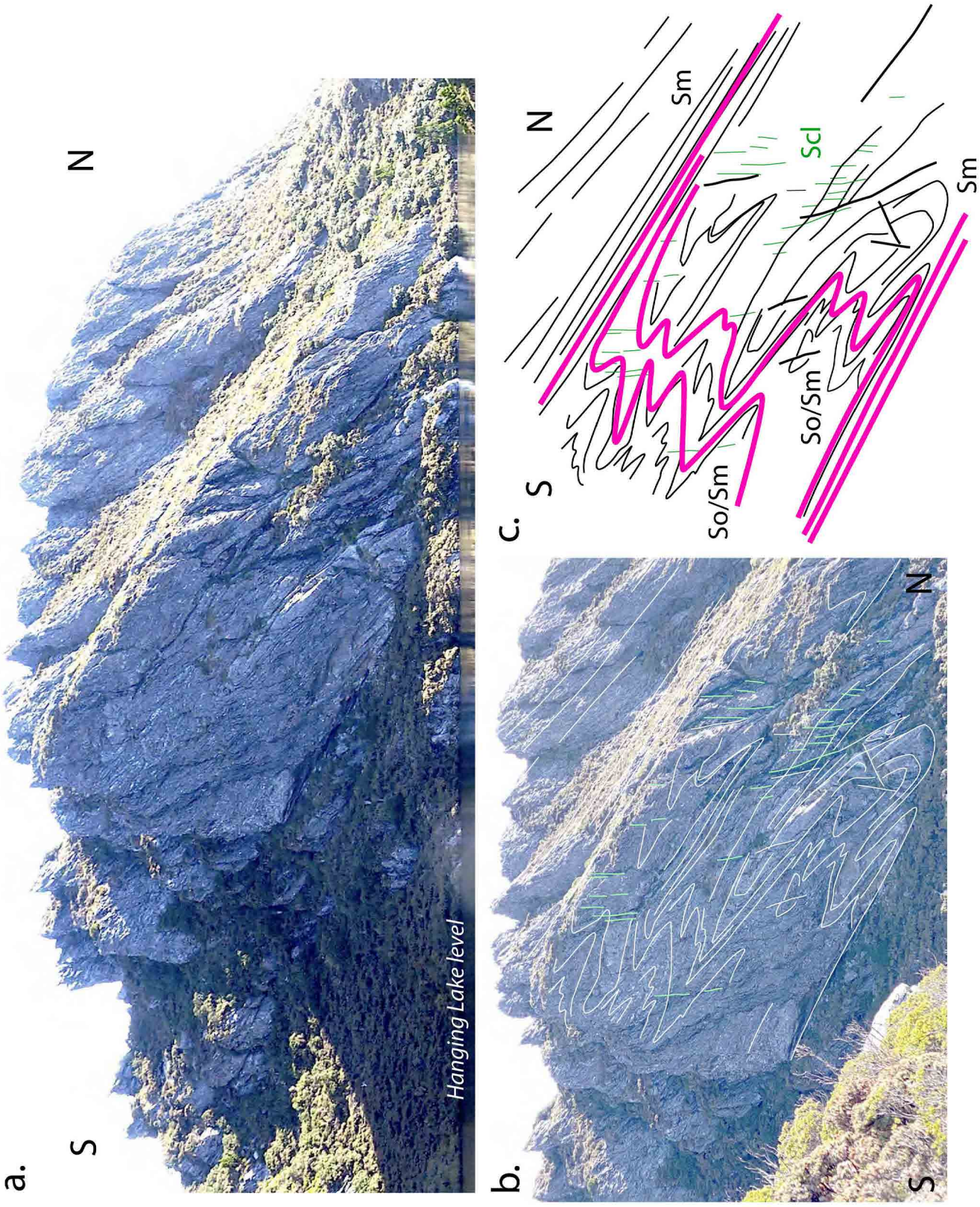

Figure 86. Folded zone in thin-bedded quartzite in cliff face on the west side of Hanging Lake. a) Cliff face with view looking to the west. b) Enlarged view of cliff face with formline interpretation on photo. c) Formline interpretation of the photo in (b). The folded layering is So/Sm bounded by intense transposition layering Sm, with both overprinted by the younger Devonian sub-vertical cleavage (Scl). Pink formlines show the asymmetry of the folded zone.

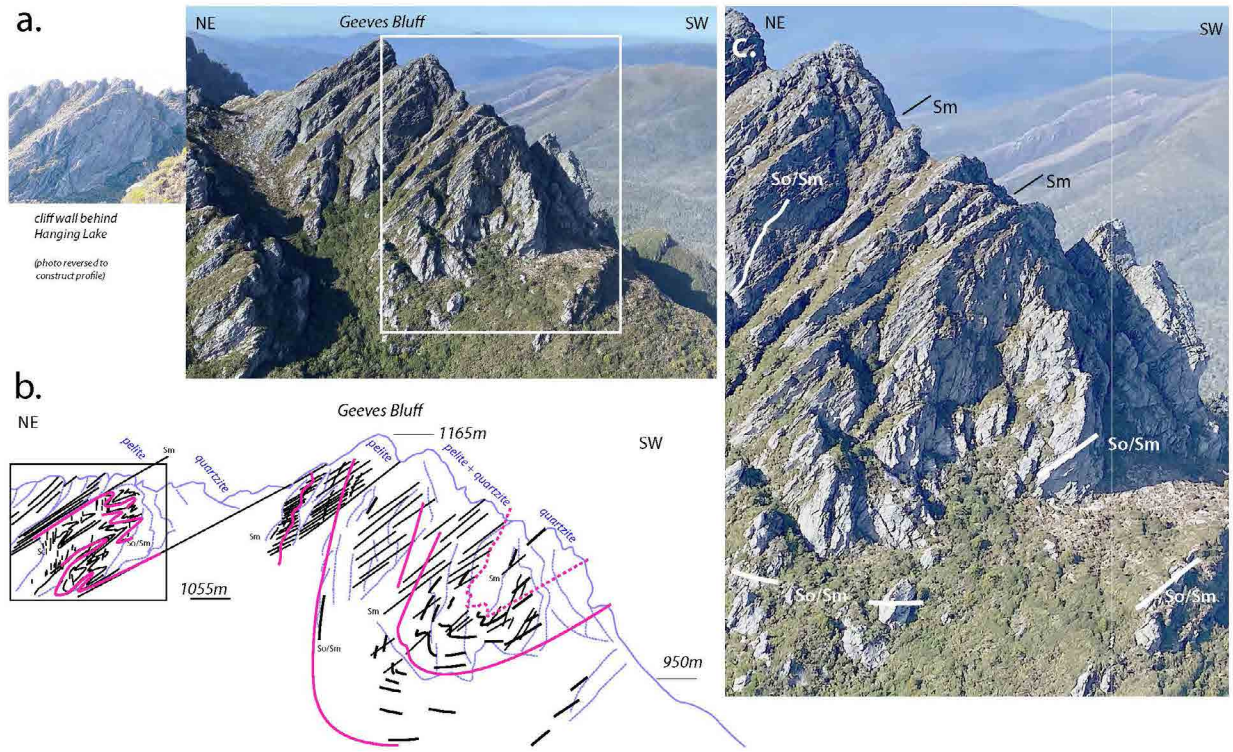

Figure 87. Geeves Bluff northeast-closing, recumbent synformal macro-fold closure exposed in the cliff face below Geeves Bluff. Pink lines are the So/Sm layering that defines the fold closure. Thin black lines are the axial surface foliation Sm.

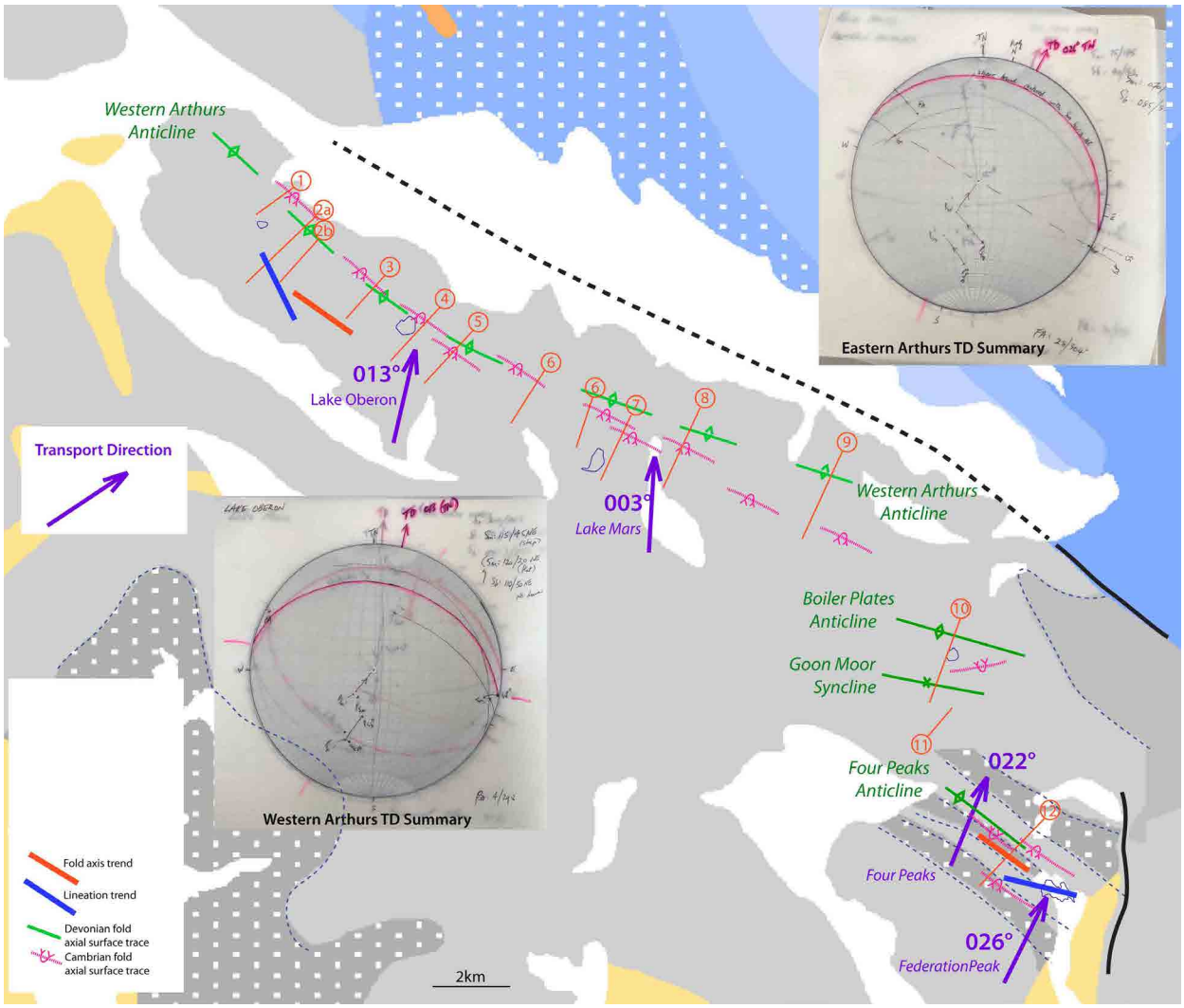

Figure 88. Transport directions for the Western and Eastern Arthurs. Purple arrows show the Transport direction (TD). Stereonets show the determinations and restoration for the Western and Eastern Arthurs shear bands.

6.0 CONCLUSIONS

The Arthur Ranges are at the extreme northeastern edge of the Southern Tyennan domain. The overall macro-structure is a series of northwest-trending regional-scale recumbent isoclinal folds that are refolded by a similarly oriented series of open, upright Devonian anticlines and synclines. The range-front along the northeast flank of the Western Arthur Range is defined by a major, northwest-trending, thrust-reverse fault network. These faults offset both the Cambrian recumbent folds and the upright Devonian folds.

The Cambrian structure of Western Arthur Range is a northeast-facing and closing recumbent macro-fold with 21 km axial surface length juxtaposed by the reverse faulting against a major southwest-closing recumbent macro-fold that has a minimum preserved length of ~14km.

The Eastern Arthur Range, and most likely the entire Arthur Range region, consists of a recumbent fold pile. Given the established northwest-fold plunge through the southern part of the Eastern Arthur Range (see Figures 61 and 74) the northeast-closing Federation Peak-Geeves Bluff recumbent macro-fold plunges below the oppositely southwest-closing Devils Thumb recumbent macro-fold (Figure 76). The northeast-closing fold is therefore at a lower structural level. Similarly, the southwest-closing The Needles-Devils Thumb recumbent fold(s) sits above this fold and is therefore at a higher structural level. The southwest-closing recumbent fold exposed in the Devils Thumb ridge is likely coincident with the southwest-closing The Needles fold in the East Portal-Goon Moor profile, but folded across the Devonian Goon Moor Syncline into the Four Peaks Anticline (Figure 61). These relationships are expressed in the Eastern Arthur Range profile (Figure 62).

Prior to the reverse faulting the Western Arthur Range most likely had an overall similar geometry to that of the Eastern Arthur Range. Given that the northeast-closing macro-fold in the Western Arthur Range is thrust over the southwest- closing recumbent macro-fold, the implication is that the northeast-closing fold has come from a lower structural level. This matches the relationships in the Eastern Arthur Range where the southwest-closing recumbent fold is at the highest structural level.

7.0 IMPLICATIONS

1. The structural geometry of this part of the Southern Tyennan domain is an isoclinally folded, low-grade metamorphic sheet dominated by a recumbent isoclinal fold pair. The fold pair consists of an upper-most southwest-closing recumbent macro-fold overlying a northeast-closing recumbent macro-fold.
2. The Arthur Ranges provide insight into the dimensions of these regional-scale recumbent isoclinal folds
   - The Western Arthur Range indicates they have hinge lengths of at least 21 km (equivalent to map axial surface trace strike-lengths);
   - The Eastern Arthur Range indicates they have limb lengths of at least 6-8 km.
3. The recumbent fold pair relationship may hold for the entire region east of Bathurst Harbour including the Ray Range, Mt Norold and the Spiro Range with an areal extent of 450-500 square kilometres.

8.0 ACKNOWLEDGEMENTS

- Andrew McNeill for providing support through the 2016-2020 Geoscience Initiative, reviewing the document and providing comments.
- Grant Dixon for supplying high-resolution images of outcrops in the Arthur Ranges (grantdixon-photography.com.au), notes on lithology changes across the Eastern Arthur Range, and comments on an early draft of the document.
- David Noble for supplying high-resolution images from his bushwalking photograph collection at www.david-noble.net and giving permission to use in this publication.
- Liz Dombrovskis for permission to reproduce photographs by Peter Dombrovskis.
- Rodney Smith for supplying high resolution photographs of Federation Peak.
- Parks and Wildlife Service (PWS) for access into the World Heritage Area and to allow measurement, sampling and photograph collection.
- Jason Bradbury DPIPWE for assistance with WHA and PWS permits for scientific research, and assistance on the Haven Lake-Mt Scorpio traverse.
- Rodney Smith from Rotorlift for helicopter transport into the Arthurs and skilled landings in difficult topography.
- Rick Allmendinger and Nestor Cardozzo for use of OSX Stereonet.

9.0 REFERENCES

Berry, R.F. 2014. Chapter 4.2 Cambrian Tectonics – The Tyennan Orogeny. In Corbett, K.D., Quilty, P.G & Calver, C.R. editors, Geological Evolution of Tasmania pp 95-110. *Geological Society of Australia Special Publication,* 24, Geological Society of Australia (Tasmania Division).

Brown, B. 2017. *Journeys into the Wild: The Photography of Peter Dombrovskis*. National Library Australia Publication. 187p.

Collins, K. 1990. *South-West Tasmania: A Natural History and Visitors Guide*. Heritage Books. 368p.

Taylor, A. M. 1959. Precambrian Rocks of the Old River Area. *Tasmanian Geological Survey Technical Report,* 4, p. 34-46.

APPENDIX 1

TABULATED STRUCTURAL MEASUREMENTS

File Download

Arthur Ranges Structural Measurements

Datum: GDA94 - MGA Zone 55

Projects	Structure	Structure Type	Dip	D/Direct	Reliability	Secondary Dip	Secondary Dip Direction	Comments	Originators	Chronostratigraphy	Collection Date	Field #	East	North	Accuracy	Location Method
Arthur Ranges	Fold axis	Haa + Pac	10	303.6	1 - Most reliable	20	353.6	FA	David Gray	Proterozoic	26/03/2020	DG.20.11.1	438203	5224470	10m	GPS
Arthur Ranges	Lineation	Lae	20	13.6	1 - Most reliable			Lm	David Gray	Proterozoic	26/03/2020	DG.20.11.2	438203	5224470	10m	GPS
Arthur Ranges	Lineation	Lae	18	53.6	1 - Most reliable			Lm	David Gray	Proterozoic	26/03/2020	DG.20.11.2	438203	5224470	10m	GPS
Arthur Ranges	Metamorphic Foliation	Sag	28	358.6	1 - Most reliable			Sm	David Gray	Proterozoic	26/03/2020	DG.20.11.2	438203	5224470	10m	GPS
Arthur Ranges	Lineation	Lae	12	293.6	1 - Most reliable			Lm	David Gray	Proterozoic	26/03/2020	DG.20.11.3	438203	5224470	10m	GPS
Arthur Ranges	Metamorphic Foliation	Sag	15	313.6	1 - Most reliable			Sm	David Gray	Proterozoic	26/03/2020	DG.20.11.3	438203	5224470	10m	GPS
Arthur Ranges	Fold axis	Haa	15	328.6	1 - Most reliable			FA	David Gray	Proterozoic	26/03/2020	DG.20.11.4	438203	5224470	10m	GPS
Arthur Ranges	Fold axis	Haa + Pac	30	313.6	1 - Most reliable	40	293.6	FA	David Gray	Proterozoic	26/03/2020	DG.20.11.5	438203	5224470	10m	GPS
Arthur Ranges	Lineation	Lae	25	263.6	1 - Most reliable			Lm	David Gray	Proterozoic	26/03/2020	DG.20.11.6	438203	5224470	10m	GPS
Arthur Ranges	Metamorphic Foliation	Sag	25	308.6	1 - Most reliable			Sm	David Gray	Proterozoic	26/03/2020	DG.20.11.6	438203	5224470	10m	GPS
Arthur Ranges	Lineation	Lae	25	343.6	1 - Most reliable			Lm	David Gray	Proterozoic	26/03/2020	DG.20.11.7	438203	5224470	10m	GPS
Arthur Ranges	Metamorphic Foliation	Sag	46	38.6	1 - Most reliable			Sm	David Gray	Proterozoic	26/03/2020	DG.20.11.7	438203	5224470	10m	GPS
Arthur Ranges	Metamorphic Foliation	Sag	15	303.6	1 - Most reliable			Sm?	David Gray	Proterozoic	26/03/2020	DG.20.12	438107	5224255	10m	GPS
Arthur Ranges	Axial Surface	Pac		13.6	1 - Most reliable	5	318.6	FA AS	David Gray	Proterozoic	26/03/2020	DG.20.13.1	438112	5224186	10m	GPS
Arthur Ranges	Fold axis	Haa	15	283.6	1 - Most reliable		283.6	FA	David Gray	Proterozoic	26/03/2020	DG.20.13.2	438112	5224186	10m	GPS
Arthur Ranges	Lineation	Lae	32	323.6	1 - Most reliable			Lm	David Gray	Proterozoic	26/03/2020	DG.20.13.3	438112	5224186	10m	GPS
Arthur Ranges	Metamorphic Foliation	Sag	45	13.6	1 - Most reliable			Sm	David Gray	Proterozoic	26/03/2020	DG.20.13.3	438112	5224186	10m	GPS
Arthur Ranges	Lineation	Lae	14	308.6	1 - Most reliable			Lrod	David Gray	Proterozoic	26/03/2020	DG.20.14.1	456998	5208823	10m	GPS

Projects	Structure	Structure Type	Dip	D/Direct	Reliability	Secondary Dip	Secondary Dip Direction	Comments	Originators	Chronostratigraphy	Collection Date	Field #	East	North	Accuracy	Location Method
Arthur Ranges	Metamorphic Foliation	Sag	76	43.6	1 - Most reliable			Sm	David Gray	Proterozoic	26/03/2020	DG.20.14.1	456998	5208823	10m	GPS
Arthur Ranges	Axial Surface	Pac		13.6	1 - Most reliable	43	199.6	FA AS	David Gray	Proterozoic	26/03/2020	DG.20.15.1	456807	5208666	10m	GPS
Arthur Ranges	Fold axis	Haa + Pac	30	289.6	1 - Most reliable	45	19.6	FA	David Gray	Proterozoic	26/03/2020	DG.20.15.2	456807	5208666	10m	GPS
Arthur Ranges	Shear Band	Sau	55	318.6	1 - Most reliable			Sb	David Gray	Proterozoic	26/03/2020	DG.20.15.3	456807	5208666	10m	GPS
Arthur Ranges	Metamorphic Foliation	Sag	40	353.6	1 - Most reliable			Sm	David Gray	Proterozoic	26/03/2020	DG.20.15.4	456807	5208666	10m	GPS
Arthur Ranges	Lineation	Lae	25	298.6	1 - Most reliable			Lrod	David Gray	Proterozoic	26/03/2020	DG.20.16.1	456731	5208298	10m	GPS
Arthur Ranges	Metamorphic Foliation	Sag	45	11.6	1 - Most reliable			Sm	David Gray	Proterozoic	26/03/2020	DG.20.16.1	456731	5208298	10m	GPS
Arthur Ranges	Lineation	Lae	35	278.6	1 - Most reliable			Lm/Lrod	David Gray	Proterozoic	26/03/2020	DG.20.16.2	456731	5208298	10m	GPS
Arthur Ranges	Metamorphic Foliation	Sag	38	253.6	1 - Most reliable			Sm	David Gray	Proterozoic	26/03/2020	DG.20.16.2	456731	5208298	10m	GPS
Arthur Ranges	Metamorphic Foliation	Sag	34	293.6	1 - Most reliable			Sm	David Gray	Proterozoic	26/03/2020	DG.20.16.3	456731	5208298	10m	GPS
Arthur Ranges	Fold axis	Haa + Pac	38	43.6	1 - Most reliable	58	253.6	FA	David Gray	Proterozoic	14/12/2020	DG20.53.1	445766	5219928	10m	GPS
Arthur Ranges	Lineation	Lae	18	346.6	1 - Most reliable			Lm	David Gray	Proterozoic	14/12/2020	DG20.53.2	445766	5219928	10m	GPS
Arthur Ranges	Metamorphic Foliation	Sag	20	213.6	1 - Most reliable			Sm	David Gray	Proterozoic	14/12/2020	DG20.53.2	445766	5219928	10m	GPS
Arthur Ranges	Fold axis	Haa + Pac	38	283.6	1 - Most reliable	90	207.6	FA	David Gray	Proterozoic	14/12/2020	DG20.54	445779	5219931	10m	GPS
Arthur Ranges	Lineation	Lae	5	13.6	1 - Most reliable			Lm	David Gray	Proterozoic	14/12/2020	DG20.54b	445789	5219931	10m	GPS
Arthur Ranges	Metamorphic Foliation	Sag	45	128.6	1 - Most reliable			Sm	David Gray	Proterozoic	14/12/2020	DG20.54b	445789	5219931	10m	GPS
Arthur Ranges	Lineation	Lae	35	208.6	1 - Most reliable			Lm	David Gray	Proterozoic	14/12/2020	DG20.55.1	446089	5220208	10m	GPS
Arthur Ranges	Metamorphic Foliation	Sag	40	193.6	1 - Most reliable			Sm	David Gray	Proterozoic	14/12/2020	DG20.55.1	446089	5220208	10m	GPS
Arthur Ranges	Fold axis	Haa		168.6	1 - Most reliable			FA or lin	David Gray	Proterozoic	14/12/2020	DG20.55.2	446089	5220208	10m	GPS
Arthur Ranges	Shear Band	Say	15	203.6	1 - Most reliable			Sb; Left lateral movement	David Gray	Proterozoic	14/12/2020	DG20.56.1	446081	5220210	10m	GPS

Projects	Structure	Structure Type	Dip	D/Direct	Reliability	Secondary Dip	Secondary Dip Direction	Comments	Originators	Chronostratigraphy	Collection Date	Field #	East	North	Accuracy	Location Method
Arthur Ranges	Fold axis	Haa	16	203.6	1 - Most reliable			FA	David Gray	Proterozoic	14/12/2020	DG20.56.2	446081	5220210	10m	GPS
Arthur Ranges	Metamorphic Foliation	Sag	38	218.6	1 - Most reliable			Sm	David Gray	Proterozoic	14/12/2020	DG20.56.3	446081	5220210	10m	GPS
Arthur Ranges	Lineation	Lae	8	213.6	1 - Most reliable			Lm	David Gray	Proterozoic	14/12/2020	DG20.56.5	446081	5220210	10m	GPS
Arthur Ranges	Metamorphic Foliation	Sag	28	293.6	1 - Most reliable			Sm	David Gray	Proterozoic	14/12/2020	DG20.56.5	446081	5220210	10m	GPS
Arthur Ranges	Metamorphic Foliation	Sag	27	283.6	1 - Most reliable			Sm	David Gray	Proterozoic	14/12/2020	DG20.56.5	446081	5220210	10m	GPS
Arthur Ranges	Fold axis	Hal	10	288.6	1 - Most reliable			FA early	David Gray	Proterozoic	14/12/2020	DG20.56.6	446081	5220210	10m	GPS
Arthur Ranges	Bedding	Baf	75	270	1 - Most reliable			So	David Gray	Proterozoic	14/12/2020	DG20.57.1	446101	5220613	10m	GPS
Arthur Ranges	Lineation	Lae	15	273.6	1 - Most reliable			Lrod	David Gray	Proterozoic	14/12/2020	DG20.57.2	446101	5220613	10m	GPS
Arthur Ranges	Metamorphic Foliation	Sag	20	133.6	1 - Most reliable			Sm	David Gray	Proterozoic	14/12/2020	DG20.57.2	446101	5220613	10m	GPS
Arthur Ranges	Cleavage	Cae	55	273.6	1 - Most reliable			S1	David Gray	Proterozoic	14/12/2020	DG20.58.1	446495	5221016	10m	GPS
Arthur Ranges	Bedding	Baf	65	198.6	1 - Most reliable			So	David Gray	Proterozoic	14/12/2020	DG20.58.1	446495	5221016	10m	GPS
Arthur Ranges	Fold axis	Haa	51	265.6	1 - Most reliable			Beta calc	David Gray	Proterozoic	14/12/2020	DG20.58.2	446495	5221016	10m	GPS
Arthur Ranges	Vein	Vad	80	98.6	1 - Most reliable			QV	David Gray	Proterozoic	14/12/2020	DG20.59.1	446708	5221087	10m	GPS
Arthur Ranges	Cleavage	Cae	70	218.6	1 - Most reliable			S1	David Gray	Proterozoic	14/12/2020	DG20.59.1	446708	5221087	10m	GPS
Arthur Ranges	Bedding	Baf	58	223.6	1 - Most reliable			So	David Gray	Proterozoic	14/12/2020	DG20.59.1	446708	5221087	10m	GPS
Arthur Ranges	Fold axis	Haa	18	301.6	1 - Most reliable			Beta calc	David Gray	Proterozoic	14/12/2020	DG20.59.2	446708	5221087	10m	GPS
Arthur Ranges	Lineation	Lae	25	278.6	1 - Most reliable			Lrod??	David Gray	Proterozoic	14/12/2020	DG20.59.3	446708	5221087	10m	GPS

Tasmanian
Government

Mineral Resources Tasmania
PO Box 56 Rosny Park
Tasmania Australia 7018
Ph: +61 3 6165 4800

info@mrt.tas.gov.au www.mrt.tas.gov.au